Hemangiomas and Vascular Malformations

7

Siegfried Peer and Ximena Wortsman

How to deal with the most common forms of vascular tumors and their ultrasound findings

Contents

7.1 Introduction

While a so-called "angel's kiss" is a harmless finding–typically with spontaneous resolution within the first 2 years of life–one in one hundred newborns is affected by a vascular soft-tissue lesion, which warrants further investigation. Our main goal is to separate the "don't touch" lesions, such as most hemangiomas–that can simply be observed for a period of time, awaiting spontaneous involution– from lesions that need to be observed more closely or those that should undergo early therapeutic intervention. Such a decision must be made by an interdisciplinary team of pediatricians, dermatologists, surgeons, and radiologists, however, "too many cooks may spoil the broth," especially if they don't speak the same language. A confusing historical nomenclature has been used for many years for the classification of a vascular anomaly: even specialists have applied the term "cavernous hemangioma" to a port wine stain, which gives the false impression of a possibility for spontaneous involution of the lesion. Various hybrid names such as "capillary hemangioma" further added to the confusion. The correct classification of a lesion by clinicians, and especially radiologists and sonographers, however, is of utmost importance to avoid misinterpretations in terms of prognosis and choice of optimal treatment.

7.2 Classification of Vascular Anomalies

The work of Mulliken and Glowacki has greatly improved our understanding of vascular anomalies [1]. In their work dating back to 1982, they classified vascular anomalies according to their endothelial characteristics into two main categories: hemangioma and vascular malformations. While a hemangioma is a benign vascular tumor, characterized by an initial rapid growth of endothelial cells, followed by later slow involution, vascular malformations by definition are not tumors; they are composed of dysplastic vascular channels without accompanying endothelial proliferation. The basic

S. Peer, MD, PhD (✉)
Department of Radiology, CTI GesmbH Innsbruck,
Klostergasse 4, Innsbruck, Tirol 6020, Austria
e-mail: info@siegfried-peer.at

X. Wortsman, MD
Department of Radiology and Dermatology,
Faculty of Medicine, Institute for Diagnostic Imaging
and Research of the Skin and Soft Tissues,
Clinica Servet, University of Chile,
Almirante Pastene 150, Providencia, Santiago, Chile
e-mail: xwo@tie.cl, xworts@yahoo.com, www.sonoskin.com

X. Wortsman, G.B.E. Jemec (eds.), *Dermatologic Ultrasound with Clinical and Histologic Correlations*,
DOI 10.1007/978-1-4614-7184-4_7, © Springer Science+Business Media New York 2013

Table 7.1 ISSVA-Classification of vascular anomalies

	Vascular Malformations	
Vascular Tumors	Simple	Combined
Hemangioma	Arterial/ Capillary	Arteriovenous fistula
		Arteriovenous malformation
		Capillary-venous malformation
		Capillary-lymphatic-venous malformation
Other	Lymphatic	Lymphatic-venous malformation
Kaposiform hemangioendothelioma		Capillary-lymphatic-arteriovenous malformation
Hemangiopericytoma		
Pyogenic granuloma		
Spindle-cell hemangioendothelioma		
	Venous	

ISSVA International Society for the Study of Vascular Anomalies

classification by Mullicken/Glowacki was later modified by Burrows et al. [2], who introduced the subclassification of vascular malformations into high-flow and low-flow varieties. Currently, a generally accepted classification is recommended by the Society for the Study of Vascular Anomalies [3], which is based on the cellular origin of the lesion, its clinical behavior, and its flow characteristics. In that classification, proliferating neoplasms are distinguished from congenital vascular malformations (Table 7.1). In terms of treatment planning, additional differentiation of lesions into "high-flow," "intermediate-flow," and "low-flow," as proposed by Kawanabe et al. and Inoue et al., is of practical value [4, 5]. While in high-flow lesions a combination of transarterial catheter embolization with or without venous embolization or sclerotherapy is feasible, percutaneous sclerotherapy alone may be the best choice for slow-flow lesions.

Teaching Point
Hemangiomas are true endothelial tumors and malformations are developmental anomalies. Correct classification is mandatory to institute optimal treatment!

7.3 General Considerations for Imaging of Vascular Anomalies

Ultrasound imaging–which will be covered in more detail later in the chapter–is definitely the first line evaluation of hemangiomas and vascular malformations, although at times additional imaging studies are needed. While conventional radiography and computed tomography (CT) have only little impact, magnetic resonance imaging (MRI), digital subtraction angiography (DSA), and venous angiography are important adjuncts for the study of vascular anomalies.

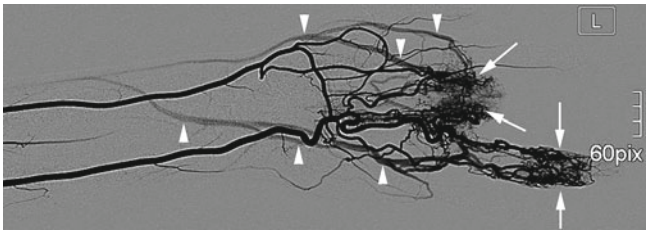

Fig. 7.1 Arterial DSA in a patient with recurrent arteriovenous malformation in the hand after previous surgery. Dense arterial nidus (*arrows*) and early venous drainage (*arrowheads*) is demonstrated

DSA is typically performed to define the arterial component of combined high-flow arteriovenous malformations and arteriovenous fistulae (Fig. 7.1). However, in hemangiomas and other types of malformations (low or intermediate flow), it is hardly indicated. The lesions that should undergo DSA can be judged through careful evaluation of the individual flow characteristics during examination with color Doppler and duplex ultrasound or MRI. Depending on the location of the lesion, DSA is performed with either retrograde or antegrade cannulation of the femoral artery and endovascular treatment is typically performed during the same session. In low-flow venous malformations, angiographic lesion visualization is performed through direct percutaneous phlebography for differential diagnosis or during sclerotherapy (Fig. 7.2). This topic is covered in more detail in the section on venous malformations.

A complete work up of a hemangioma is normally feasible with ultrasound alone, whereas an indication for MRI is in critical regions in deep lying hemangiomas, such as the pelvic area or in distinct locations of the craniofacial region (orbit, nasopharyngeal space, etc.). Typically, hemangiomas are hyperintense on T2-weighted images and isointense to muscle on T1-weighted sequences with marked enhancement after administration of a contrast agent (Fig. 7.3).

In cases with large or multiple vascular malformations we opt for a combination of ultrasound with MRI and magnetic resonance angiography (MRA) which can provide the complete extent of the lesion and its relationship to surrounding soft tissues (muscles, nerves, bone, tendons, subcutaneous tissue, and skin).

Teaching Point
Combined ultrasound and MRI is ideal for imaging of large and multiple vascular malformations. It combines functional and morphological information.

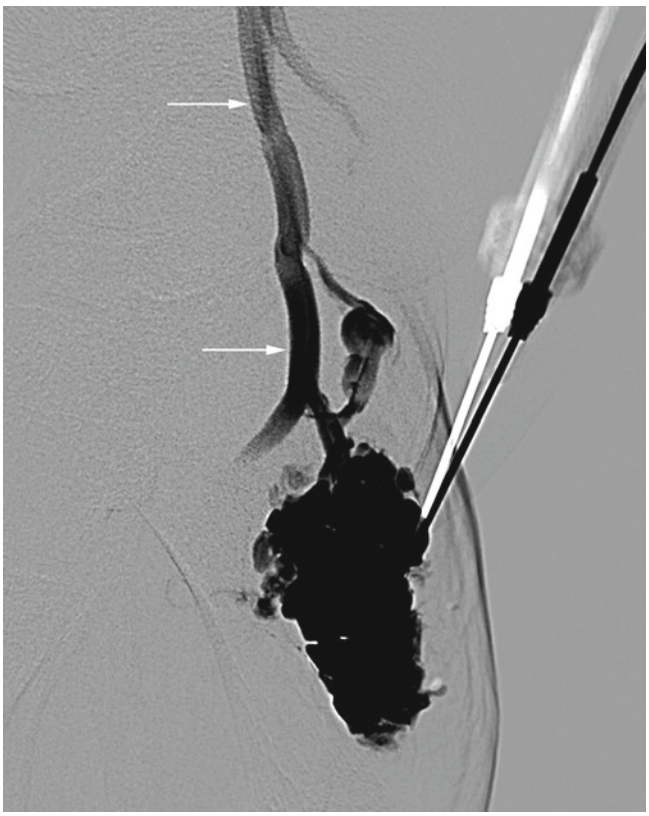

Fig. 7.2 Direct puncture phlebography in a patient with a venous malformation around the knee. Rapid venous drainage into the superficial femoral vein (*arrows*) is demonstrated

Vascular malformations are best distinguished from adjacent fatty structures on fat-suppressed sequences (STIR [short tau inversion recovery] or frequency selective fat saturation) (Fig. 7.4). Low-flow venous malformations consist of blood-filled pouches of variable size that appear as homogeneous hyperintense areas without flow void signals on T2-weighted or STIR images (Fig. 7.4). In contrast, high-flow malformations are characterized by signal voids in serpiginous structures corresponding to high-flow feeders (Fig. 7.5). A pathognomonic feature of venous malformations is intralesional phleboliths caused by stagnation of blood flow with partial thrombosis and calcification of clot, and can be detected as low signal foci on T2-weighted or STIR images (Fig. 7.6). MRA has gained widespread acceptance in the pre-treatment evaluation of vascular malformations (Fig. 7.7), and in terms of technique, it can be performed as conventional MRA, typically with fast 3D gradient-echo sequences in coronal orientation after intravenous injection of 0.1 mmol/kg of a gadolinium contrast agent. A more timely approach is contrast-enhanced time-resolved MRA, which combines high temporal resolution and the ability to visualize flow dynamics in a manner similar to that of DSA [6].

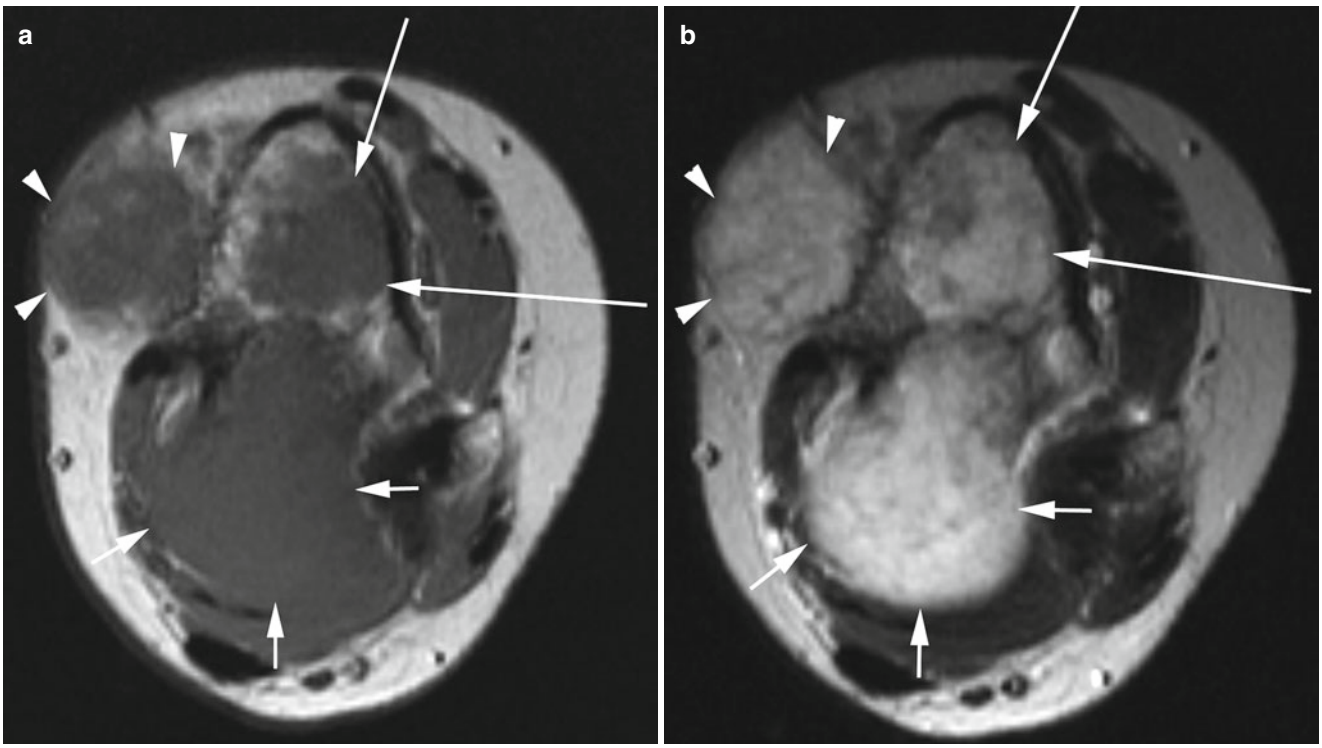

Fig. 7.3 (**a**–**c**) Multiple hemangiomas in a patient with Mafucci syndrome, located in the subcutaneous tissue (*arrowheads*), muscle (*short arrows*), and bone (*long arrows*). In the T1-weighted image (**a**) intramuscular hemangioma (*short arrows*) is isointense to muscle tissue and hardly discernible from normal muscle. In the T2-weighted image (**b**) the hemangiomas are hyperintense and thus more easily discerned from muscle but not so from subcutaneous tissue. In the T1-weighted image after administration of gadolinium contrast (**c**) all hemangiomas show marked inhomogeneous uptake

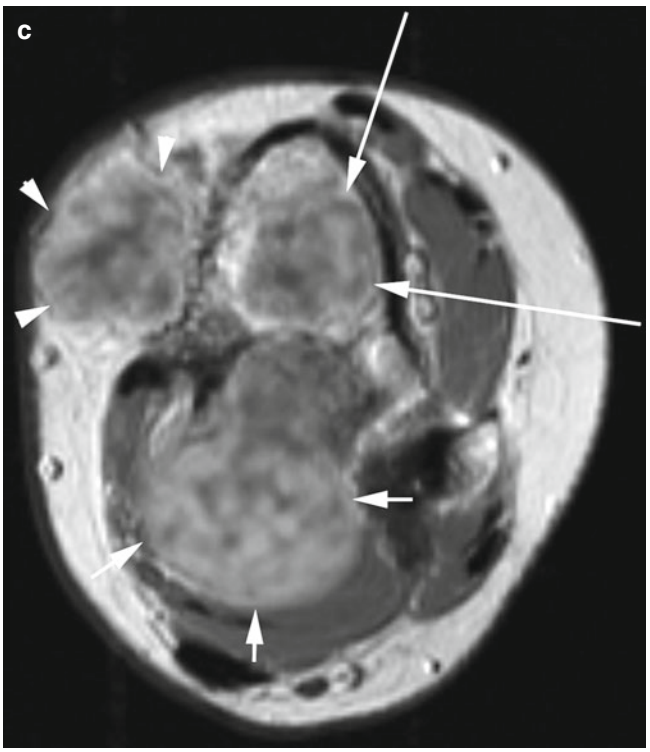

Fig. 7.3 (continued)

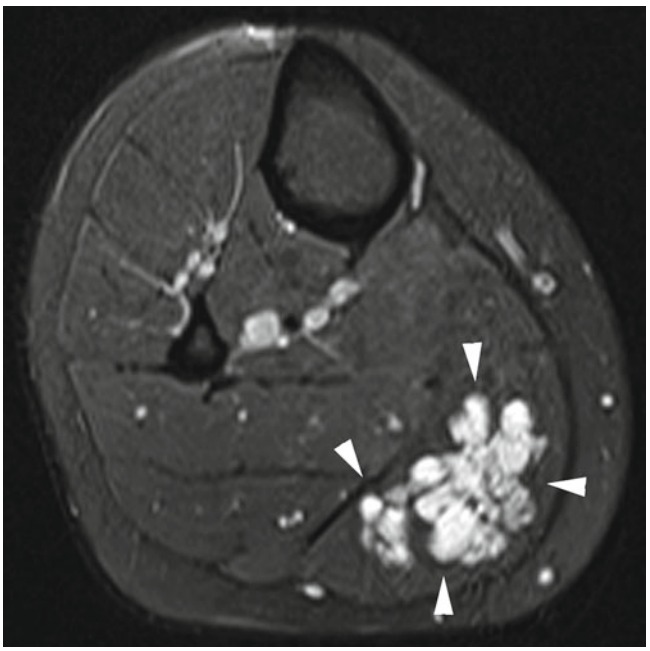

Fig. 7.4 Fat saturated transverse MR image in a patient with a slow-flow venous malformation (*arrowheads*) inside the medial gastrocnemius muscle. High signal intensity fluid-filled venous caverns are demonstrated

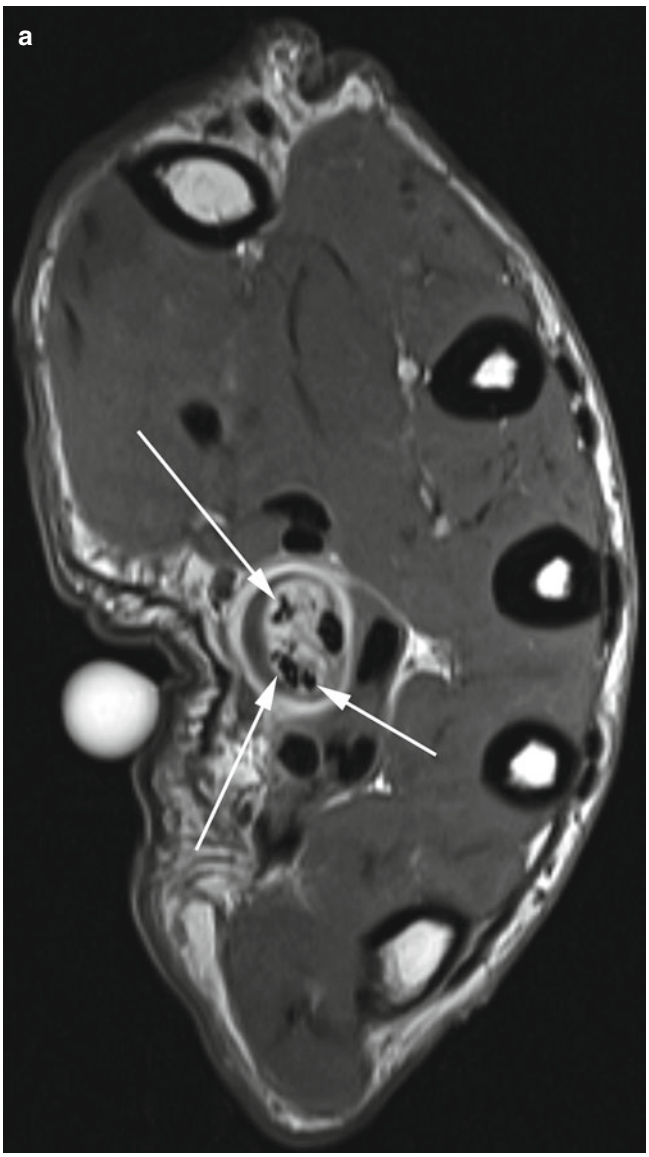

Fig. 7.5 (**a**) T1-weighted MR image in a patient with high-flow AVM. Multiple small signal voids (*arrows*) are seen inside carpal tunnel and adjacent to the flexor tendons. (**b**) Grey scale ultrasound image shows hypoechoic longitudinal vascular channels (*arrows*) interspersed with flexor tendons (*arrowheads*). (**c**) Duplex ultrasound demonstrates high arterial systolic flow velocity arterial feeder

Fig. 7.5 (continued)

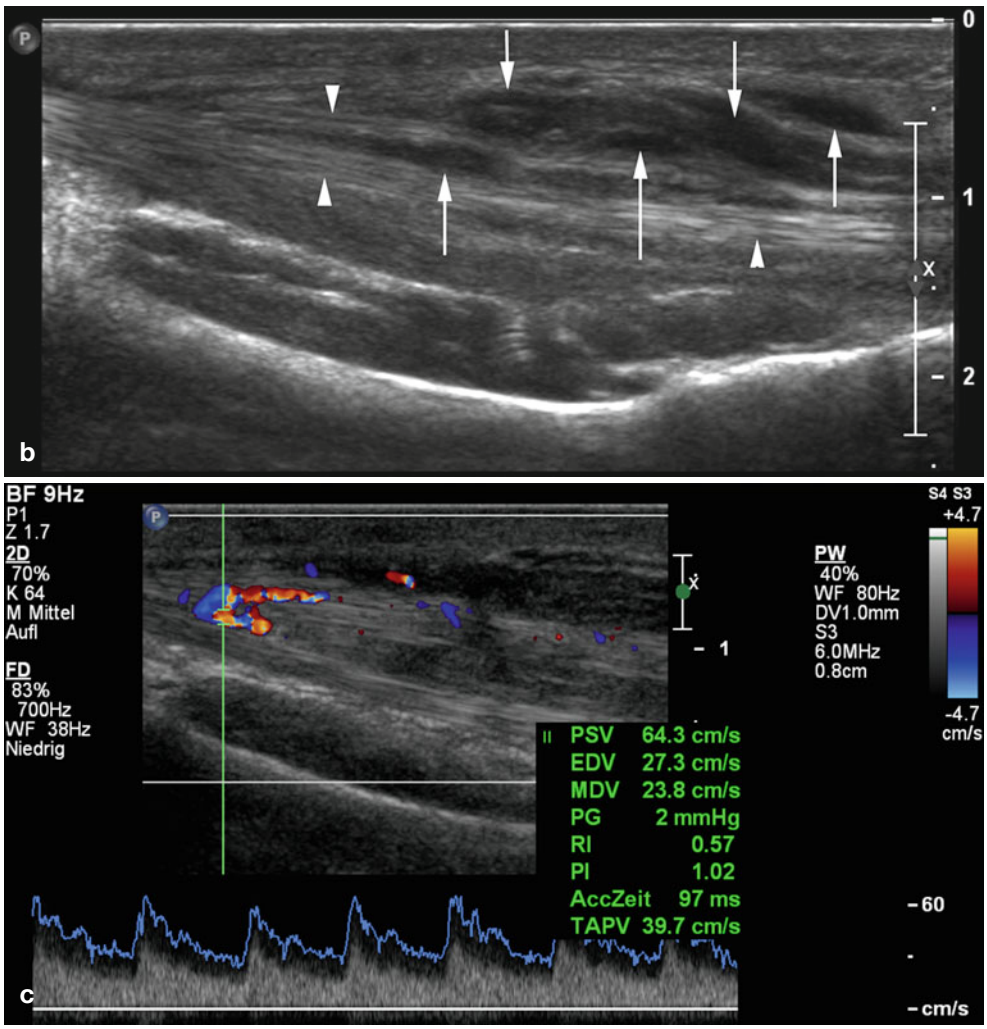

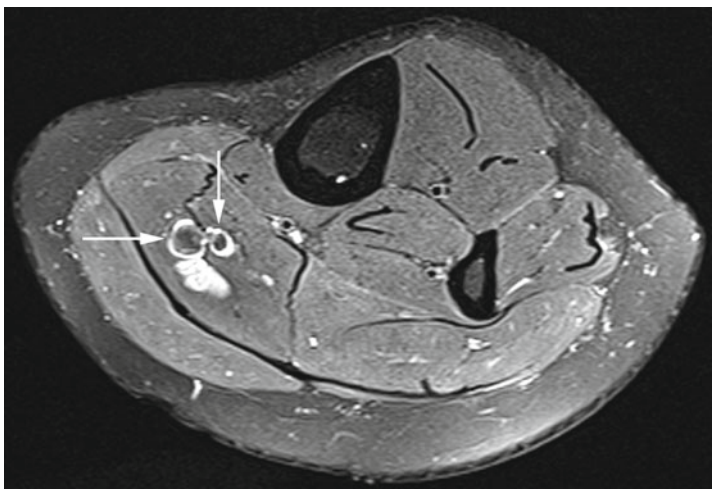

Fig. 7.6 Axial T2-weighted fat saturated MR image in a patient with a venous malformation. The venous malformation is of hyperintense fluid equivalent signal with two small roundish low signal structures = phleboliths (*arrows*)

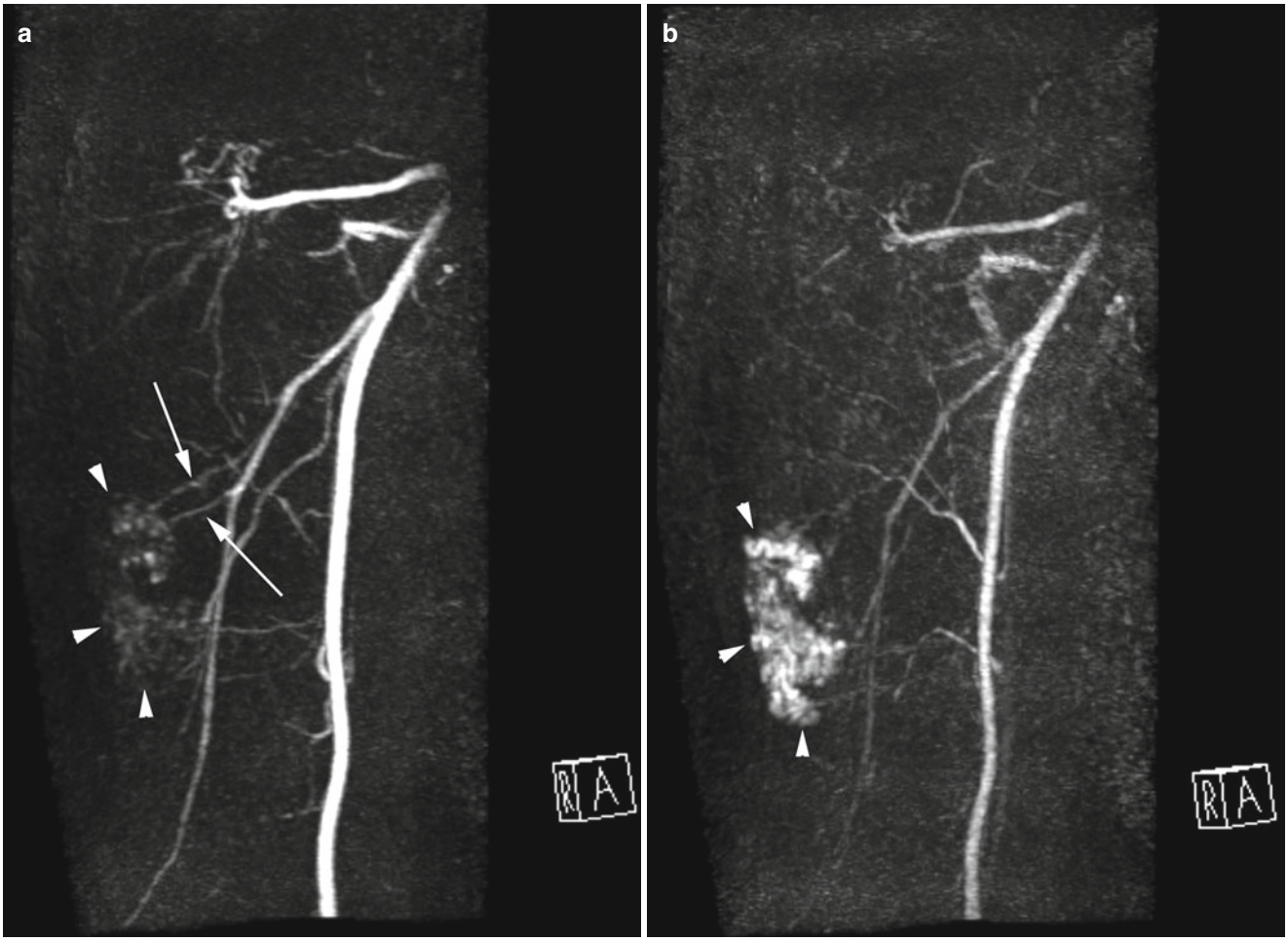

Fig. 7.7 (**a**–**b**) MR angiography of low-flow arteriovenous malformation (*arrowheads*): (**a**) early angiographic phase, (**b**) late angiographic phase. Slow progressive filling of malformation through small arterial feeders (*arrows* in **a**)

7.4 Ultrasound: General Considerations and Technical Requirements

A modern ultrasound equipment with high-resolution scanning software is well suited for the imaging of vascular anomalies. Companies combine special beam-forming software with broad-band transducers, which enhances the system's ability for high-resolution imaging and powerful color Doppler and duplex ultrasound. New matrix transducers deliver an ultra-thin, targeted ultrasound beam, which results in extraordinary tissue uniformity, while decreasing noise surrounding the region of interest. This results in fewer artifacts and better image quality in terms of resolution and image sharpness.

All lesions are initially evaluated in B mode and documented and measured in two orthogonal planes. We carefully evaluate the echotexture of the lesion (hypo- or hyperechoic, homogeneous or heterogeneous) and its borders toward surrounding tissue (well delineated, infiltrative, etc.). We especially look for any solid component, which is an important finding for the differentiation of a "true" tumor (i.e., hemangioma) and a malformation (Fig. 7.8). Any presence of cystic or tubular vascular channels inside a lesion is also recorded.

Color Doppler ultrasound is used to define the vascular pattern of a lesion (optimized low-flow color Doppler settings must be used to permit detection of small vessels, low-velocity arteries, and veins); hypovascular lesions are differentiated from lesions with little or dense vascularization. Vessel location is categorized as predominantly central, peripheral, or combined (central and peripheral). Vessel density inside a tumor is documented in a modified semi-quantitative fashion according to Dubois et al. [7, 8] (Fig. 7.9): the area of greatest vascular density is identified and color flow signals can be counted within an area of 1 cm^2. A vessel is defined as a linear or punctuate colored signal not associated with adjacent color noise (optimized setting of color gain is of utmost importance to reduce artifacts). Vessel density is defined as low (fewer than two vessels per square centimeter), moderate (2–4 vessels per square centimeter), or high (five or more vessels per square centimeter).

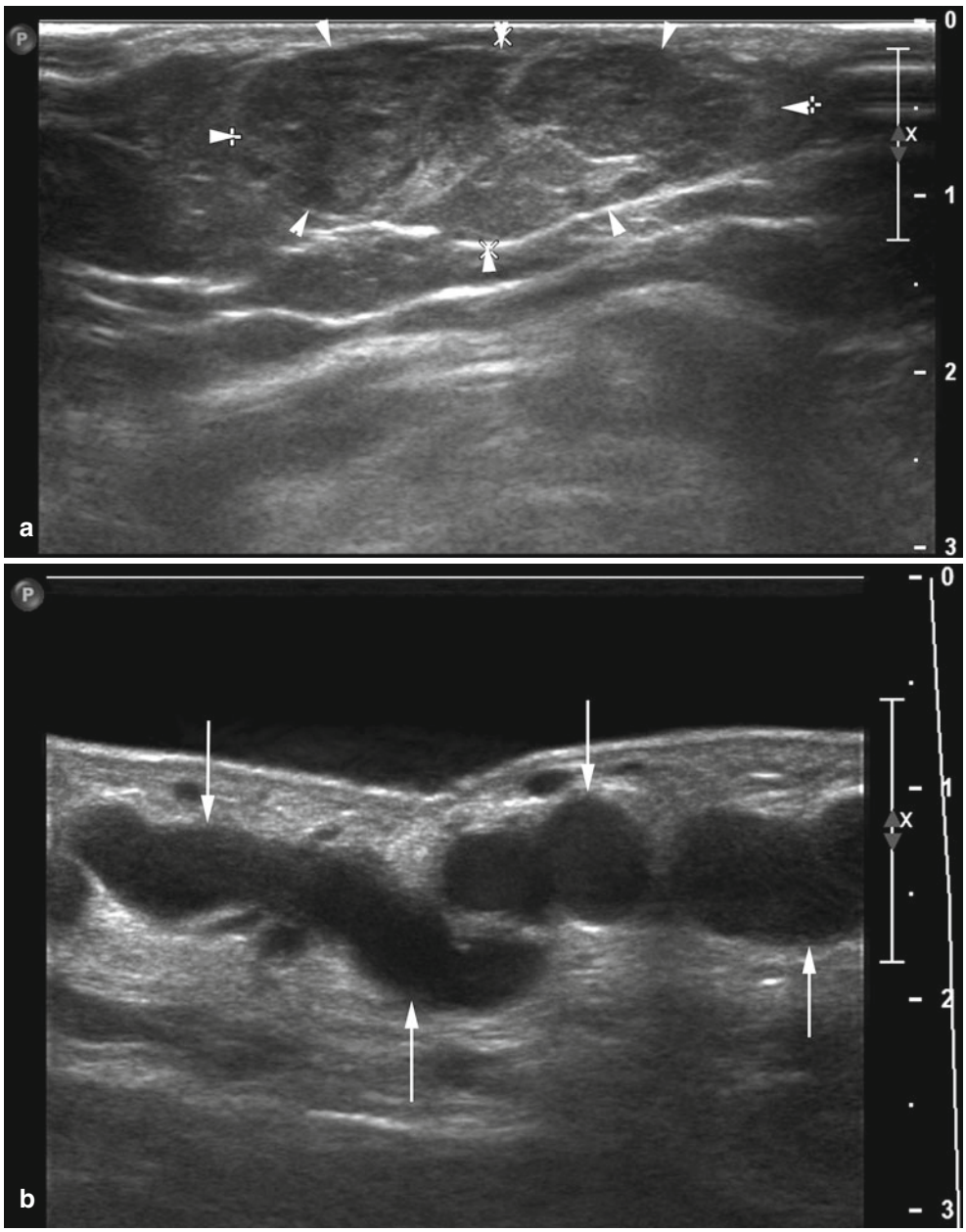

Fig. 7.8 (**a**) Typical hemangioma presenting a slightly hyperechoic and heterogeneous lobulated solid mass with distinct outer contour i.e., "true" soft-tissue tumor (*arrowheads*). (**b**) In contrast an arteriovenous malformation consisting of dilated anechoic vascular channels only (*arrows*) without a solid component

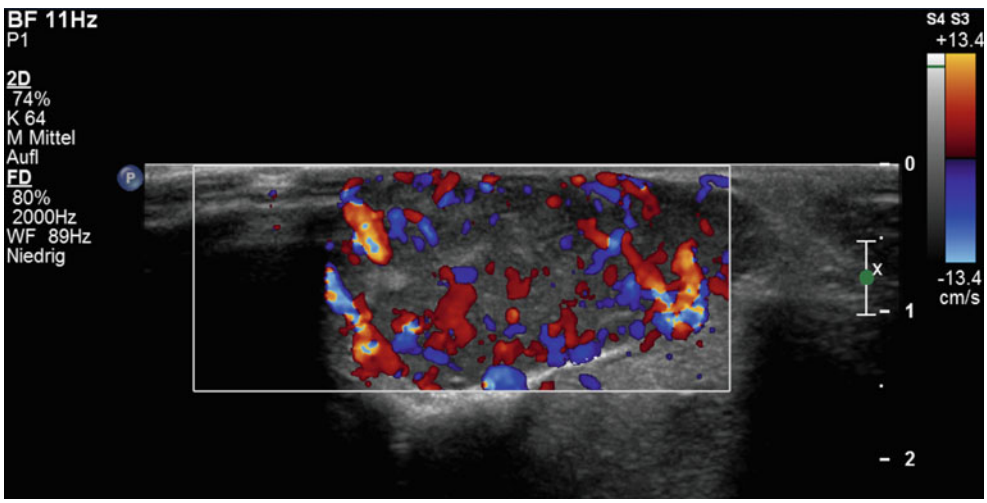

Fig. 7.9 Periorbital hemangioma in a child: a high vessel count of >5 is demonstrated inside a region of one square centimeter

An important additional tool for the differentiation of lesions with color Doppler ultrasound is the "compression test": with light compression of a lesion and subsequent release of transducer pressure a bidirectional venous flow can be induced inside the blood filled pouches of a venous malformation. A corresponding change of color encoding from red to blue is seen in the image, depending on transducer pressure (Fig. 7.10).

Teaching Point
A color Doppler ultrasound compression test shows bidirectional flow inside a lesion typical for venous malformations.

Duplex ultrasound and spectral wave analysis are used to characterize the types of vessels that exist inside the lesion: presence of venous/arterial vessels, arteriovenous shunts (high diastolic flow and resistive index (RI) below 0.5) (Fig. 7.11), and measurement of flow velocities to define a lesion as low, intermediate, or high flow. In the latter, flow volume or shunt volume across the lesion should also be evaluated (Fig. 7.12).

Contrast-enhanced ultrasound (CEUS) with application of microbubble contrast agents is not essentially new, but the value of CEUS for the examination of vascular anomalies has not been studied in detail [9]. Microbubbles circulate freely inside the body and constitute a true intravascular contrast agent; therefore, they permit analysis of tumor perfusion and regional blood flow. It is known from CEUS of soft-tissue tumors that microbubble-enhanced ultrasound can improve

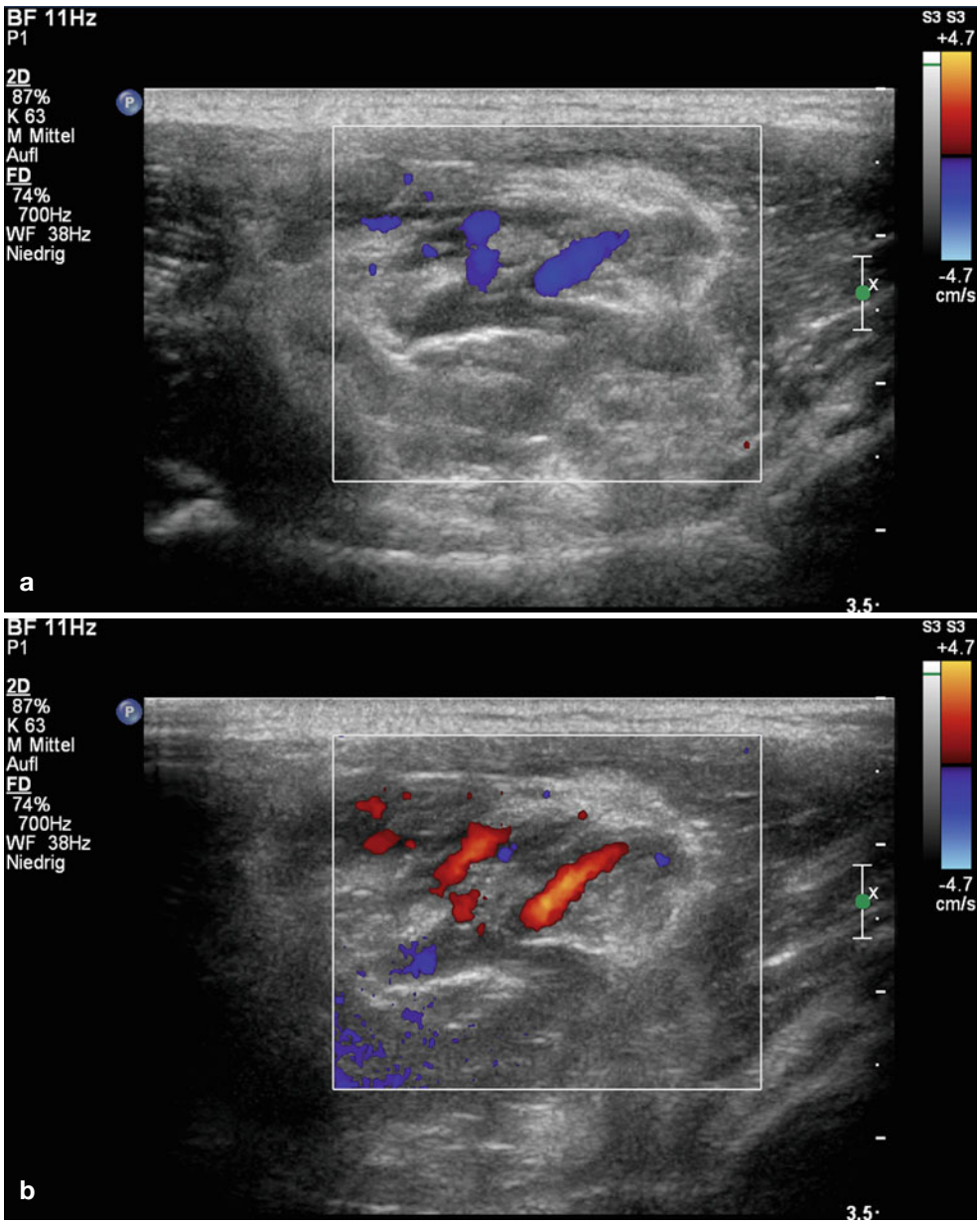

Fig. 7.10 (**a**, **b**) Compression ultrasound in a patient with low flow venous malformation: note color change from red to blue during the compression test confirming bidirectional venous flow

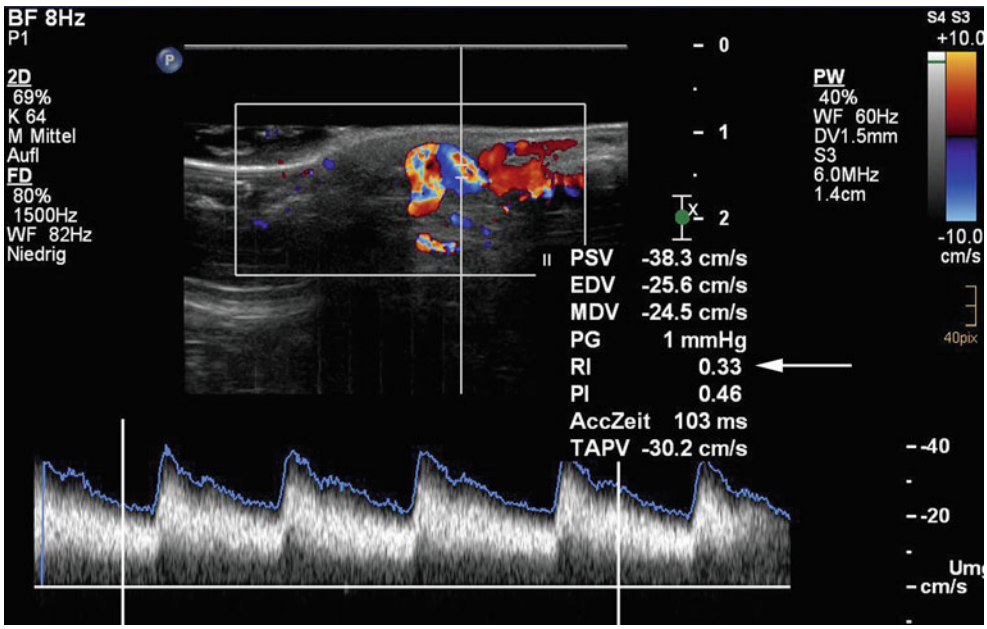

Fig. 7.11 High flow arteriovenous malformation, spectral wave analysis: demonstration of arteriovenous shunt flow with RI (resistive index) < 0.5 (*arrow*)

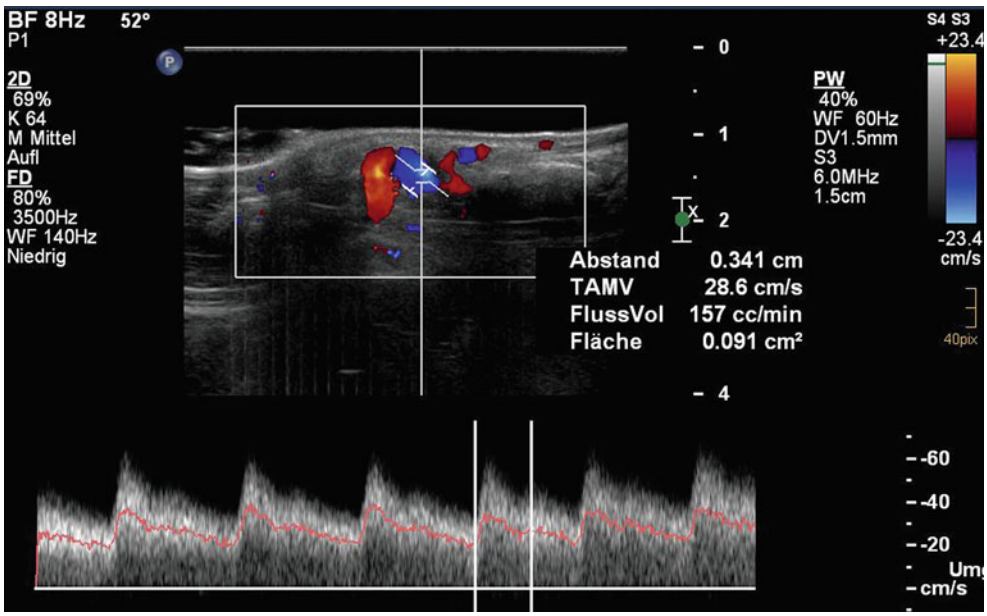

Fig. 7.12 Measurement of flow volume across the shunt: a shunt volume of 157 ml/min is demonstrated

the detection of perfusion compared with color Doppler ultrasound: in a substantial number of tumors that appear only sparsely vascularized with color Doppler ultrasound, CEUS gives a completely different impression by depicting more vessels and more intense perfusion. In particular, CEUS may offer improved detection of small arteriovenous shunts, which might have an impact on the grading of vascular anomalies into low-flow or intermediate/high-flow subtypes, and especially on evaluation of therapeutic success (extent of devascularization) after sclerotherapy (Fig. 7.13).

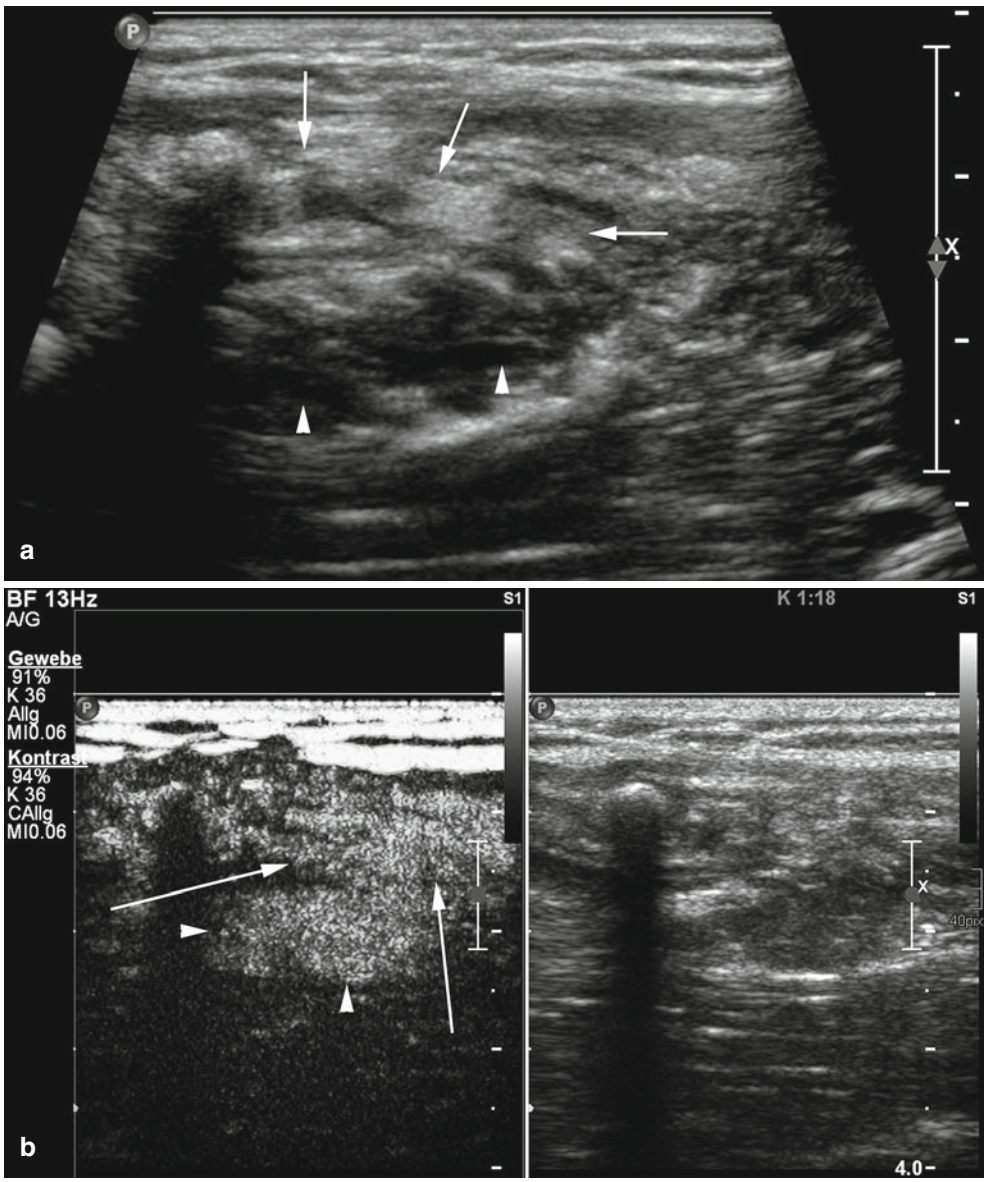

Fig. 7.13 (**a**) Grey scale ultrasound image in a patient with venous malformation after sclerotherapy. While some deep-lying blood-filled venous caverns are seen (*arrowheads*), the superficial part of the malformation seems largely fibrotic (*arrows*) corresponding with at least partial success. (**b**) Contrast-enhanced ultrasound image in the same patient (split screen image, left: tissue harmonic imaging mode, right: corresponding grey scale image): note dense contrast enhancement in venous caverns (*arrowheads*) and the superficial part of the malformation also (*arrows*) which was considered fibrotic on grey scale images

7.5 Hemangioma

7.5.1 Clinical Background

Hemangiomas of infancy are benign vascular tumors typically present at birth. In contrast to vascular malformations, hemangiomas show an initial proliferative phase, followed by slow involution during early childhood. A second proliferative phase may precede regression in some hemangiomas. The time at which regression occurs differs substantially: around 50 % of hemangiomas regress completely by the age of 5 years and almost 90 % by the age of 9–10 years. Despite involution, the prognosis of a hemangioma can be disappointing resulting from cosmetic impairment, and furthermore, hemangiomas may pose a clinical problem, depending on their location: perioral, perianal, or orbital hemangiomas may bleed, impair vision, or cause other problems [10]. In contrast to simple hemangiomas, an extensive imaging work-up is advocated in the latter type. Ultrasound may often suffice, but for particularly deep-lying hemangiomas (such as lesions inside the orbit), MRI may be a better choice. In contrast to vascular malformations, most hemangiomas do not need invasive treatment.

7.5.2 Ultrasound Characteristics

Hemangiomas differ in their appearance according to the phase; thus, lesions in the proliferative stage appear as hypoechoic hypervascular ill-defined structures on ultrasound

that become heterogeneous (i.e., hypoechoic and hyperechoic areas) during partial involution. The intensity of the vascularity that can be detected within the lesions also varies during the different degrees of involution going from hypervascular to hypovascular. In the end stage of involution, hemangiomas tend to show hyperechogenicity and hypo- or lack of vascularity (Figs. 7.14, 7.15, 7.16, 7.17, 7.18, 7.19, 7.20, 7.21, 7.22, 7.23, 7.24, and 7.25).

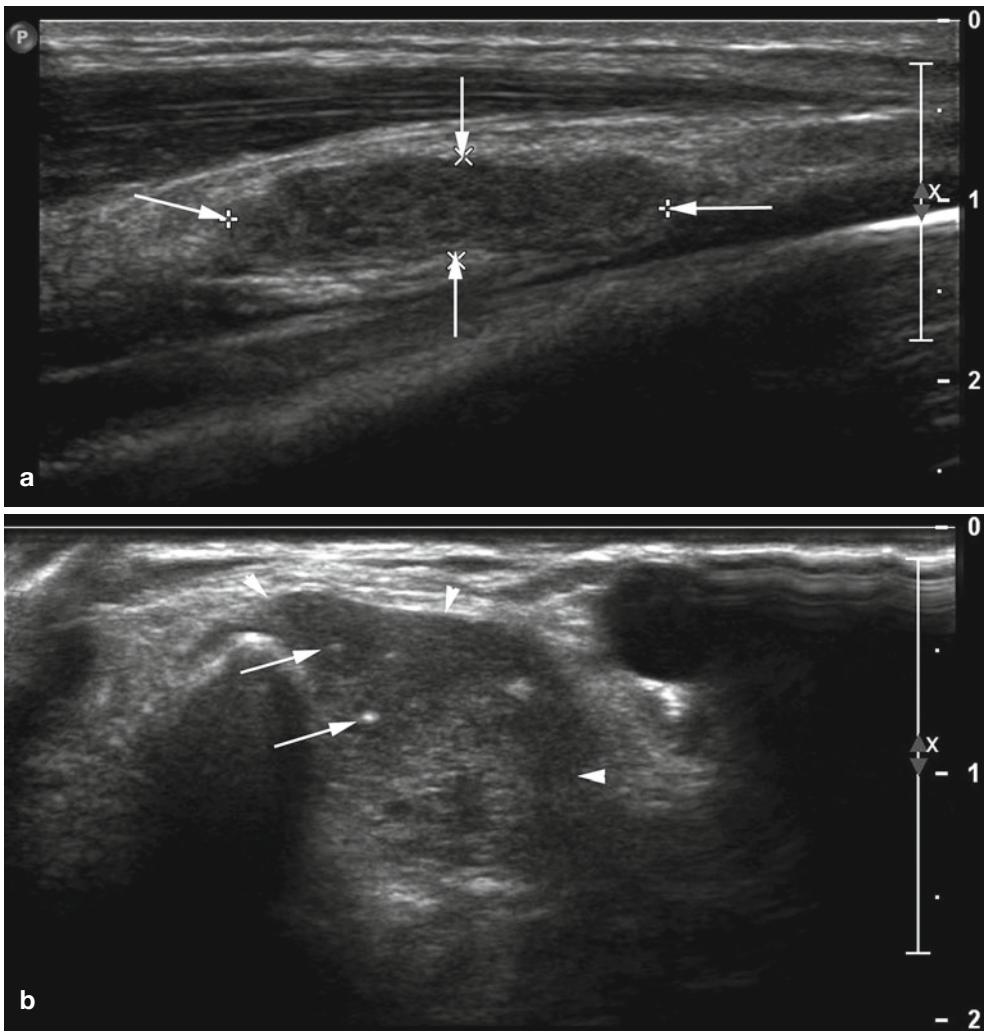

Fig. 7.14 (**a**) Hemangioma with distinct outer border and relatively homogeneous texture, slightly hyperechoic to muscle. (**b**) Hemangioma in another patient with distinct capsule (*arrowheads*) but more inhomogeneous texture and tiny calcific foci (*arrows*)

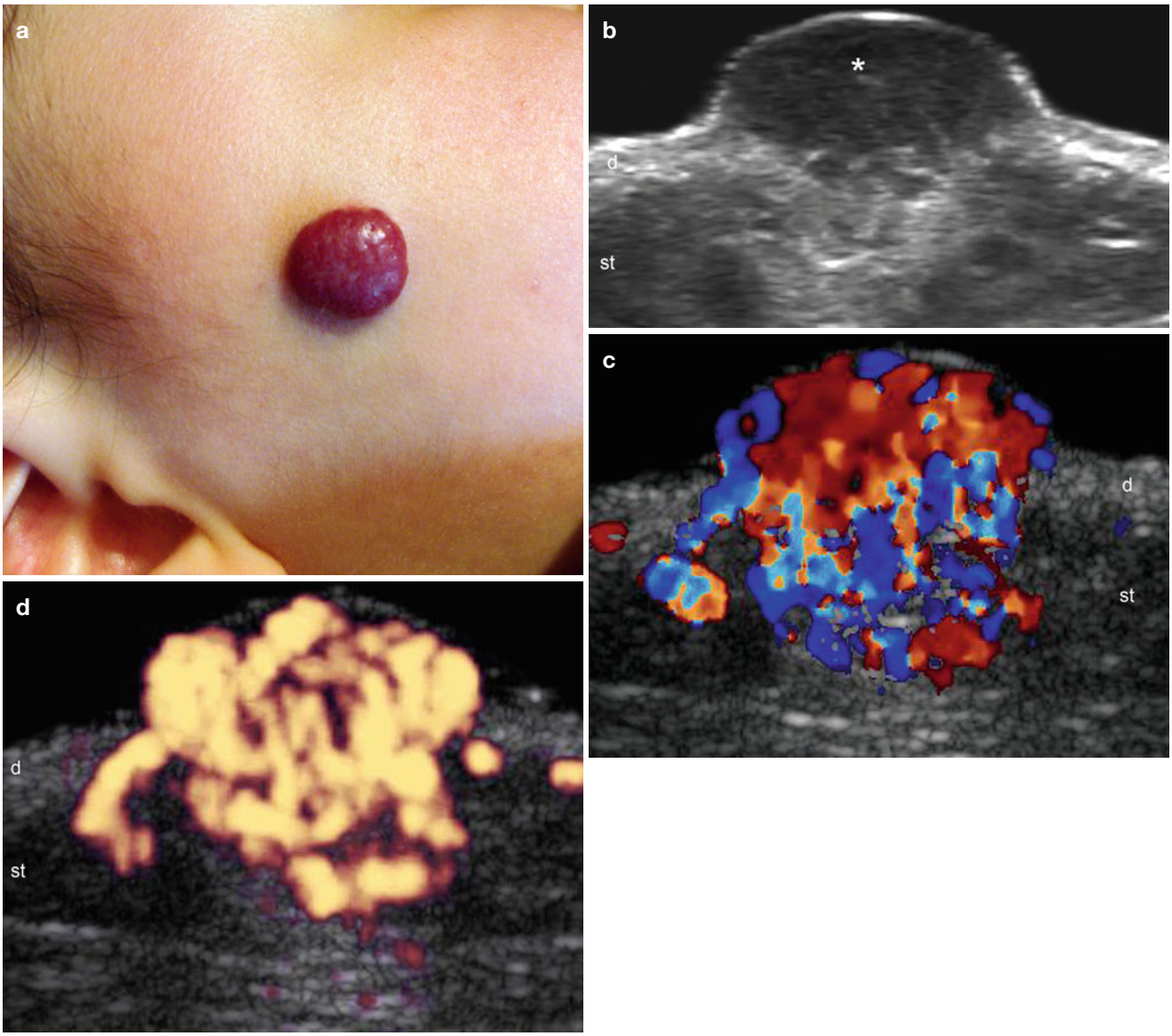

Fig. 7.15 (**a**–**f**) Hemangioma (proliferative phase). (**a**) Clinical erythematous bump in the right cheek. (**b**) Grey scale ultrasound image (transverse view) shows hypoechoic tissue (*) in the dermis that displaces the epidermis upward. Hyperechogenicity of the subcutaneous tissue is also detected. (**c**) Color Doppler ultrasound image and (**d**) power Doppler ultrasound image (transverse view) demonstrates prominent vascularity in the lesional area. (**e**, **f**) Color Doppler ultrasound spectral curve analysis (transverse view) shows arterial (**e**) and venous (**f**) flow within the mass. *Abbreviations*: *d* dermis, *st* subcutaneous tissue

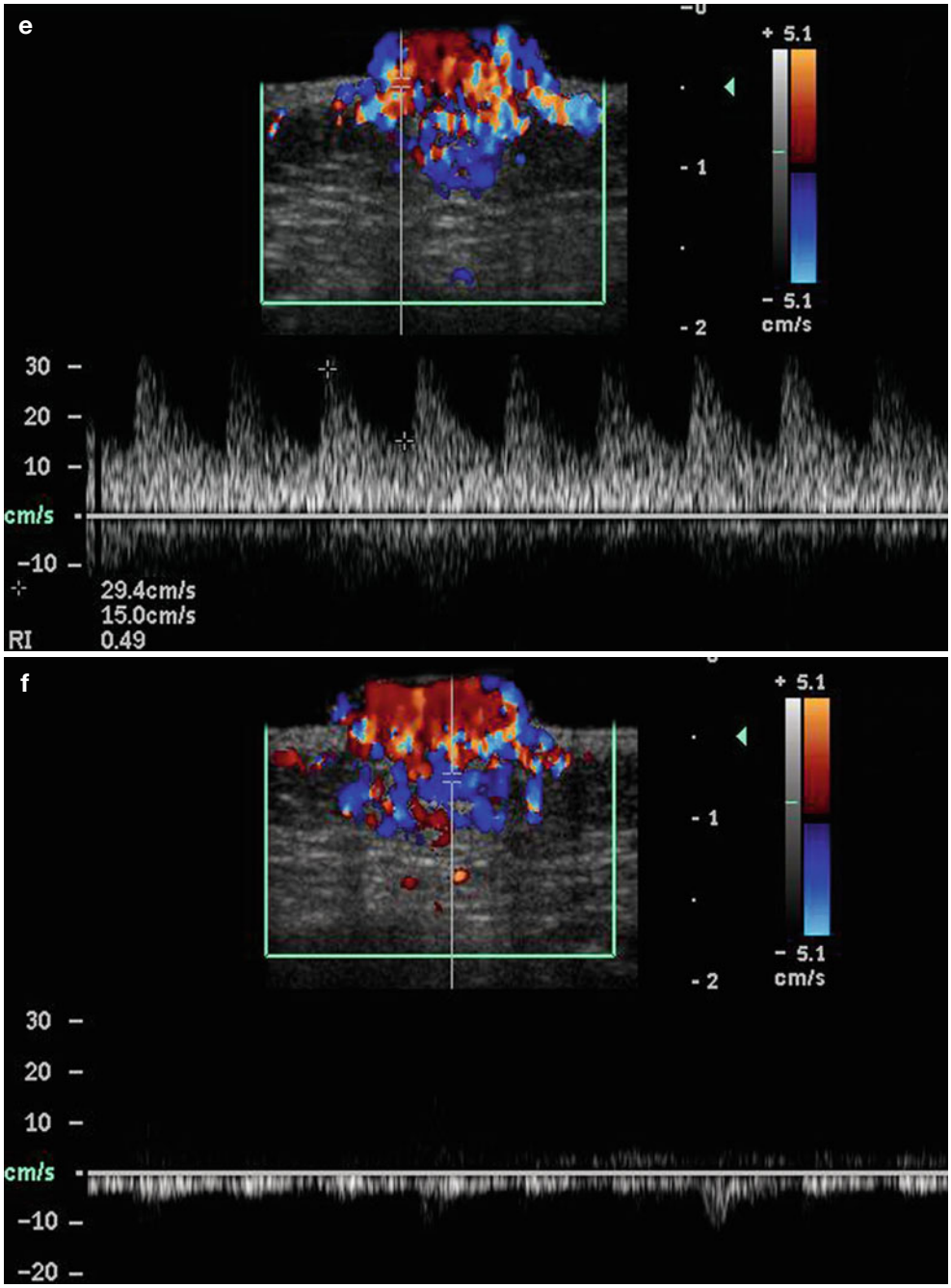

Fig. 7.15 (continued)

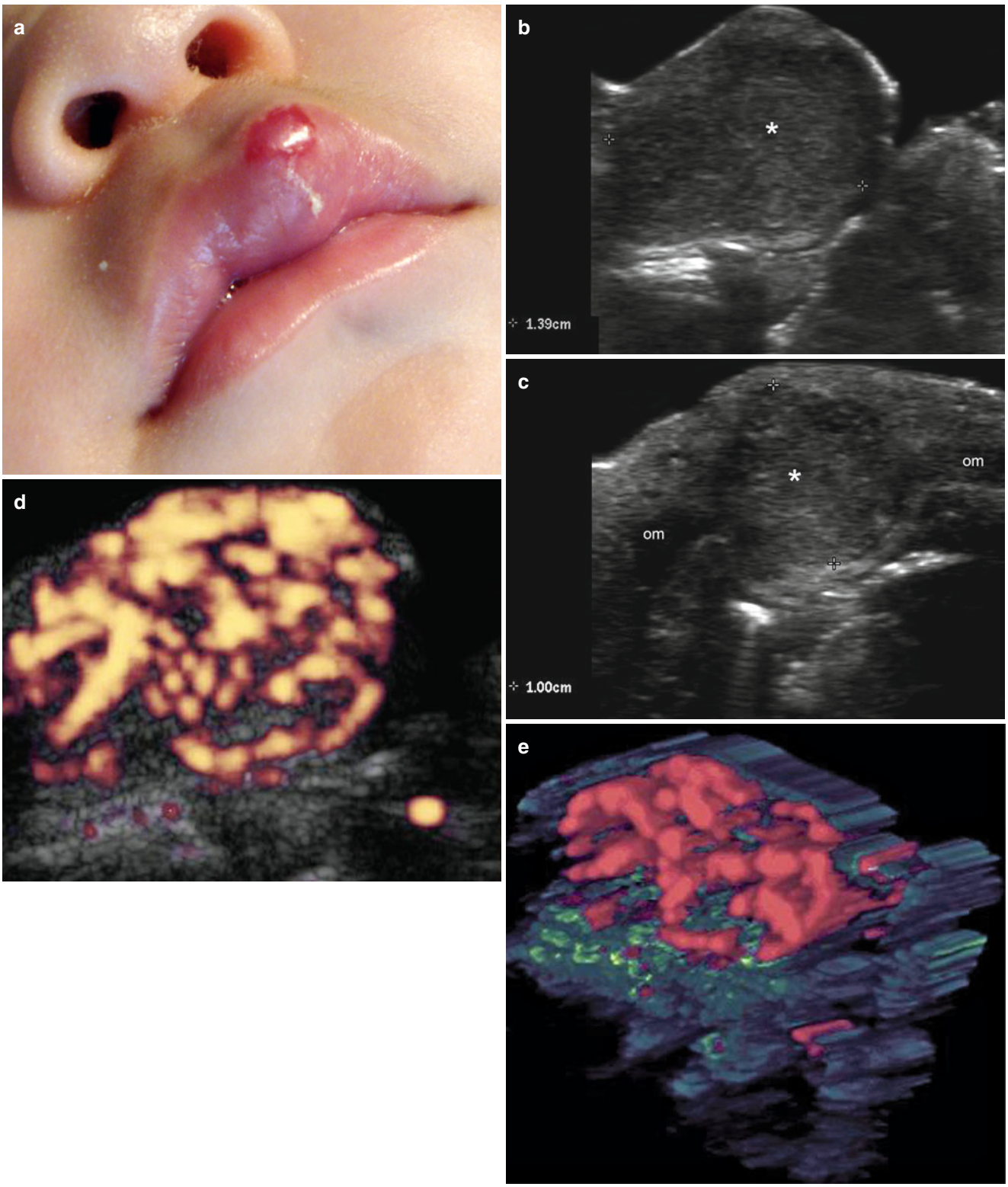

Fig. 7.16 (**a**–**g**) Hemangioma (proliferative phase) (**a**) Clinical lesion shows erythematous swelling in the upper lip. (**b**) Grey scale ultrasound image (longitudinal view) demonstrates 1.39 cm long hypoechoic mass (*) in the upper lip that involves the cutaneous layers and the orbicularis muscle. (**c**) Grey scale ultrasound image (transverse view) shows 1.0 cm depth hypoechoic mass. Notice the discontinuity of the orbicularis muscle (*om*). (**d**) Power Doppler ultrasound image and (**e**) 3D reconstruction power angio (longitudinal view) demonstrates the prominent vascularity within the mass. (**f**, **g**) Spectral curve analysis shows the arterial (**f**) and arterialized venous flow shunts (**g**) in the same mass

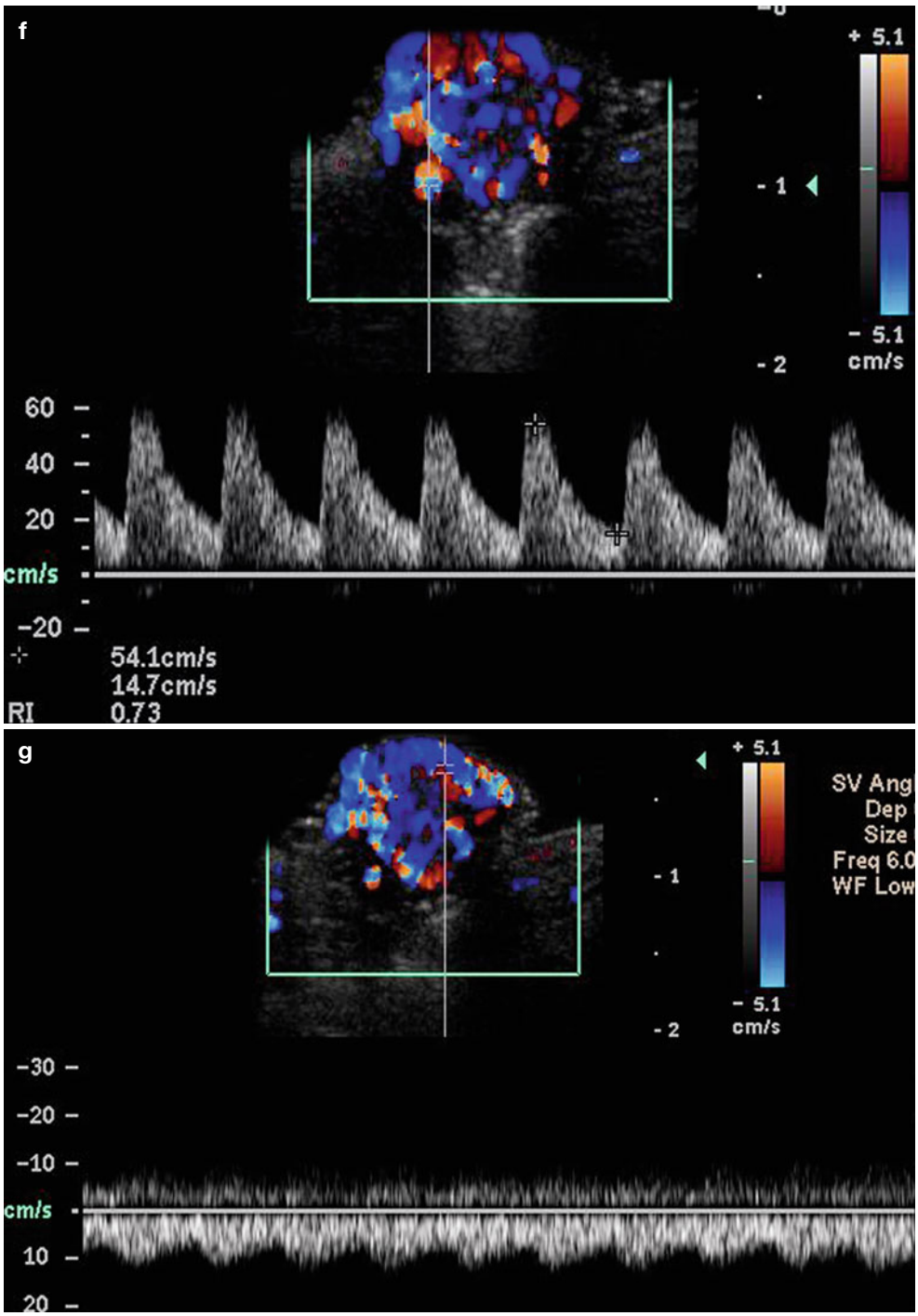

Fig. 7.16 (continued)

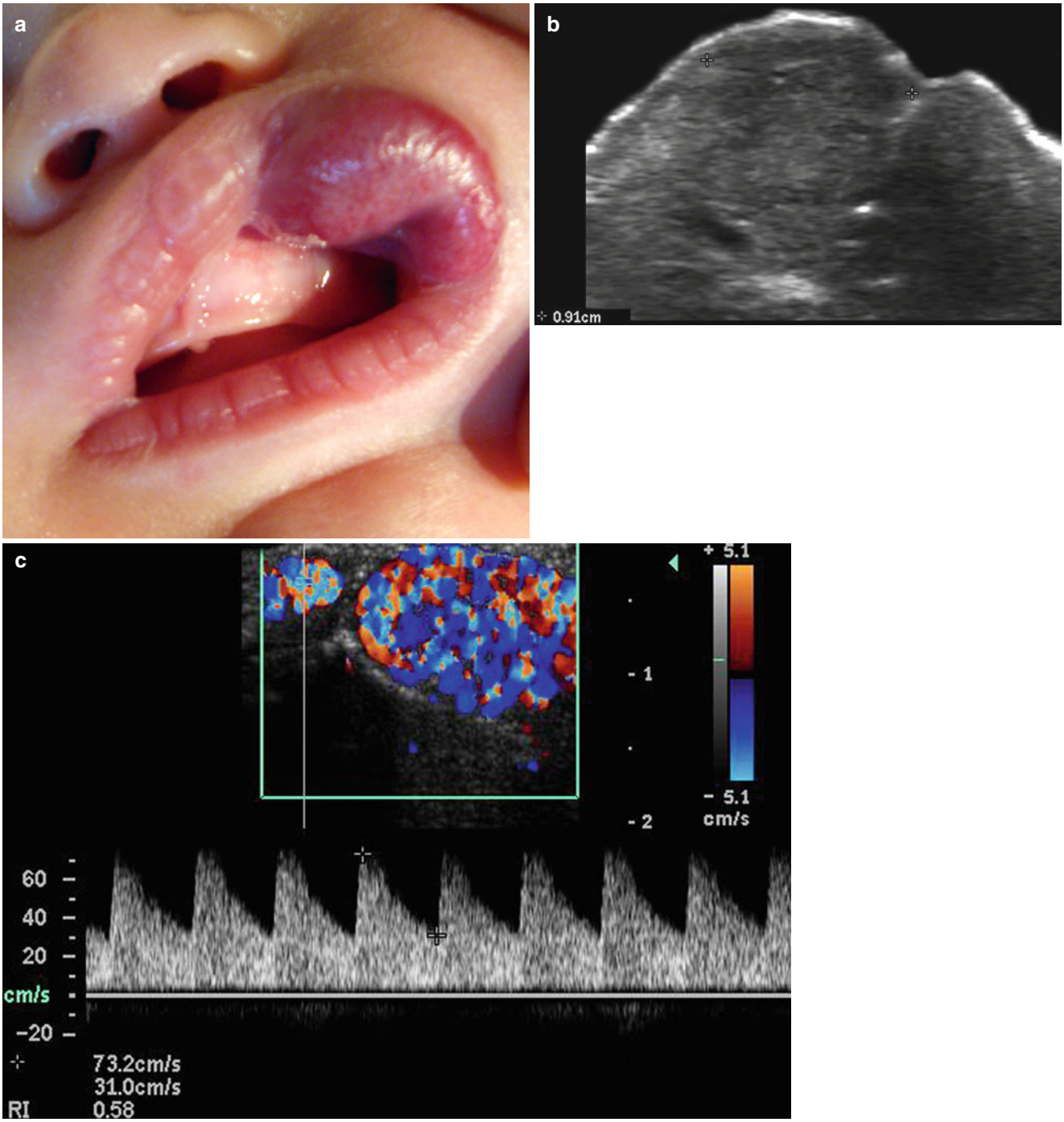

Fig. 7.17 (**a**–**d**) Hemangioma (proliferative phase). (**a**) Clinical image shows erythematous swelling, retraction, and deformation of the upper lip. (**b**) Grey scale ultrasound image (longitudinal view) demonstrates 0.9 cm long ill-defined hypoechoic mass that affects the cutaneous layers and the orbicularis oris muscle. (**c**) Color Doppler ultrasound spectral curve analysis (transverse view) shows a high peak of systolic velocity within the arterial vessels (73.2 cm/s). (**d**) Power angio 3D reconstruction demonstrates the hypervascularity of the mass

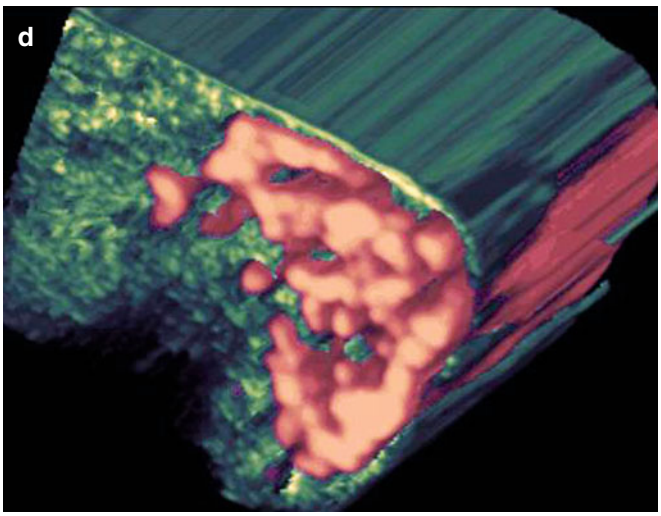

Fig. 7.17 (continued)

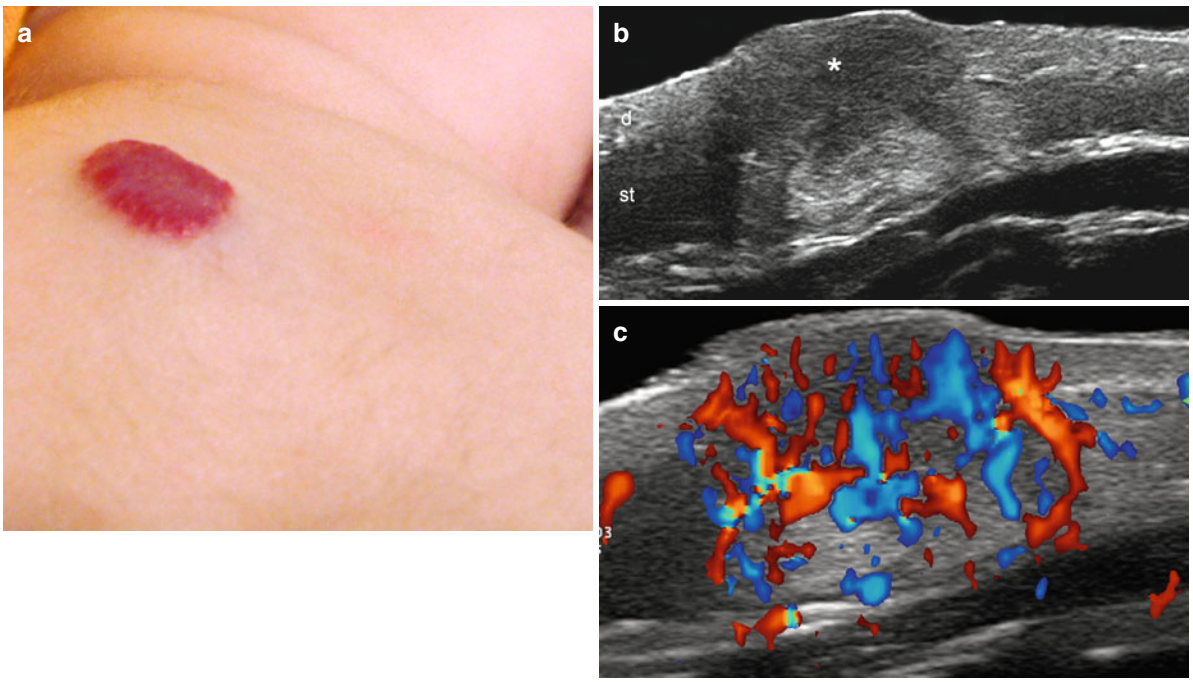

Fig. 7.18 (**a**–**c**) Hemangioma (mostly proliferative phase). (**a**) Clinical lesion shows erythematous bump in the dorsal region. (**b**) Grey scale ultrasound image (transverse view) demonstrates a mass with prominent hypoechogenicity (*) in the dermis and upper subcutaneous tissue. Hyperechogenicity is detected in the lower subcutaneous tissue. (**c**) Color Doppler ultrasound image (transverse view) shows hypervascularity within the mass. *Abbreviations*: *d* dermis, *st* subcutaneous tissue

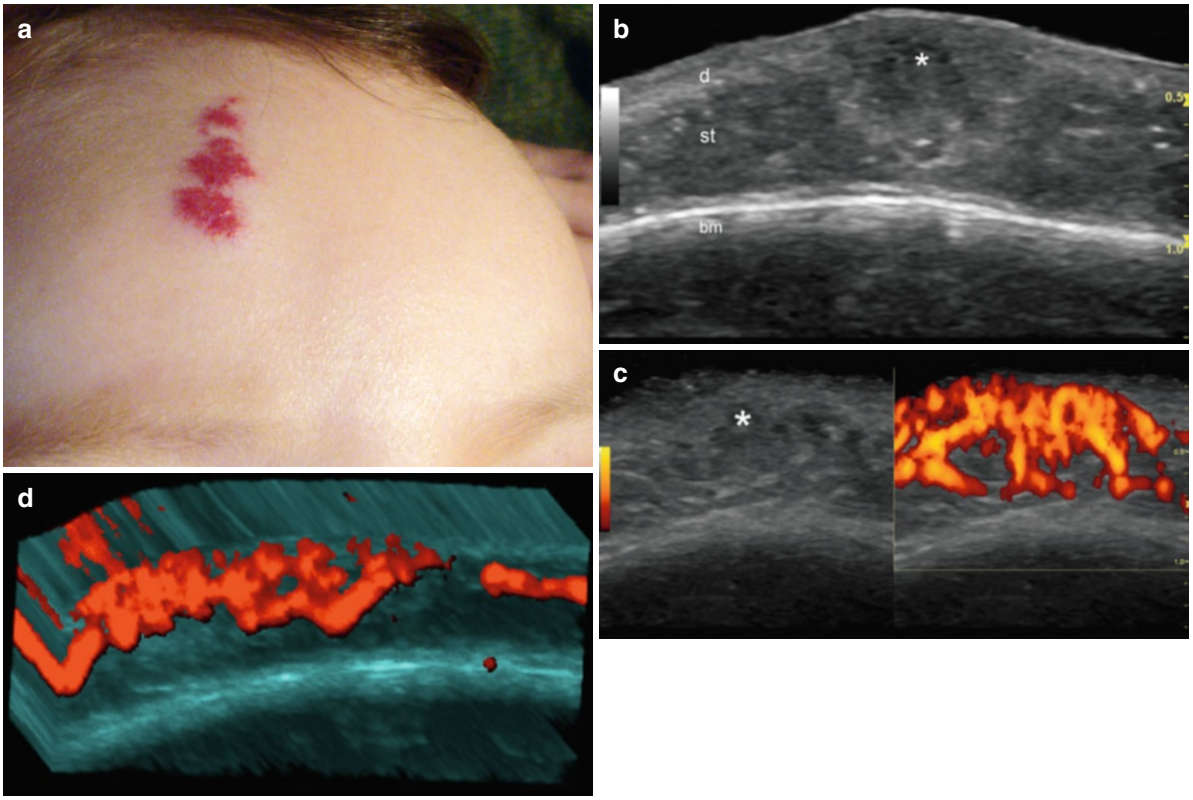

Fig. 7.19 (**a**–**d**) Hemangioma (mostly proliferative phase). (**a**) Clinical image demonstrates an erythematous swelling in the right frontal region. (**b**) Grey scale ultrasound image (transverse view) shows ill-defined hypoechoic lesion (*) that affects the dermis and upper subcutaneous tissue. (**c**) Grey scale ultrasound image and power. Doppler ultrasound image (comparative images) demonstrates prominent vascularity within the mass (*). (**d**) Power angio 3D reconstruction (5–8 s) of the lesion. *Abbreviations*: *d* dermis, *st* subcutaneous tissue, *bm* bony margin of the skull

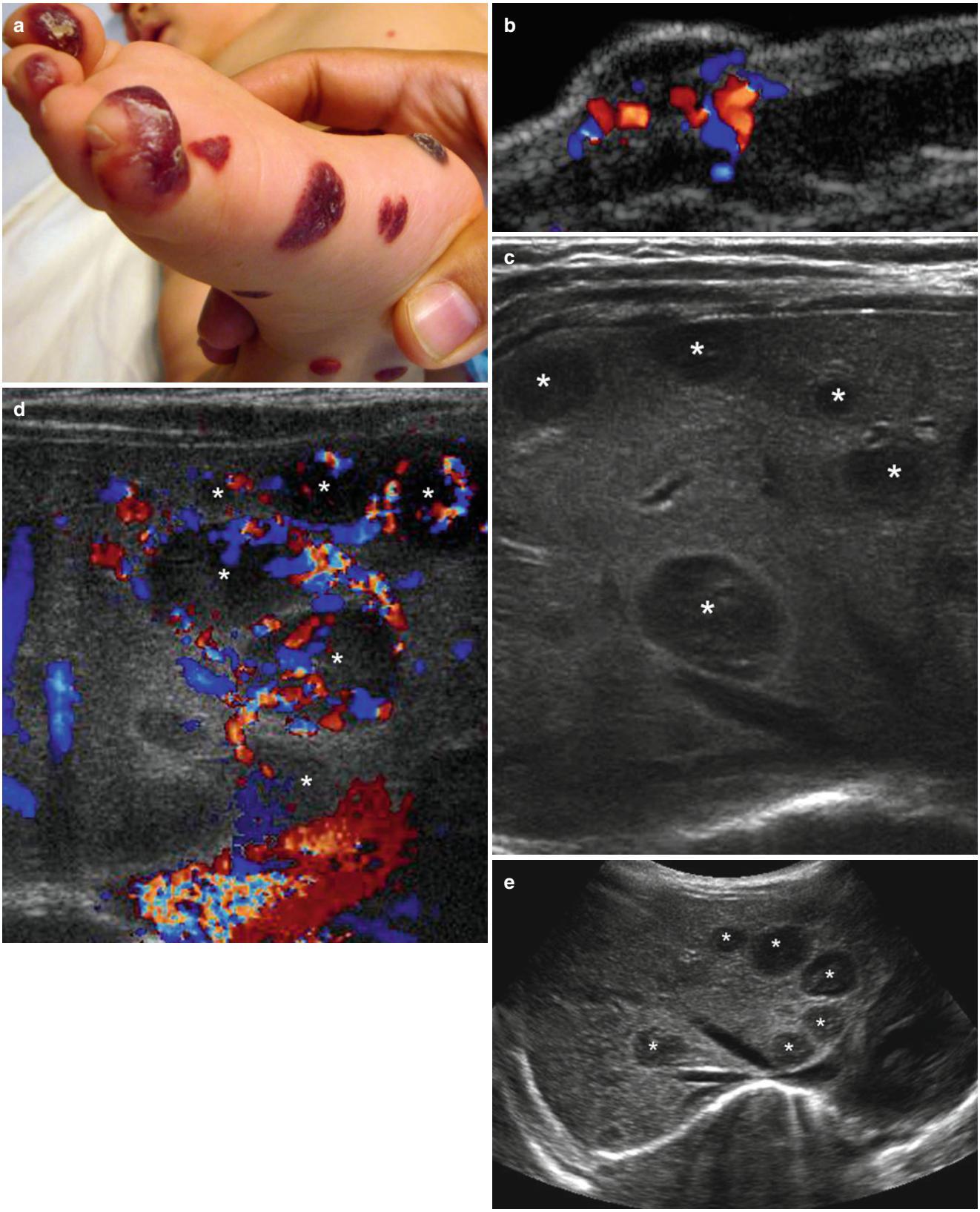

Fig. 7.20 (**a**–**e**) Multiple cutaneous and hepatic hemangiomatosis (proliferative phase). (**a**) Clinical image shows multiple cutaneous hemangiomas in the right foot. (**b**) Grey scale ultrasound image (transverse view) of one of the lesions demonstrates hypoechoic mass affecting dermis and subcutaneous tissue with increased blood flow. (**c**) Grey scale ultrasound image of the liver (transverse view) in the same patient shows multiple hypoechoic nodules suggestive of hemangiomas. (**d**) Color Doppler ultrasound image (transverse view) demonstrates increased vascularity in the periphery and within the hepatic nodules (*). (**e**) Grey scale ultrasound image (extended transverse axis) shows a wider view of the multiple hepatic nodules (*)

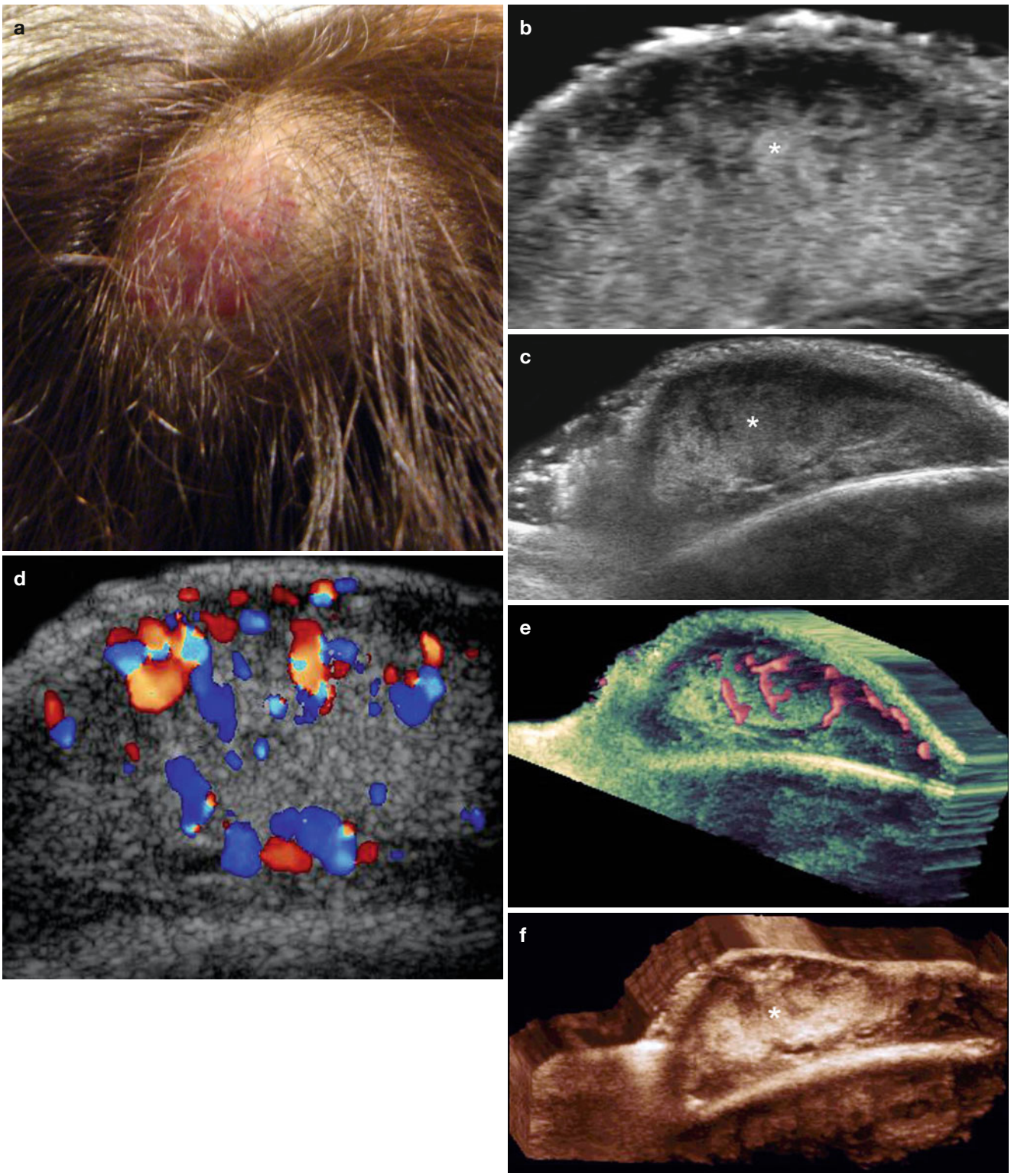

Fig. 7.21 (**a**–**f**) Hemangioma (partial regression phase). (**a**) Clinical erythematous lesion in the scalp. (**b**) Grey scale ultrasound image (transverse view) and (**c**) Grey scale ultrasound image (extended transverse view) shows a mixed echogenicity ill-defined mass (*) that involve dermis and subcutaneous tissue (*). (**d**) Color Doppler ultrasound image (transverse view) demonstrates increased vascularity within the mass. Nevertheless, the blood flow is less prominent compared with the previous cases in proliferative phase. (**e**) 3D power and (**f**) grey scale reconstructions of the hemangioma

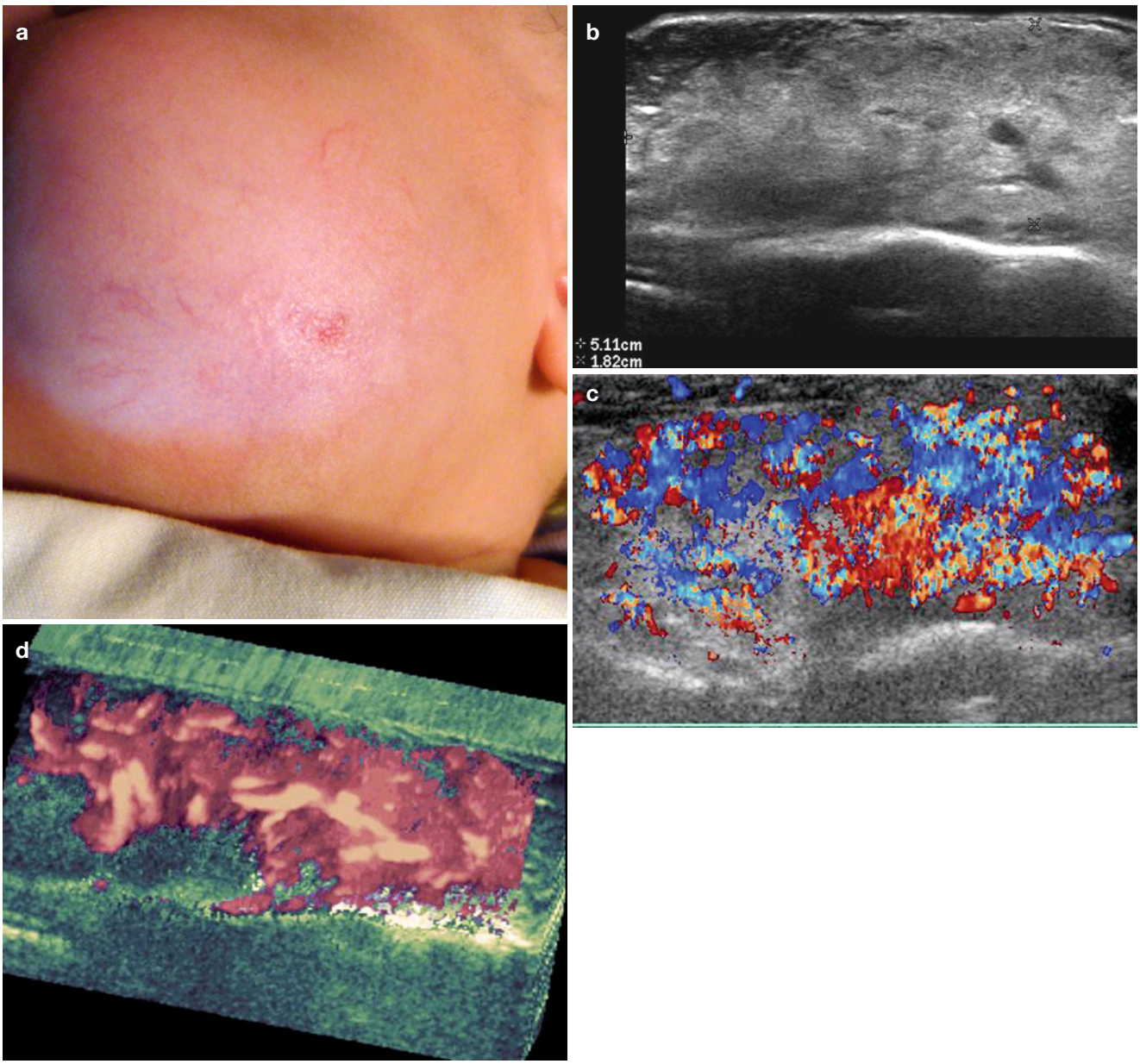

Fig. 7.22 (**a**–**d**) Hemangioma (partial regression phase). (**a**) Clinical erythematous lesion in the left cheek. (**b**) Grey scale ultrasound image (transverse view) that shows 5.11 × 1.82 cm Ill-defined heterogeneous mass that involves dermis, subcutaneous tissue and the masseter muscle. (**c**) Color Doppler ultrasound image (transverse view) and (**d**) 3D Power angio reconstruction (transverse view, 5–8 s) demonstrate increased vascularity within the mass

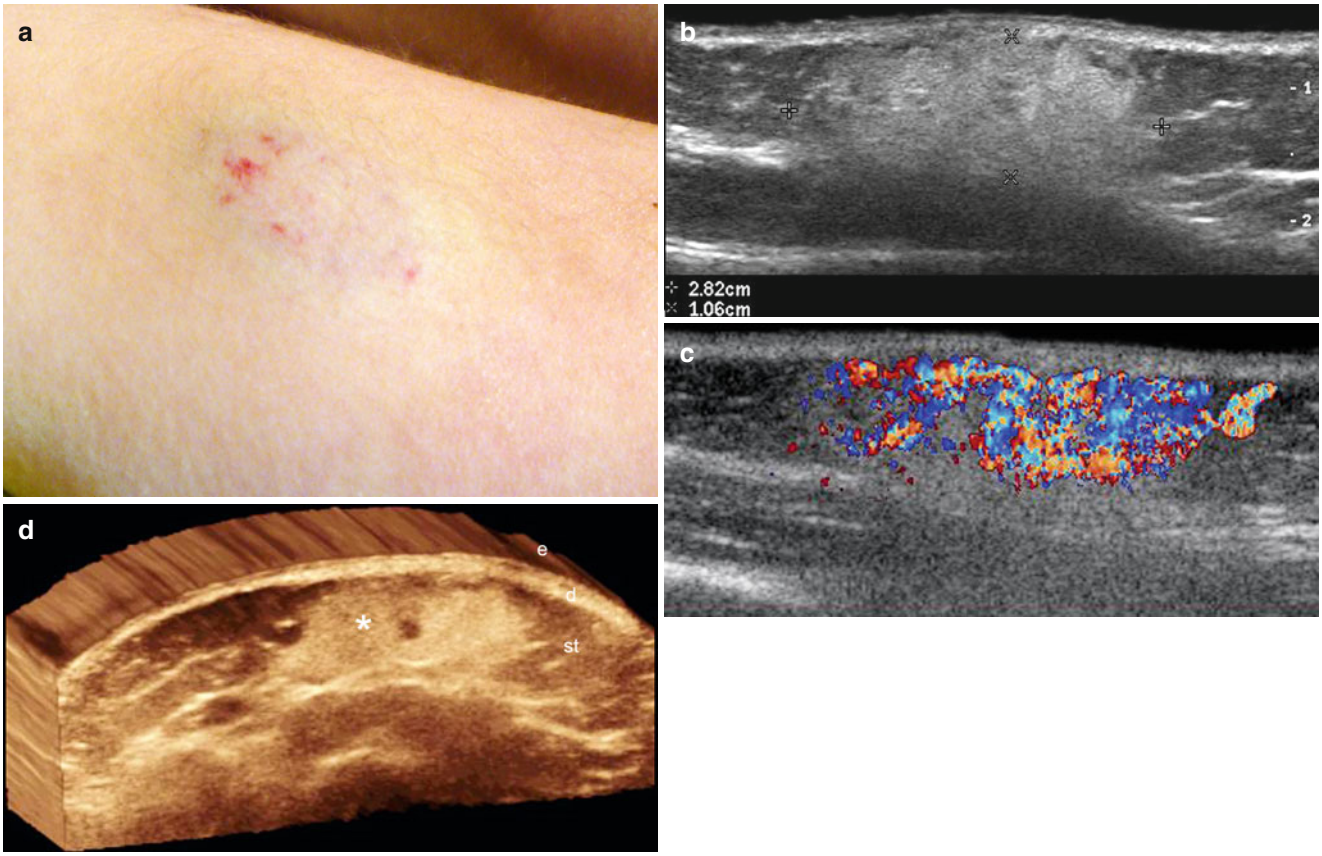

Fig. 7.23 (**a**–**d**) Hemangioma (partial regression phase). (**a**) Clinical image shows erythematous lesion in the left arm. (**b**) Grey scale ultrasound image (longitudinal view) demonstrates 2.82 × 1.06 cm Ill-defined hyperechoic and heterogeneous mass that mostly affects the subcutaneous tissue. (**c**) Color Doppler ultrasound image (longitudinal view) shows increased turbulent blood flow within the lesion. (**d**) 3D reconstruction (transverse view, 5–8 s) of the lesion (*). *Abbreviations*: *e* epidermis, *d* dermis, *st* subcutaneous tissue

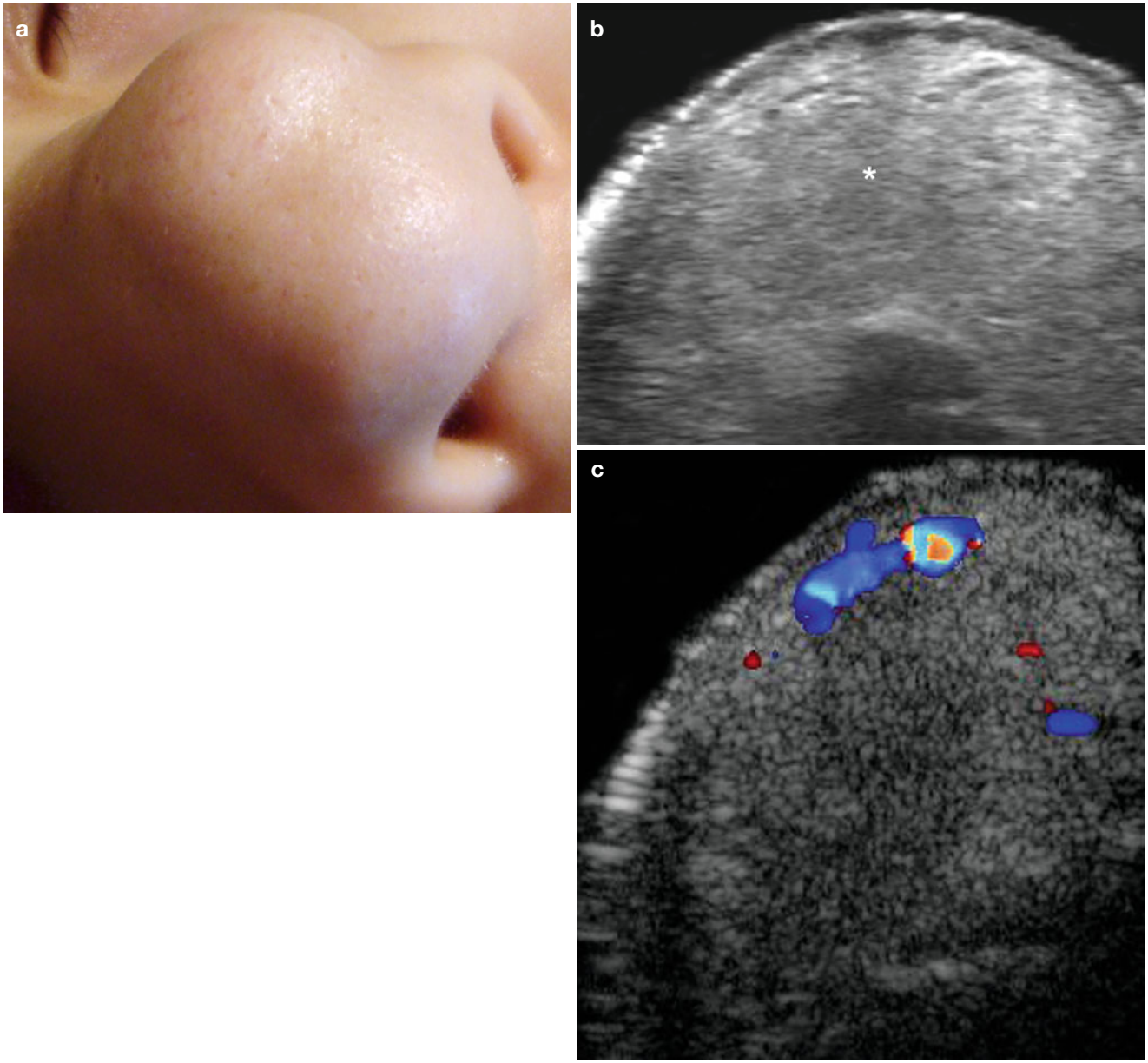

Fig. 7.24 (**a**–**c**) Hemangioma (complete regression phase). (**a**) Clinical image shows a lump in the tip of the nose. (**b**) Grey scale ultrasound image (transverse axis) demonstrates ill-defined hyperechoic mass (*) that affects the cutaneous layers and the nasal cartilages. (**c**) Color Doppler ultrasound image (transverse view) shows scarce presence of vascularity within the mass in comparison with the previous cases

Vascular channels, pouches, or pseudocystic structures large enough to be seen on B-mode are not a typical feature of hemangiomas [7]. Nevertheless, most hemangiomas show blood flow through many small vessels that may not be detectable with B-mode ultrasound. Therefore, on color Doppler ultrasound, hemangiomas are typically hypervascular with intense perfusion and high vessel density according to the criteria mentioned above (five or more vessel counts per square centimeter) (Fig. 7.24). With duplex ultrasound the arterial vessels inside a hemangioma have a Doppler shift of >2 KHz, or in other words show high systolic flow velocities (Fig. 7.26). Together with a high vessel count this is a highly specific feature for the diagnosis of hemangiomas and the combination of high vessel count and high-flow velocity results in a positive predictive value of 97 % [7]. Proliferative hemangiomas show prominent arterial blood flow, low-velocity venous vessels, and occasionally arteriovenous shunts. During the involution phase, the arteriovenous shunts start to disappear and the peak systolic velocity of the arterial vessels tends to decrease.

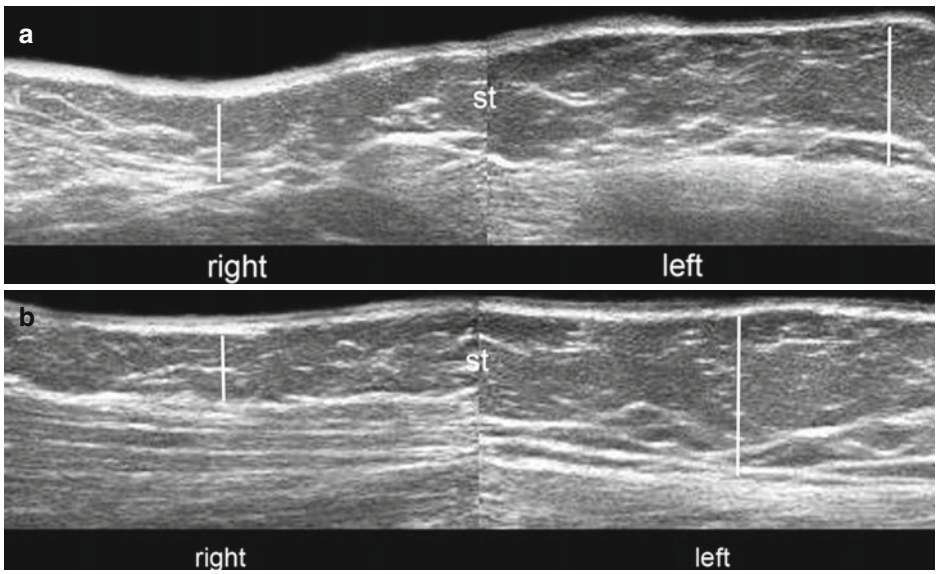

Fig. 7.25 (**a**, **b**) Hypertrophic lipodystrophy secondary to a hemangioma (total regression phase). Grey scale ultrasound images in (**a**) (transverse view) and (**b**) (longitudinal view) show side by side comparisons of the chest region. Notice the hypertrophy of the subcutaneous tissue in the left side (hemangioma site) in comparison with the normal right side (*white vertical lines*). The echogenicity of the subcutaneous tissue is unremarkable (total regression phase). *Abbreviation*: *st* subcutaneous tissue

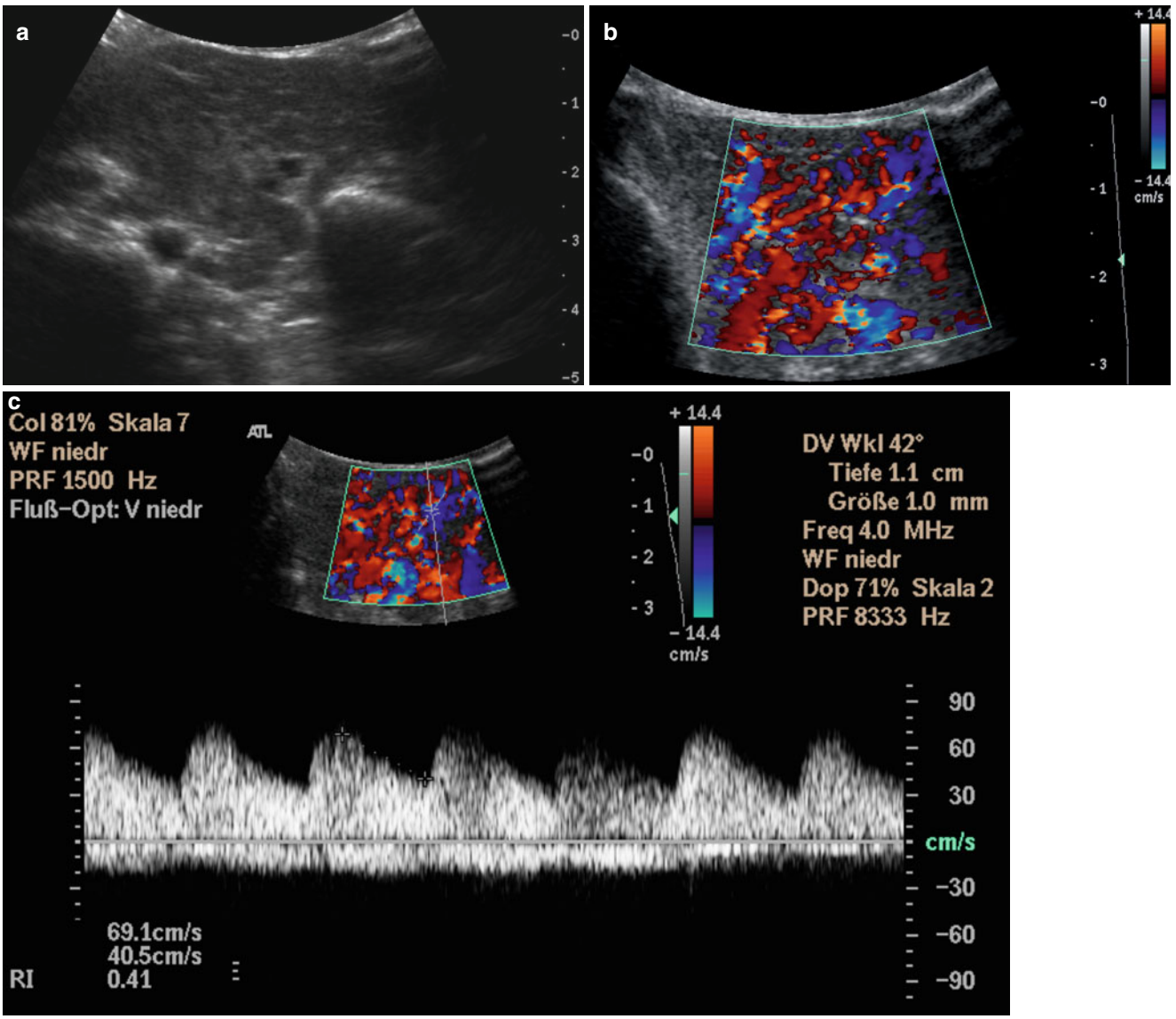

Fig. 7.26 (**a**) Transverse grey scale image of hemangioma inside the parotid gland. (**b**) Color Doppler ultrasound image shows a high vascular density with more than five vessel counts per square centimeter. (**c**) Spectral curve analysis: maximum systolic flow velocity of 70 cm/s and high diastolic flow resulting in an resistive index (RI) of < 0.5 is demonstrated

Teaching Point
A high vessel density throughout the entire lesion along with high velocity arterial and venous signals inside a solid lesion is highly specific for hemangioma.

As mentioned previously, hemangiomas (benign lesions) and soft-tissue sarcomas are not easily differentiated using B-mode ultrasound alone. What about color Doppler ultrasound and duplex ultrasound? The problem is that both types of lesions (hemangiomas and malignant tumors) are capable of stimulating the host into creating new vessels, usually from existing endothelial cells, by secreting angiogenesis factors. This is the reason why hemangiomas, in contrast to other benign soft-tissue tumors, show high vascularization. These newly produced vessels lack normal wall architecture (the muscularis layer is absent) and therefore have a high velocity with low resistance. In this regard, hemangiomas may resemble malignant soft-tissue tumors, however, in the latter, vessels are mostly found at the periphery of the tumor (active infiltrative tumor tissue) while in hemangioma the vessels are distributed more evenly throughout the lesion [11] (Fig. 7.27), which is why a high vessel density throughout the lesion is unlikely to be found in a malignant soft-tissue sarcoma.

7.6 Vascular Malformations

7.6.1 Arterial and ArterioVenous Malformations

7.6.1.1 Clinical Background

Arterial and arteriovenous malformations (AVMs) have no relationship to endothelial proliferation, but represent abnormal differentiation of vessels during embryogenesis. They are congenital lesions that are typically present at birth but often initially not detected. Additional growth, vascular factors, trauma, or endocrine changes result in clinical manifestation of the evolutive lesions, resulting in detection that is sometimes delayed into adolescence. Unlike hemangiomas, vascular malformations typically increase in size during growth. The main locations are the head and neck (40 % of cases), extremities (40 %), and torso (20 %) [12]. They represent a superficial soft-tissue mass that is typically soft and patchy with bluish or red discoloration of the skin. They derive from aberrant vessels and consist of a nest of arterial vessels or direct connections between arterial, venous, capillary, and also lymphatic vessels. This collection of tortuous vessels is called a nidus where shunting between vessels occurs, without existence of a capillary bed. These high-flow vascular malformations can contain several such nidi.

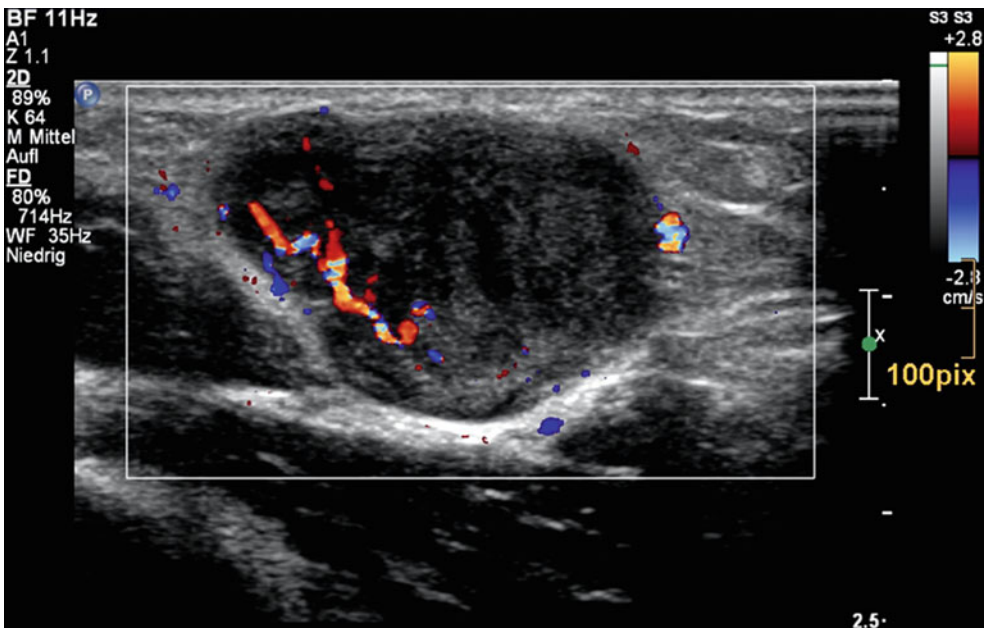

Fig. 7.27 Hypervascularized soft-tissue tumor (leiomyosarcoma) with slightly inhomogeneous texture and in contrast to hemangioma peripherally located vessels (compare with distribution of vessels in Figs. 7.9 and 7.26)

Teaching Point
A nidus with arteriovenous shunting is the hallmark of an AVM and several such nidi may exist inside a single malformation.

The high recurrence rate of vascular malformations results from their cellular origin from early mesenchymal cells, and have the potential to enlarge and recur. Because of this feature, AVMs can progress into highly destructive lesions with gross deformity of a finger or limb and substantial cosmetic impairment.

7.6.1.2 Ultrasound Characteristics

The presentation of arterial and AVMs on B-Mode ultrasound is quite variable. Typically located superficially in the subcutaneous tissue and they may result in thickening of the skin and subcutis. A nest of anechoic ducts can usually be detected, even though in some cases a anechoic pseudocystic appearance can be encountered (Figs. 7.28, 7.29, 7.30, 7.31, and 7.32). Additionally, a mixed pattern composed by hyperechoic vascular stroma and anechoic vascular channels of different size and diameter may be found [8]. The overall appearance of AVMs can be quite inhomogeneous, especially because of the different amount of arterial and venous elements inside the lesion (Figs. 7.33 and 7.34). Typically arterial malformations and AVMs do not have a soft-tissue component [8]. If the latter is encountered, the physician should always be concerned about a different differential diagnosis, such as a highly vascularized soft-tissue tumor. A criterion which may help is the distribution of vessels inside the lesions: while vessels and shunts are mainly centered inside the lesion in AVMs, in soft-tissue sarcomas, these vessels are more often found in the periphery because of their infiltrative growth. A coexisting surrounding edema or infiltrative borders are also a hallmark of sarcomas. AVMs often have indistinct outer borders and sometimes the vessels inside an AVM are so small that they are hardly seen with B-Mode ultrasound, and only detected when color Doppler ultrasound is applied.

Teaching Point
AVMs do not have soft-tissue components. If high-flow vessels and shunting are present together with a soft-tissue mass–think sarcoma.

As mentioned previously, AVMs consist of arterial and venous connections forming a so-called vascular nidus. The arterial feeders and draining veins of the AVM may sometimes be detected in the periphery of the lesion, but this is not always possible. A characteristic of all AVMs however, which must be sought as it comprises a diagnostic feature, is the presence of arteriovenous shunt flow. With color Doppler ultrasound, this is represented by aliasing inside the lesion; in this regard the correct setting of the scanner is of utmost importance to not take artifacts for true aliasing! With duplex ultrasound arteriovenous shunts show high diastolic flow above the baseline and resistance indices below 0.5 (Figs. 7.33 and 7.34). The differentiation of high-flow and low-flow AVMs is important in terms of treatment planning and therefore direct measurement of shunt flow across the lesion with duplex ultrasound is mandatory.

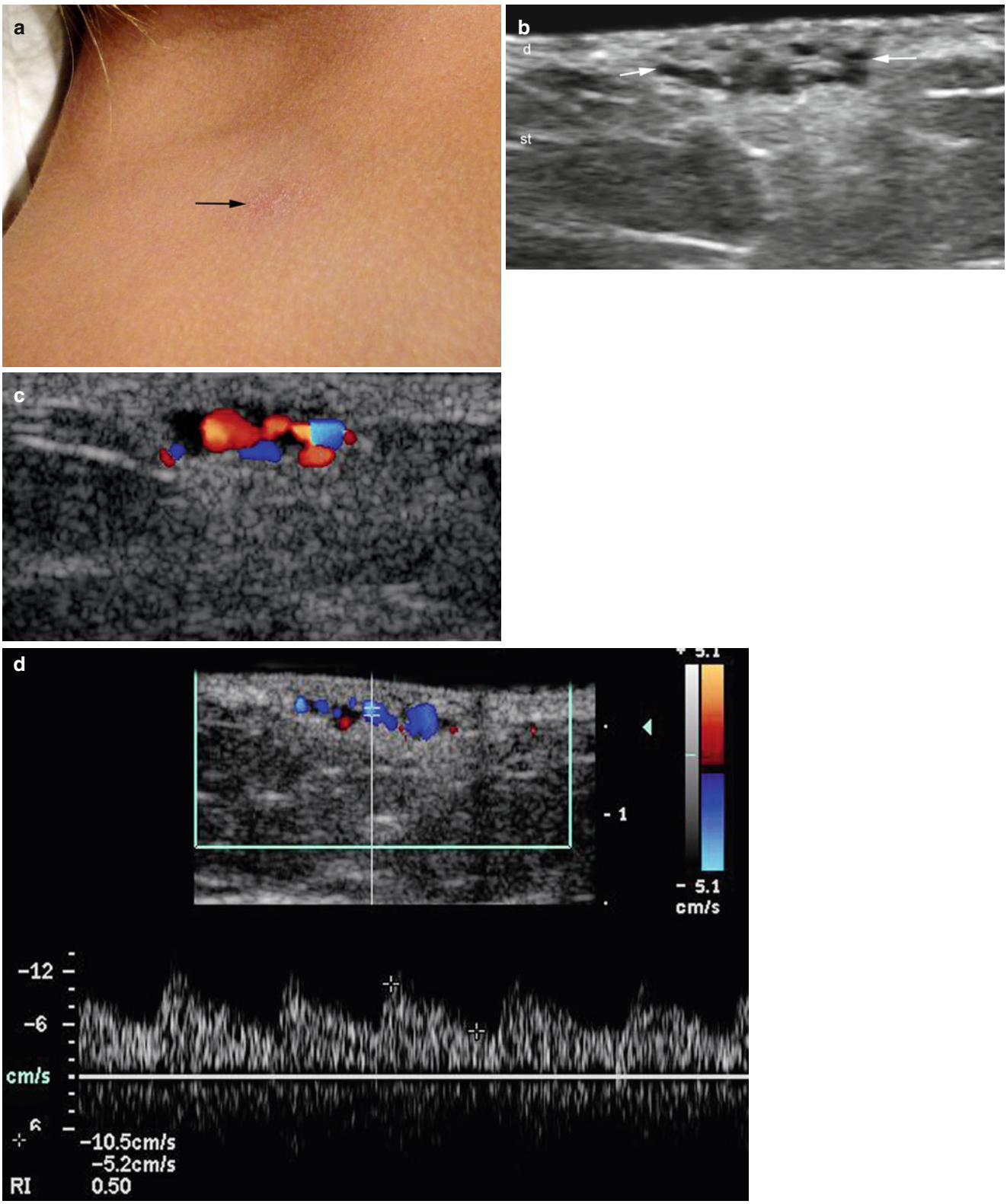

Fig. 7.28 (**a**–**d**) High-flow arterial vascular malformation. (**a**) Clinical erythematous and scaly lesion in the right clavicular region. (**b**) Grey scale ultrasound image (transverse view) shows multiple anechoic tubules (*arrows*) in the dermis and subcutaneous tissue. (**c**) Color Doppler ultrasound image (transverse view) demonstrates increased blood flow within the channels. (**d**) Color Doppler ultrasound spectral curve analysis shows arterial flow in the tubules. *Abbreviations*: *d* dermis, *st* subcutaneous tissue

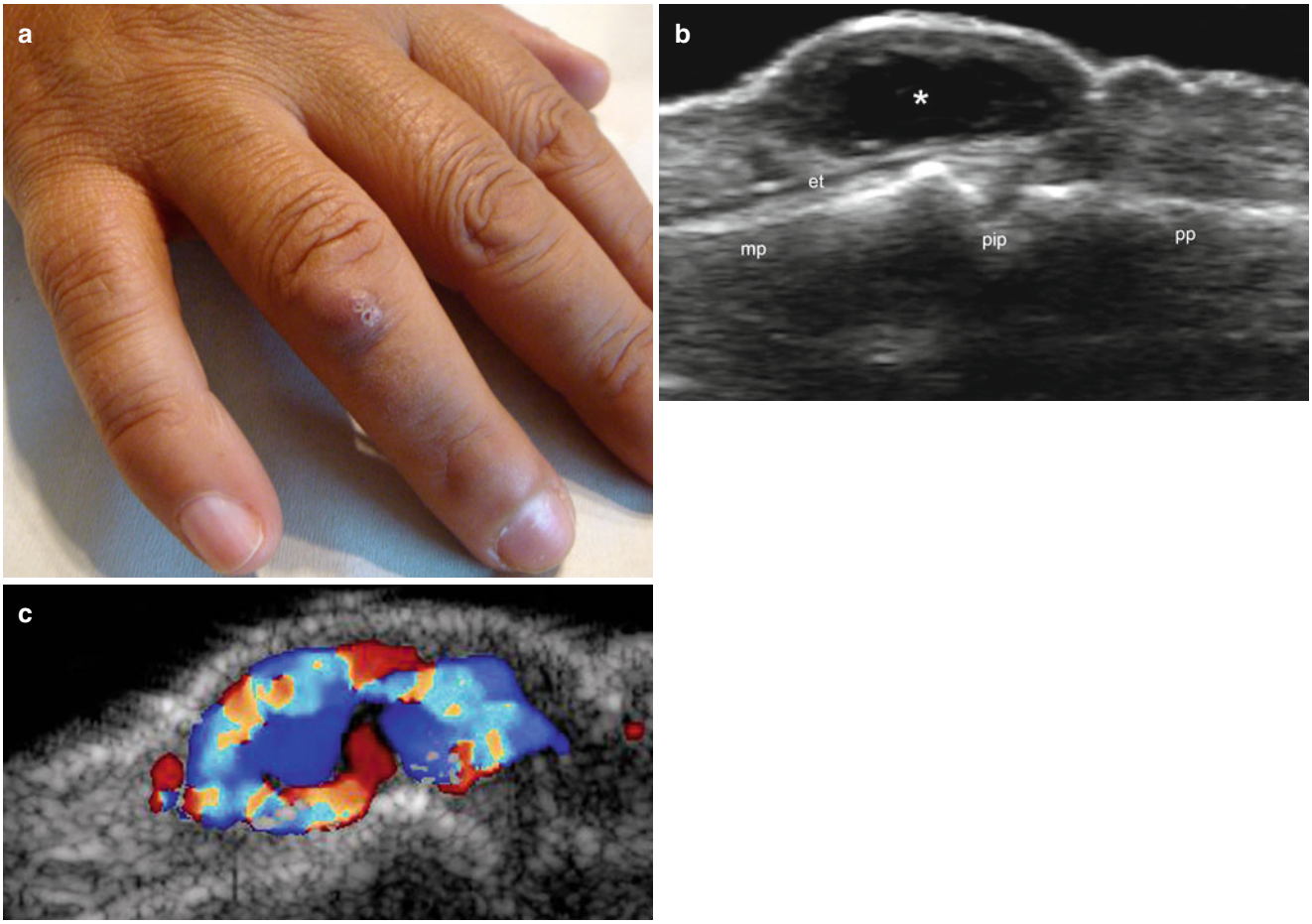

Fig. 7.29 (**a**–**e**) High-flow arterial vascular malformation. (**a**) Clinical image shows erythematous and scaly bump in the right ring finger. (**b**) Grey scale ultrasound image (longitudinal view) demonstrates oval-shaped anechoic pseudocystic structure in the subcutaneous tissue on top of the extensor tendon and proximal interphalangeal joint. (**c**) Color Doppler ultrasound image (longitudinal view) shows a nest of vessels filling the pseudocystic structure. (**d**) Color Doppler ultrasound spectral curve analysis demonstrates arterial flow within the vessels. (**e**) 3D power angio reconstruction of the lesion. *Abbreviations*: *et* extensor tendon, *mp* middle phalanx, *pp* proximal phalanx, *pip* proximal interphalangeal joint

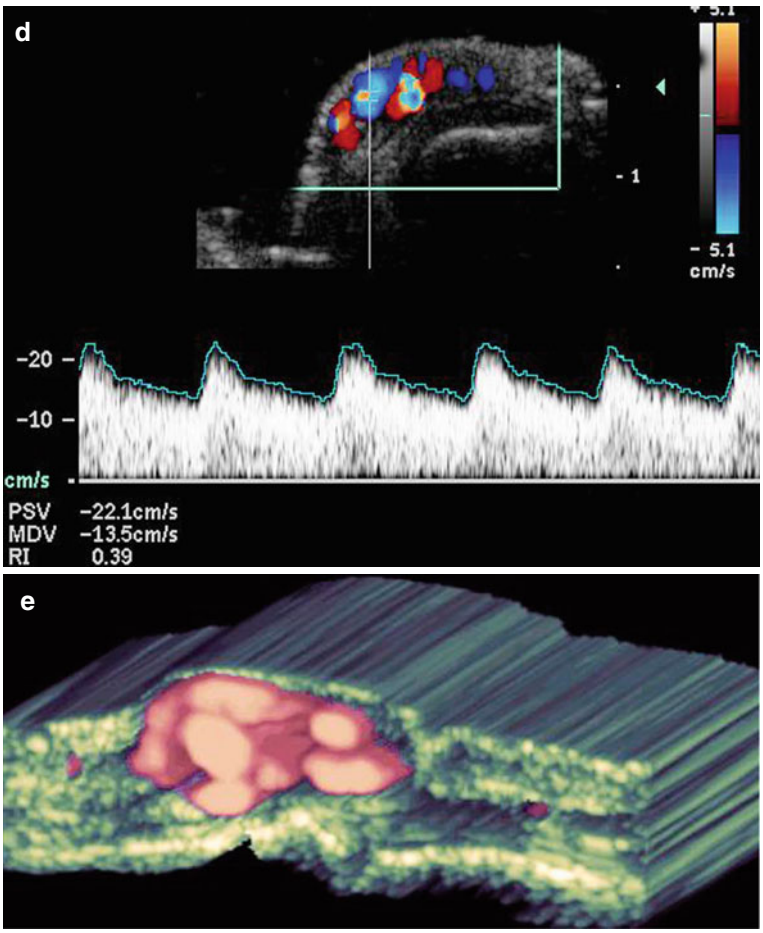

Fig. 7.29 (continued)

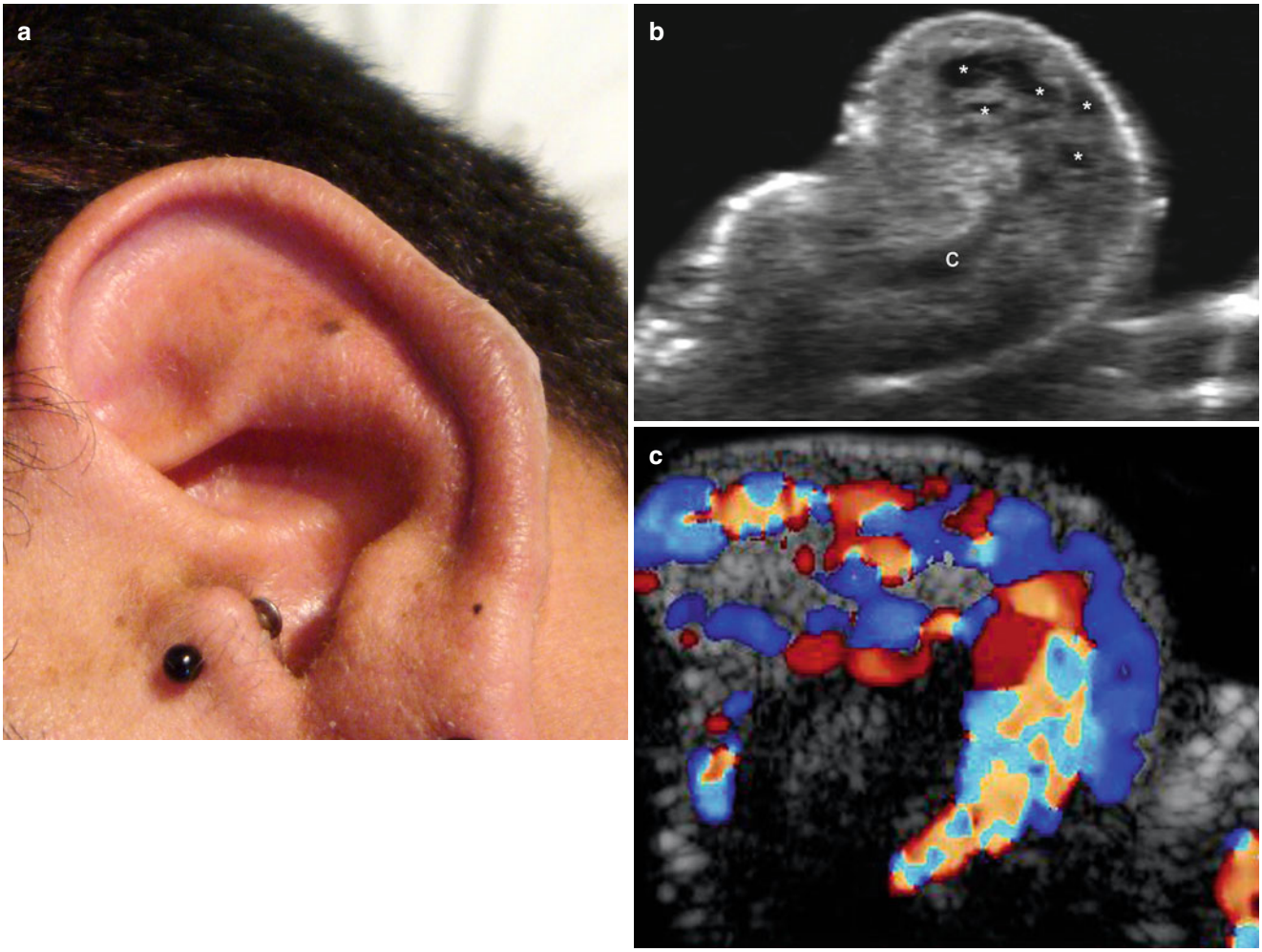

Fig. 7.30 (**a**–**e**) High-flow arterial vascular malformation. (**a**) Clinical lesion shows erythematous swelling in the helix of the left ear pinna. (**b**) Grey scale ultrasound image (transverse view) demonstrates multiple anechoic tubules (*) affecting the dermis and part of the auricular cartilage. (**c**) Color Doppler ultrasound image (transverse view) shows prominent vascularity within the tubules. (**d**) Color Doppler ultrasound spectral curve analysis shows high arterial flow within the tubules (peak systolic velocity: 87 cm/sec). (**e**) 3D power angio reconstruction of the vascular lesion

Fig. 7.30 (continued)

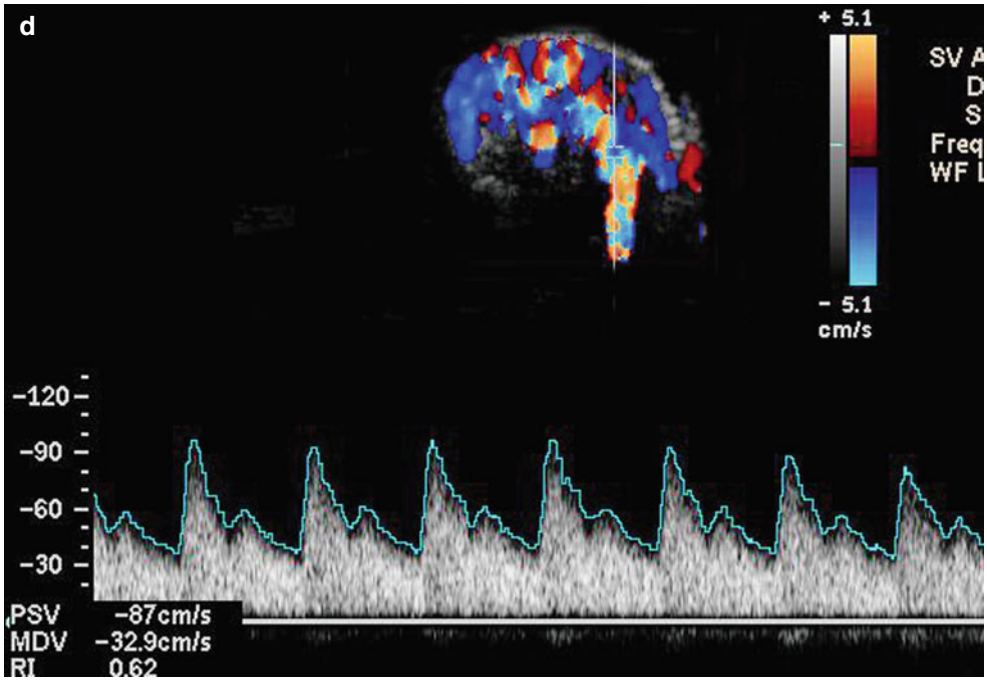

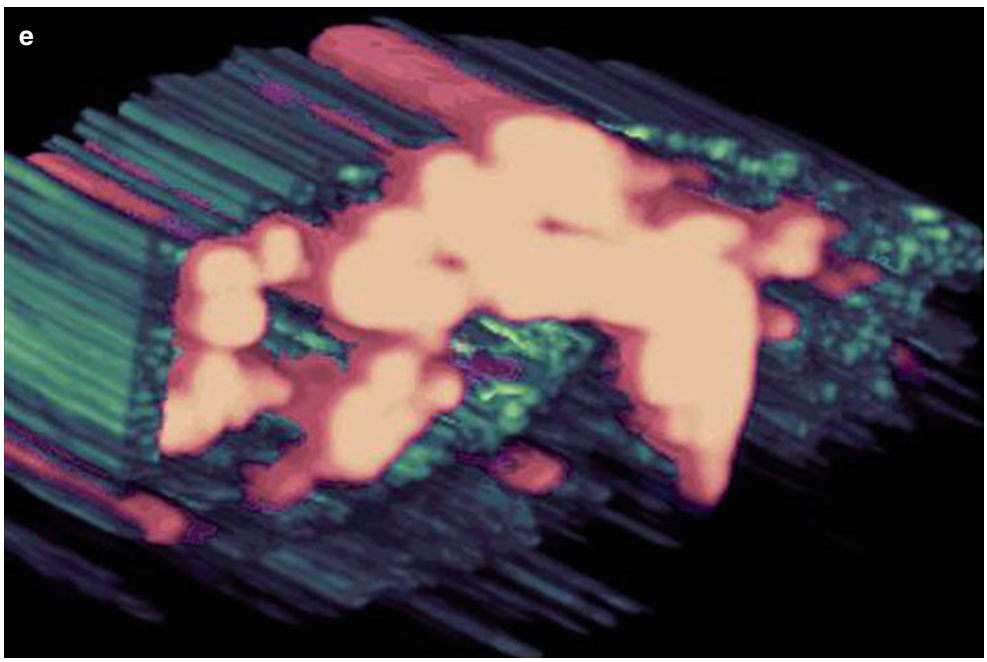

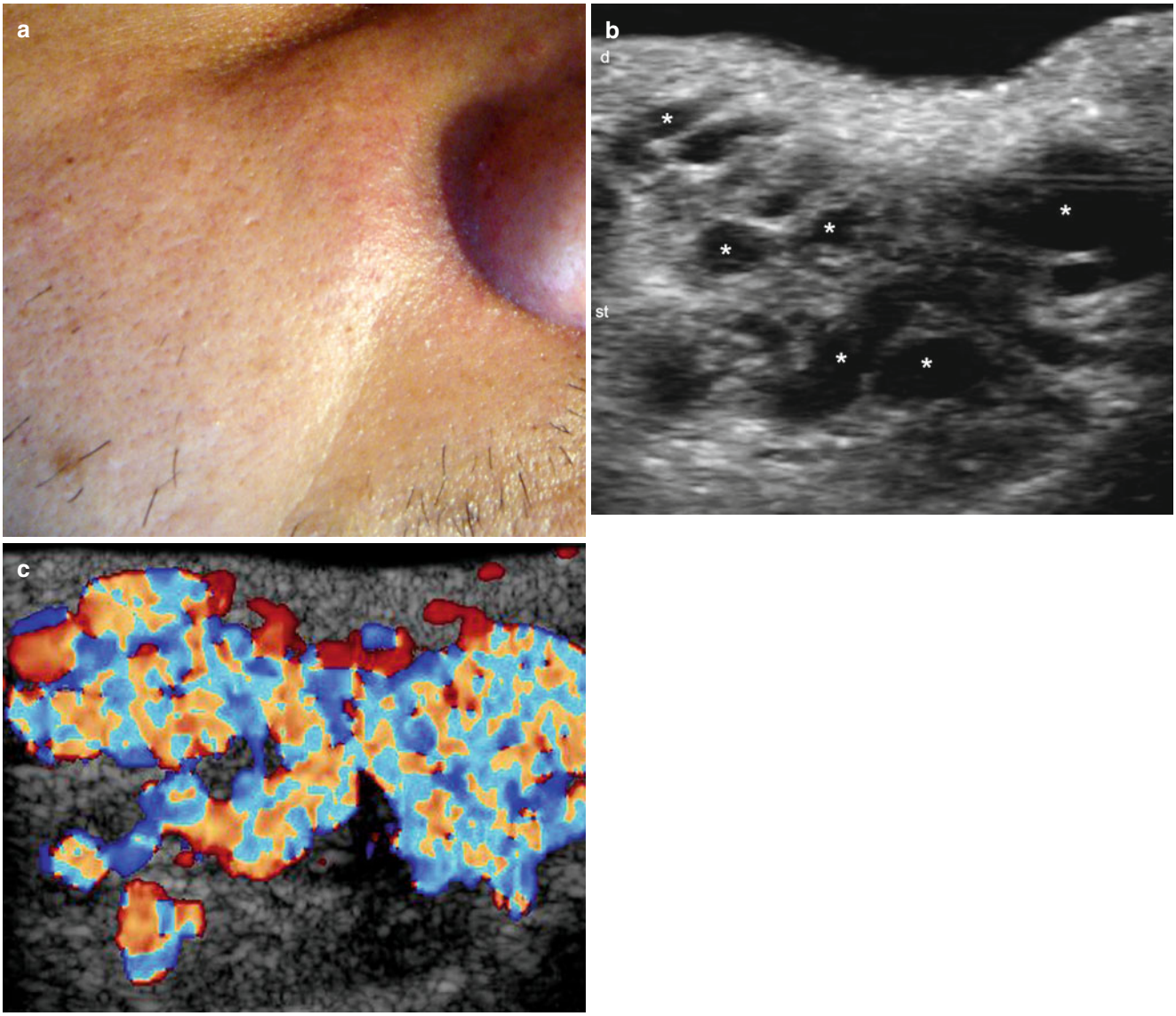

Fig. 7.31 (**a**–**e**) High-Flow arteriovenous vascular malformation. (**a**) Clinical lesion shows slightly erythematous swelling in the right cheek. (**b**) Grey scale ultrasound image (transverse view) demonstrates multiple anechoic ducts (*) in the subcutaneous tissue without a solid component. (**c**) Color Doppler ultrasound image (transverse view) shows high and turbulent flow within the ducts. (**d**, **e**) Color Doppler ultrasound spectral curve analysis demonstrates high velocity arterial (**d**) and venous (**e**) in the channels

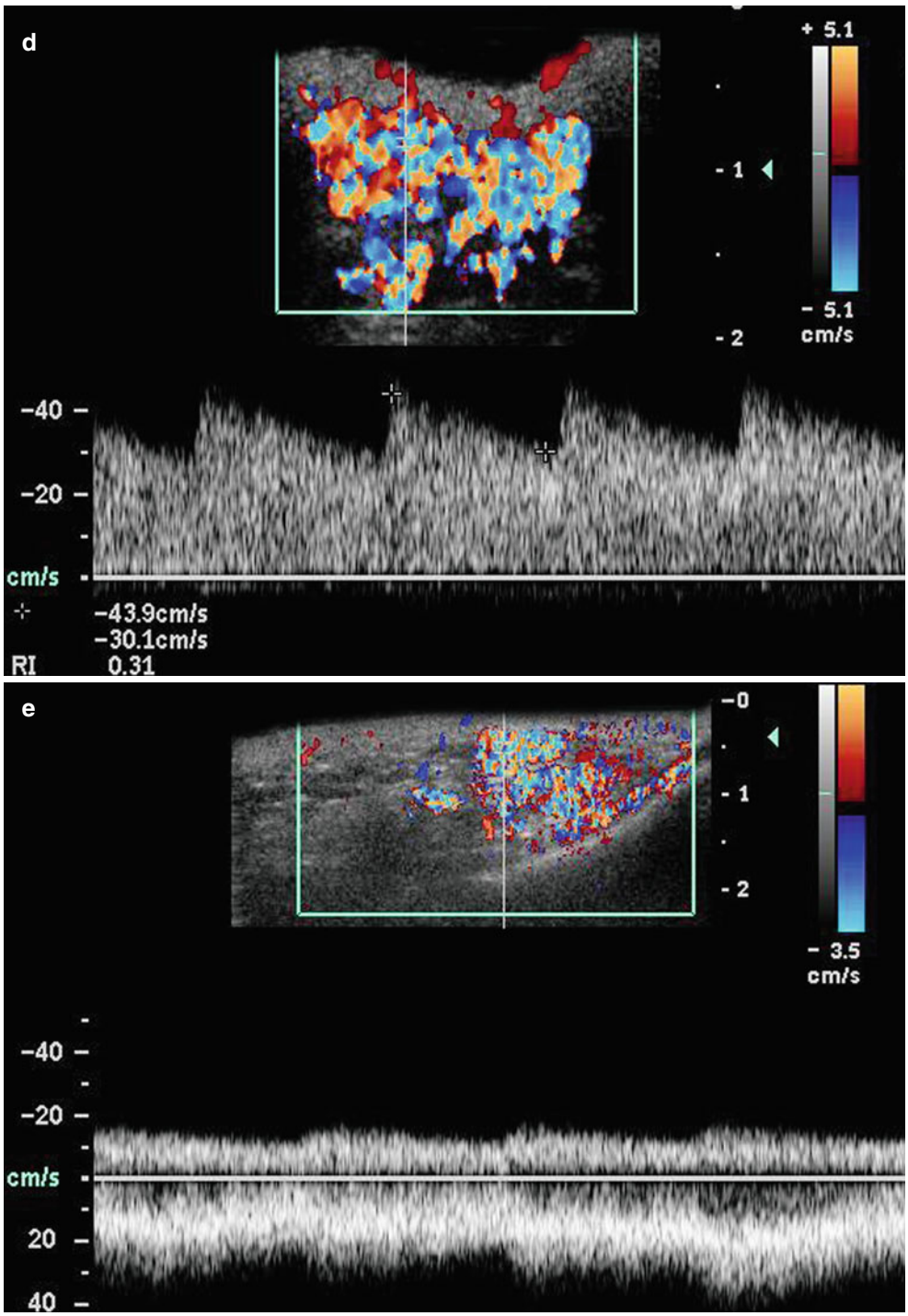

Fig. 7.31 (continued)

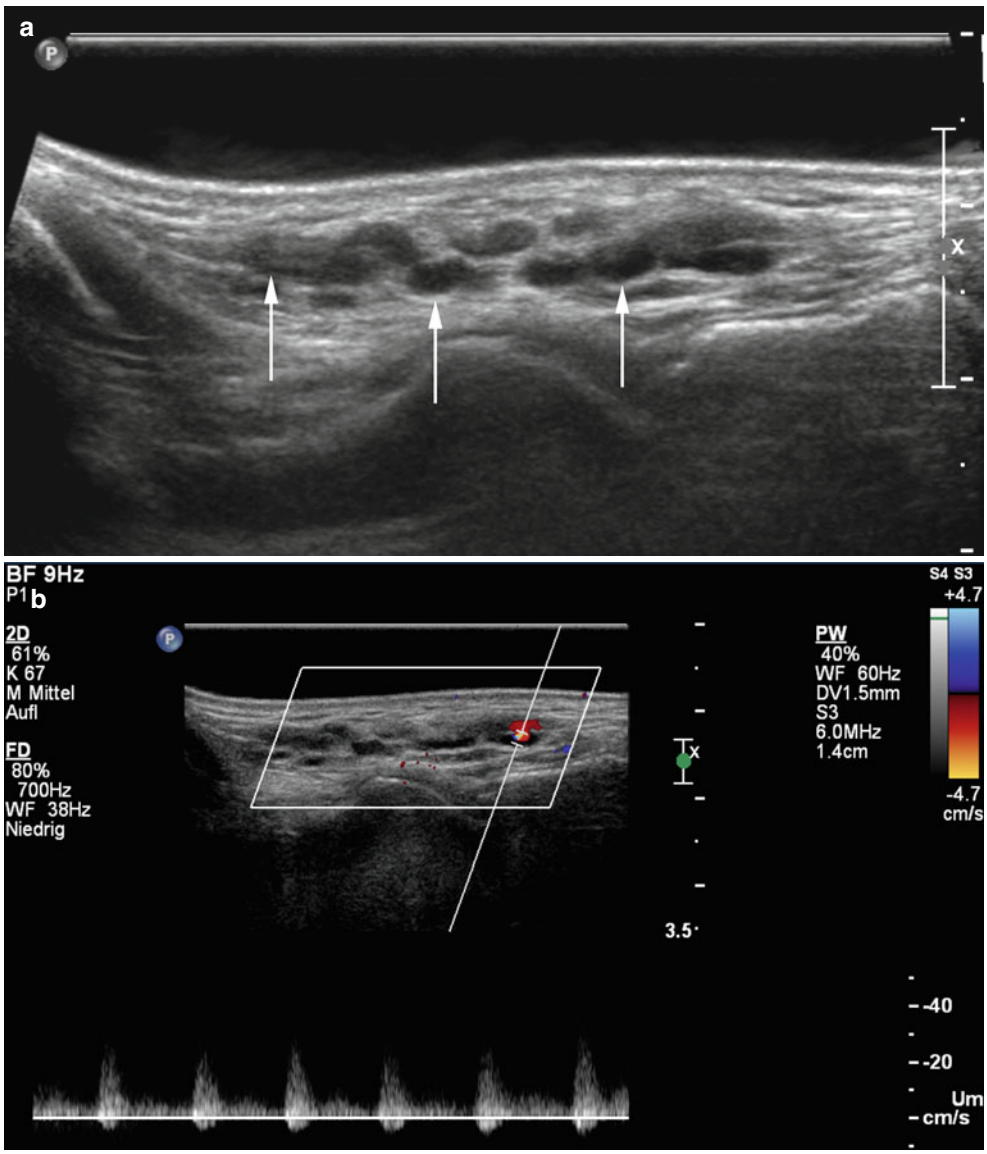

Fig. 7.32 (**a**, **b**) High-flow arteriovenous vascular malformation. (**a**) Grey scale ultrasound image of a small subcutaneous lesion consisting mainly of tortuous venous components (*arrows*). (**b**) At the lower pole of the lesion however a small arterial feeder is demonstrated, corresponding with a high-flow arteriovenous malformation

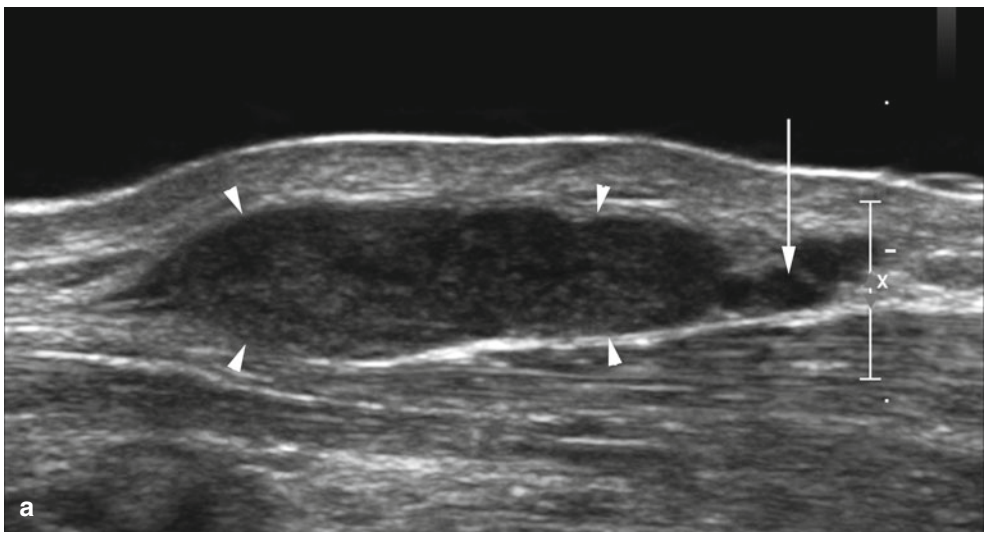

Fig. 7.33 (**a**–**c**) High-flow arteriovenous vascular malformation. (**a**) Grey scale ultrasound image of subcutaneous soft tissue mass (*arrowheads*) with a thick vascular structure on its right border (*arrow*). (**b**) Duplex ultrasound confirms highly vascularized lesion with a large peripheral high flow feeding artery and (**c**) draining vein

Fig. 7.33 (continued)

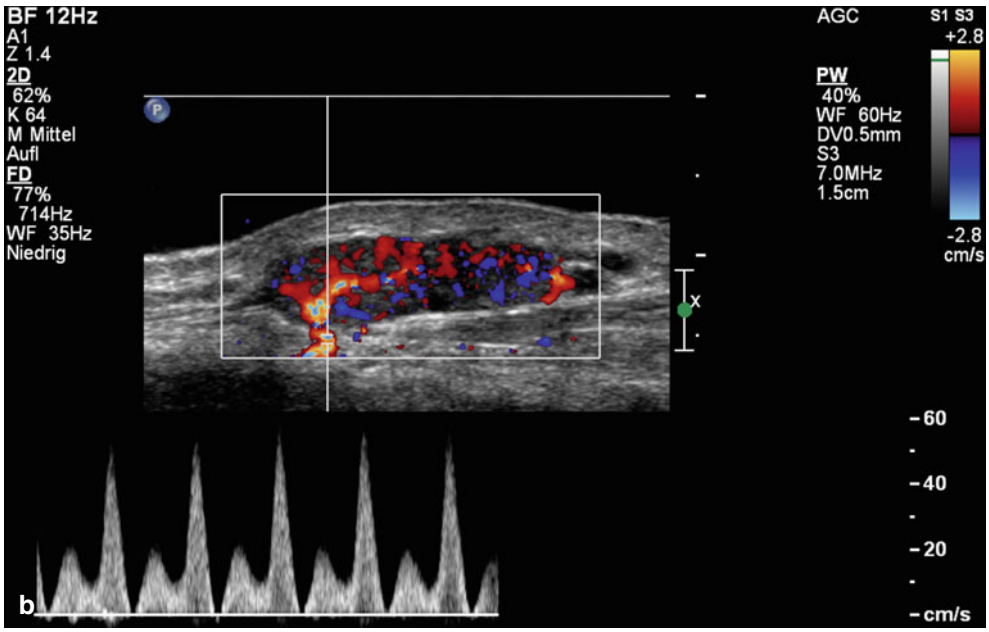

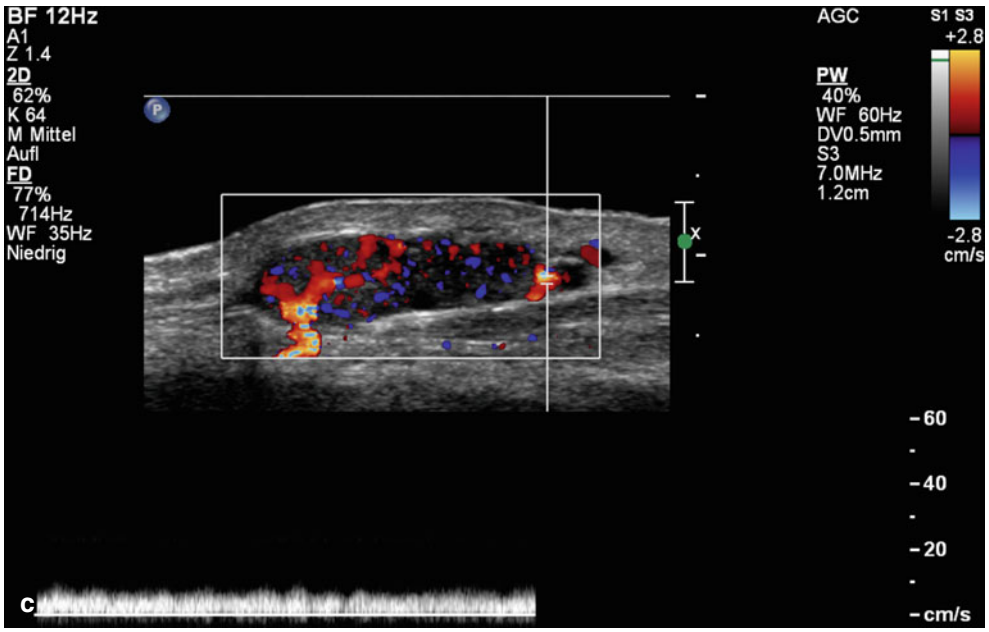

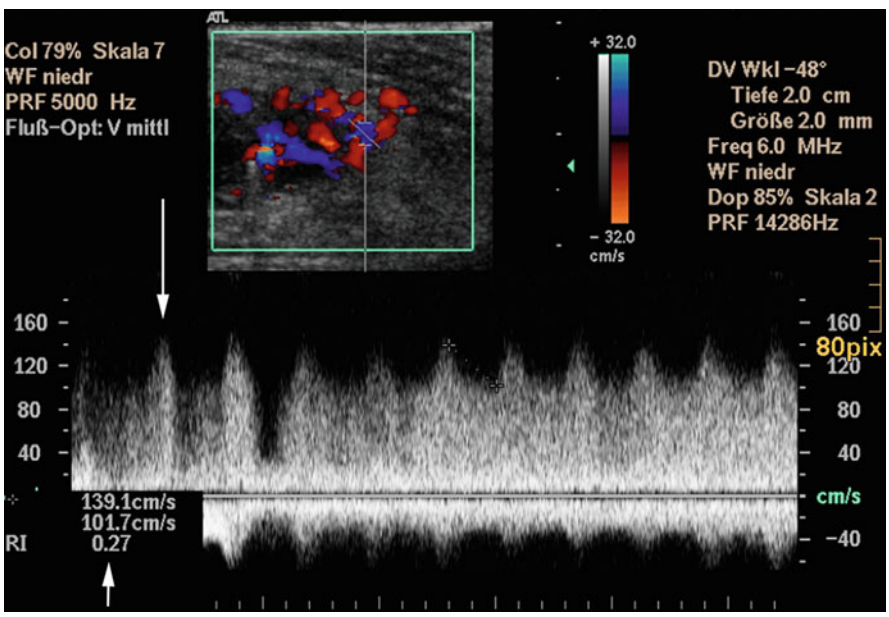

Fig. 7.34 High-flow arteriovenous malformation. Duplex ultrasound: note high-flow velocity of around 139.1 cm/s (*long arrow*) and high diastolic flow resulting in resistive index (RI) < 0.5 (*short arrow*) corresponding with marked arterio-venous shunting

7.6.2 Venous Malformations

7.6.2.1 Clinical Background

Venous malformations have certain similarities to arterial malformations and AVMs: both are congenital, both do not regress, but may most commonly enlarge during growth and both may go undetected for a period of time until they become clinically symptomatic. Venous malformations are bluish in color, they are compressible, and typically increase in size during a Valsalva maneuver [13]. While venous malformations are often asymptomatic, they may become painful when thrombophlebitis or thrombosis occurs, or in the case of involvement of muscles and joints. Histologically, they consist of venous channels with dilated, sponge-like caverns of different sizes. In terms of treatment planning, venous malformations may be further divided into four subtypes according to a classification system proposed by Puig et al. [14] (Table 7.2). The classification is based on lesion drainage and has important implications on sclerotherapy because types 3 and 4 lesions carry a higher risk of complications.

Teaching Point
The type of drainage has implications on the treatment of venous malformations as type 3 and type 4 lesions have a higher rate of complications during sclerotherapy.

A variety of syndromes can be associated with venous malformations: Klippel-Trenaunay syndrome (venous and lymphatic malformations in combination with capillary malformations and skeletal or soft-tissue hypertrophy), Parkes-Weber syndrome (similar to Klippel-Trenaunay but with presence of additional high-flow malformations), Sturge-Weber syndrome (cutaneous, facial venular malformations; i.e., port wine stain in the facial area supplied by the V1 branch of the trigeminal nerve and subcutaneous lymphatic malformations with secondary maxillofacial bone hypertrophy), Maffuci syndrome (a variant of Ollier's disease, with venous malformations associated with multiple enchondromas), among others.

Table 7.2 Classification of venous malformations based on venous drainage according to Puig et al. [14]

Type	Description
Type I	Isolated malformation without peripheral drainage
Type II	Malformation drains into normal veins
Type III	Malformation drains into dysplastic veins
Type IV	Venous ectasia

7.6.2.2 Ultrasound Characteristics

Venous malformations are anechoic or slightly hypoechoic, sponge-like structures on B-mode sonograms and they consist of multiple blood-filled caverns of different sizes. Varicose veins, complex and communicating venous channels are seen in only about 50 % of lesions [15]. Typically venous malformations have only little fibrous stroma, but the walls of the individual caverns range from very thin septae to thick fibrous bridges (Figs. 7.35, 7.36, and 7.37), which is why approximately 80 % of venous malformations are somewhat inhomogeneous on B-mode with a mixture of hypoechoic caverns and sometimes hyperechoic septations [16]. If large parts of the malformation are filled with thrombotic material, it can resemble a soft-tissue tumor with mixed echogenity making it difficult to differentiate from hemangiomas or other soft-tissue lesions [16, 17]. The inhomogeneous texture of the lesion can sometimes prevent distinction from surrounding normal tissue and exact measurement of size, this is especially the case when tiny finger-like protrusions of the lesion invade into the surrounding soft tissues. Tiny roundish calcifications resembling phleboliths inside thrombosed caverns are a diagnostic hallmark of venous malformations but are seen in only 20 % of lesions [15, 16] (Figs. 7.36, 7.37, 7.38, 7.39, 7.40, and 7.41). Echotexture alone does not allow differentiation of venous malformations from hemangioma or lymphangioma, in contrast to the latter however, venous malformations are easily compressed with the transducer. A color Doppler ultrasound compression test is a comparable and important equivalent test for the diagnosis of a venous malformation. With correct color Doppler ultrasound settings, the signal inside the blood-filled caverns shows a change from red to blue and vice versa during transducer pressure/release of pressure on the malformation (Fig. 7.10). No flow is detected in approximately 15–20 % of lesions; this may be due to either thrombosis, substantially low flow inside the malformation, or to inappropriate Doppler settings [15]. In lesions with low flow, no color signal may be seen at all unless light pressure is applied. Nevertheless, flow inside venous malformations could be quite variable, and according to Trop et al. [16], 16 % of lesions do not show any flow at all, 78 % have slow monophasic venous flow, and 6 % have biphasic low flow. Venous malformations do not harbor arteriovenous shunts, therefore, it is important to search for regions with aliasing (turbulence) using color Doppler ultrasound and for shunt flow with spectral wave analysis. If a shunt is detected, the lesion is by definition not a venous malformation but either an arteriovenous malformation and this is an important distinction in terms of treatment planning.

Teaching Point
If arteriovenous shunts are detected inside a malformation it is by definition not a simple venous malformation.

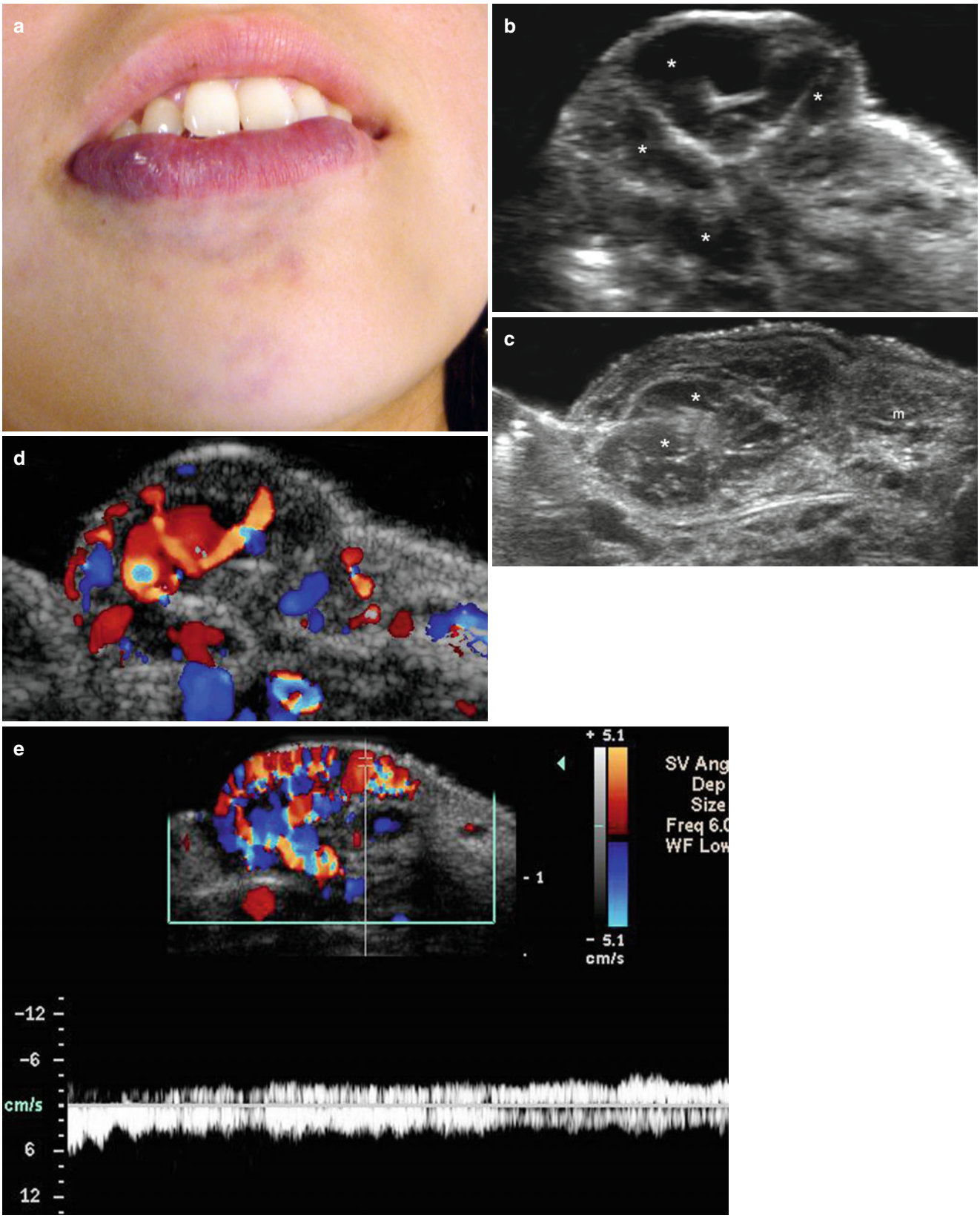

Fig. 7.35 (**a**–**e**) Low-flow venous vascular malformation. (**a**) Clinical erythematous lesion in the right border of the lower lip. (**b**) Grey scale ultrasound image (longitudinal view) and (**c**) (transverse extended view) show multiple anechoic tubules and pseudocytic structures (*) that involve the dermis and the orbicularis muscle. (**d**) Color Doppler ultrasound image demonstrates increased blood flow within the tubules. (**e**) Spectral curve analysis shows venous flow in the ducts

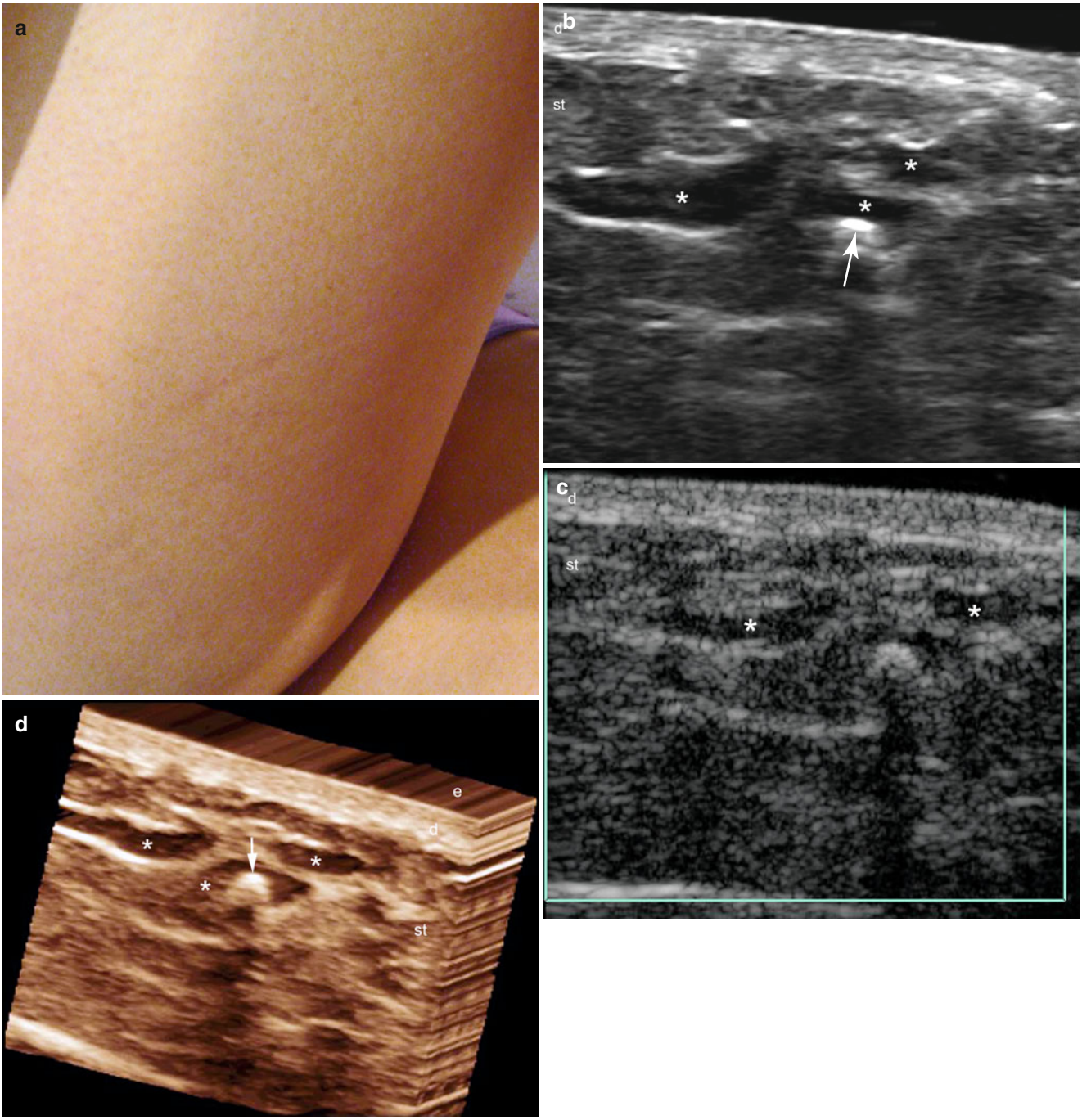

Fig. 7.36 (**a**–**d**) Low-flow venous vascular malformation. (**a**) Clinical lesion demonstrates slight erythema in the posterior aspect of the right thigh. (**b**) Grey scale ultrasound image (transverse view) shows anechoic ducts (*) in the subcutaneous tissue. Notice the hyperechoic nodule that corresponds to a phleboliths (*arrow*). (**c**) Color Doppler ultrasound image demonstrates no detectable vascularity within the lesion. (**d**) 3D ultrasound reconstruction (5–8 s sweep) of the lesion highlighting the anechoic tubules (*) and the phlebolith (*arrow*)

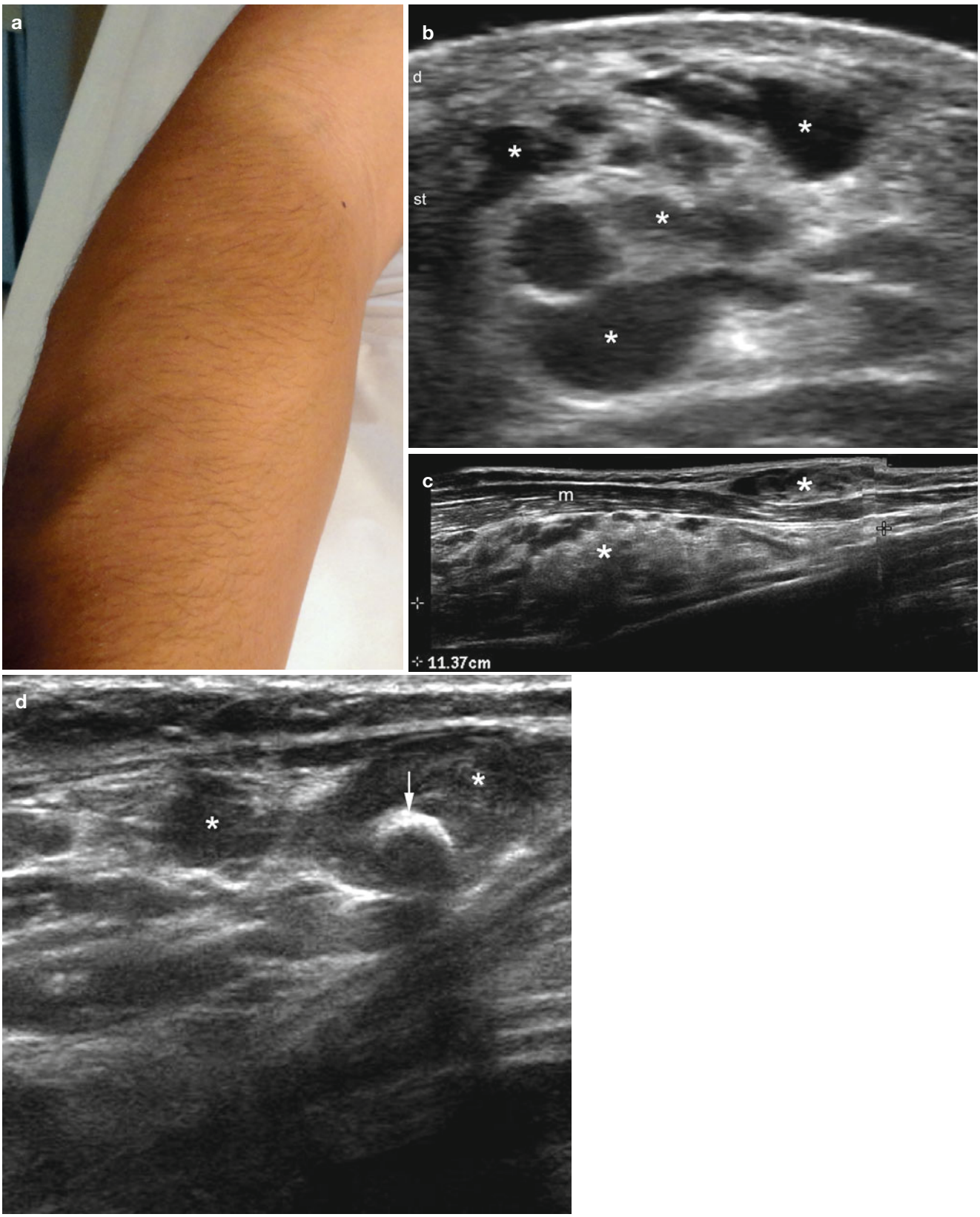

Fig. 7.37 (**a**–**e**) Low-flow venous vascular malformation. (**a**) Clinical lesion shows a swelling in the right arm and forearm. (**b**) Grey scale ultrasound image (transverse view) shows multiple anechoic pseudocystic structures (*) in the subcutaneous tissue. (**c**) Grey scale ultrasound image (extended field longitudinal view) in the forearm demonstrates subcutaneous and miofascial involvement (*). (**d**) Grey scale ultrasound image (longitudinal view) shows an hyperechoic phlebolith (*arrow*) within the pseudocystic cavities (*). (**e**) Color Doppler ultrasound spectral curve analysis with monophasic venous flow. *Abbreviation: m* muscle

Fig. 7.37 (continued)

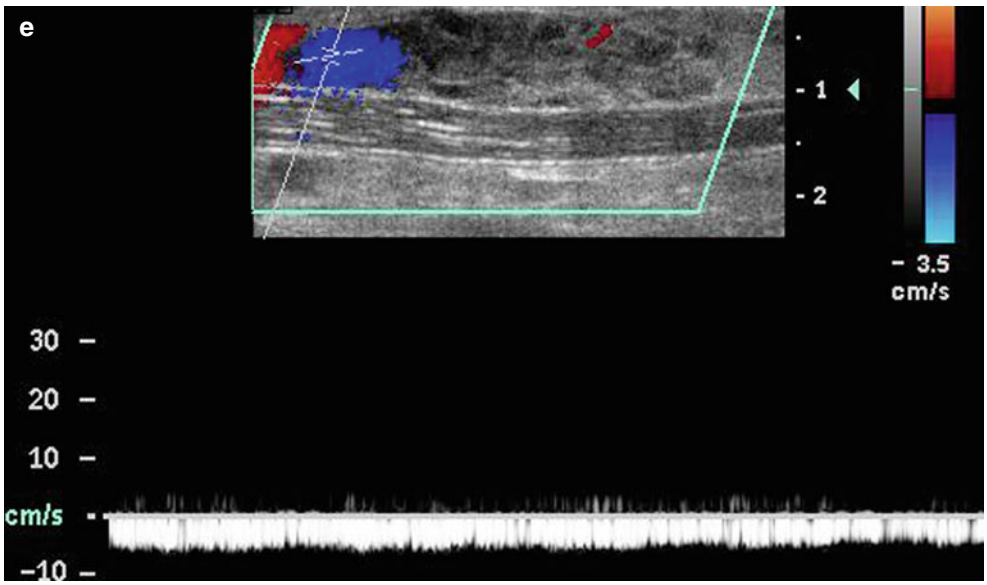

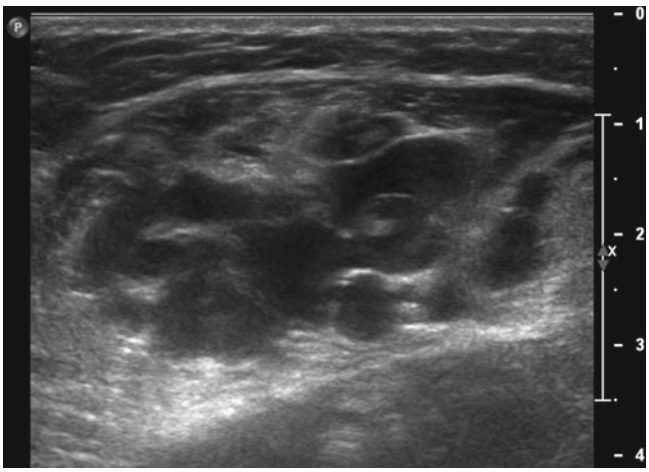

Fig. 7.38 Grey scale ultrasound image of a patient with a venous malformation at the distal thigh consisting of thin walled anechoic sponge-like caverns

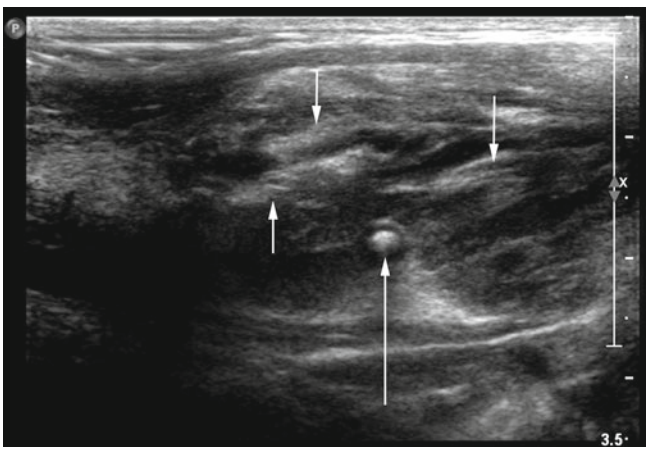

Fig. 7.39 In contrast to the lesion in Fig. 7.38, this venous malformation shows thick fibrous septae (*small arrows*). A small phlebolith is also demonstrated (*long arrow*)

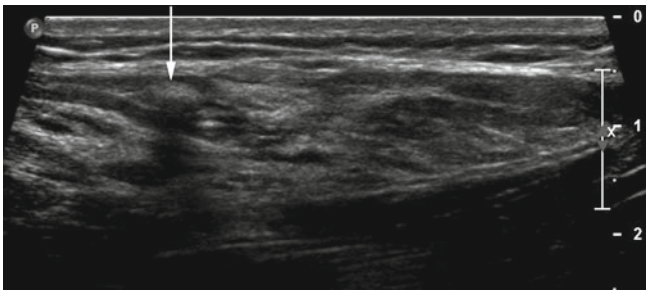

Fig. 7.40 Transverse grey scale image showing large roundish calcification (*arrow*) inside venous channel, a hallmark of a low flow venous malformation

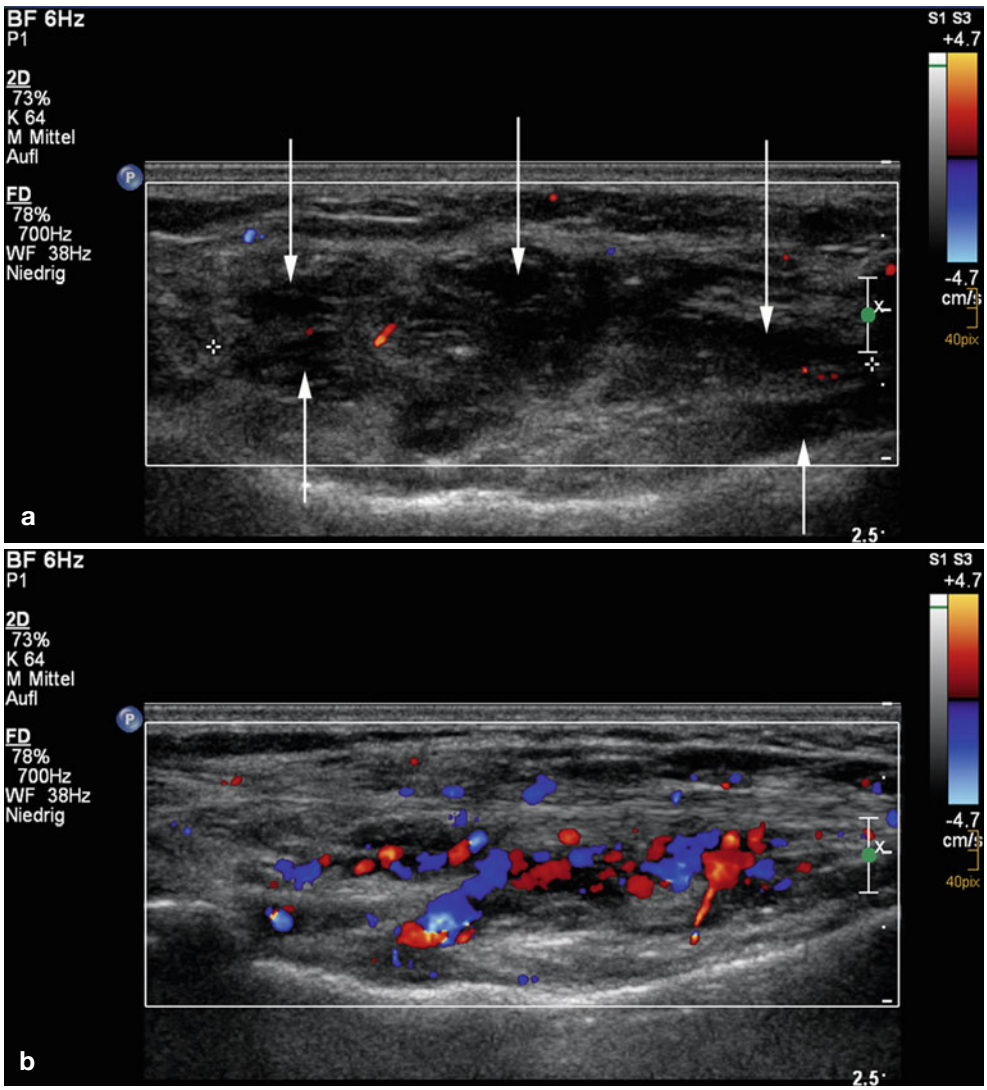

Fig. 7.41 (**a**) Soft-tissue lesion consisting of anechoic and hypoechoic caverns (*arrows* in **a**) with no detectable flow during normal ultrasound. Only with compression (**b**) venous flow inside the lesion is demonstrated

7.6.2.3 Direct Percutaneous Phlebography

The value of direct percutaneous phlebography in venous anomalies is twofold: it can be performed as a diagnostic procedure and if contrast-filled abnormal venous cavities are demonstrated, this confirms the presence of a venous malformation and virtually excludes the presence of a soft-tissue tumor. The second, and in our opinion, more important aspect, is to perform direct percutaneous phlebography as the first step during sclerotherapy of a venous malformation (Fig. 7.42): A 21-gauge needle is inserted into the malformation under ultrasound guidance and connected to a syringe via a length of tubing. Under suction, the needle is positioned until blood is withdrawn and 5 ml of iodinated contrast is injected by hand to observe the characteristics of venous opacification and filling of the drainage vein. According to Puig et al. [14] and Dubois et al. [15], different drainage patterns may be observed: some malformations are mere fluid-filled caverns without any detectable drainage. The most common is a cavitary pattern with late and slow venous drainage without detection of abnormal veins. The third is a malformation consisting of spongy vascular channels draining into dysplastic veins, with the fourth a venous ectasia with rapid drainage. In cases with immediate drainage, compression of the drainage vein using a tourniquet to avoid spilling of the sclerosant into the systemic circulation and to increase local exposure inside the malformation, is strongly advised (Fig. 7.42b).

Teaching Point

Direct puncture phlebography is necessary before sclerotherapy to define the type of drainage in malformations.

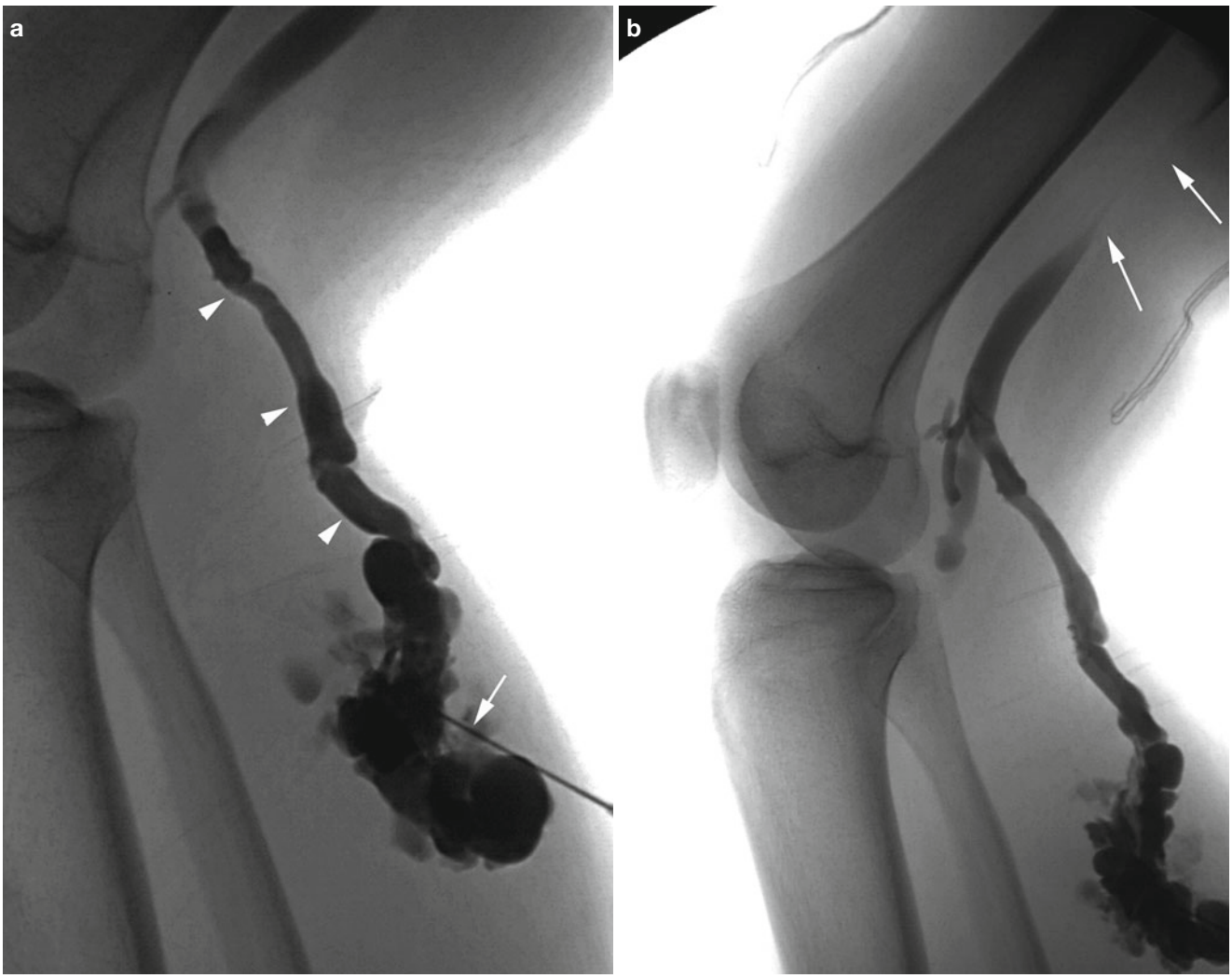

Fig. 7.42 (**a**) Direct puncture phlebography via a 21-gauge needle (*arrow*) in a patient with a large venous malformation inside the medial gastrocnemius muscle. Rapid drainage via a large communicating vein (*arrowheads* in **a**) into the distal femoral vein is seen. (**b**) Venous drainage is largely reduced after fastening of a tourniquet (*arrows* in **b**) and sclerotherapy with slow injection of the sclerosant is begun

7.6.3 Lymphatic Malformations

7.6.3.1 Clinical Background

Lymphatic malformations also called lymphangiomas, arise from a developmental defect in the communication between lymph vessels and their draining channels during embryogenesis [17, 18]. Histologically, they are thin-walled fluid-filled cysts of different sizes surrounded by a variable amount of connective tissue stroma; while the microcystic variant consists of multiple tiny cysts within a thick solid matrix, macrocystic variants consist mainly of large thin-walled spaces filled with proteinaceous fluid. The head and neck are most frequently affected and cervicofacial lymphatic malformations represent a rough 70 % of cases. About 60 % of lymphatic malformations are present at birth and the other 40 % become symptomatic during the first 2 years of life. The macrocystic variants may enlarge with growth of the child and compress surrounding soft tissues. Involvement of the tongue and orbit is well known and may result in impaired vision or speech. Tissue overgrowth may result in macroglossia, deformities of the bony palate and jaw, and thus problems with dentition or malocclusion. The infiltrative growth is more common with microcystic variants and can result in considerable cosmetic impairment. Lymphatic malformations in the limbs can also result in progressive lymphedema and skin changes.

The distinction of lymphatic malformations from other congenital vascular anomalies is important because they represent proliferative lesions, which warrants closer observation and more aggressive treatment. Lymphatic malformations may exist alone or be part of several syndromes with a complex mixture of arteriovenous and lymphatic anomalies such as Klippel-Trenaunay or Proteus syndrome. In terms of

therapy, lymphatic malformations pose a severe problem: while surgical resection is considered the gold standard, complete resection is often impossible, the recurrence rate is high, and the risk of severe cosmetic impairment is considerable. Therefore, various approaches for percutaneous treatment under ultrasound or CT/MRI guidance are reported in the literature [19, 20]: simple direct drainage, aspiration, and sclerotherapy with ethanol or picibanil (OK-432) are most frequently used with varying success.

7.6.3.2 Ultrasound Characteristics

Simple macrocystic lymphatic malformations are septate caverns of large size filled with anechoic fluid (Figs. 7.43, 7.44, 7.45, 7.46, 7.47, 7.48). Bleeding or infection may sometimes result in mixed echogenity of fluid in different caverns and/or the presence of debris layered at the bottom of the caverns. The lesion itself may be mobile against the surrounding soft tissues, but typically the caverns themselves are not compressible with the transducer; as previously mentioned, this is an important sign for the differential diagnosis of venous malformations. Microcystic malformations may exhibit extremely small cysts barely visible with sonography, tightly packed within a solid echoic matrix. This is why they may sometimes resemble proliferating hemangioma on B-mode.

Using color Doppler ultrasound, small arteries or veins may be found inside cyst walls or the surrounding stroma of mere lymphatic malformations, and according to Paltiel et al. [8], that is the case in approximately 60 % of cases. However, cysts themselves are not vascularized at all, unless a combined venolymphatic malformation is present. Only in the latter can a color change be seen in a color Doppler ultrasound compression test. Only slow flow is detected inside veins and arteries of lymphatic malformations using spectral wave analysis.

Teaching Point

A negative result using the color Doppler ultrasound compression test in a cavernous malformation is diagnostic for cystic lymphangioma.

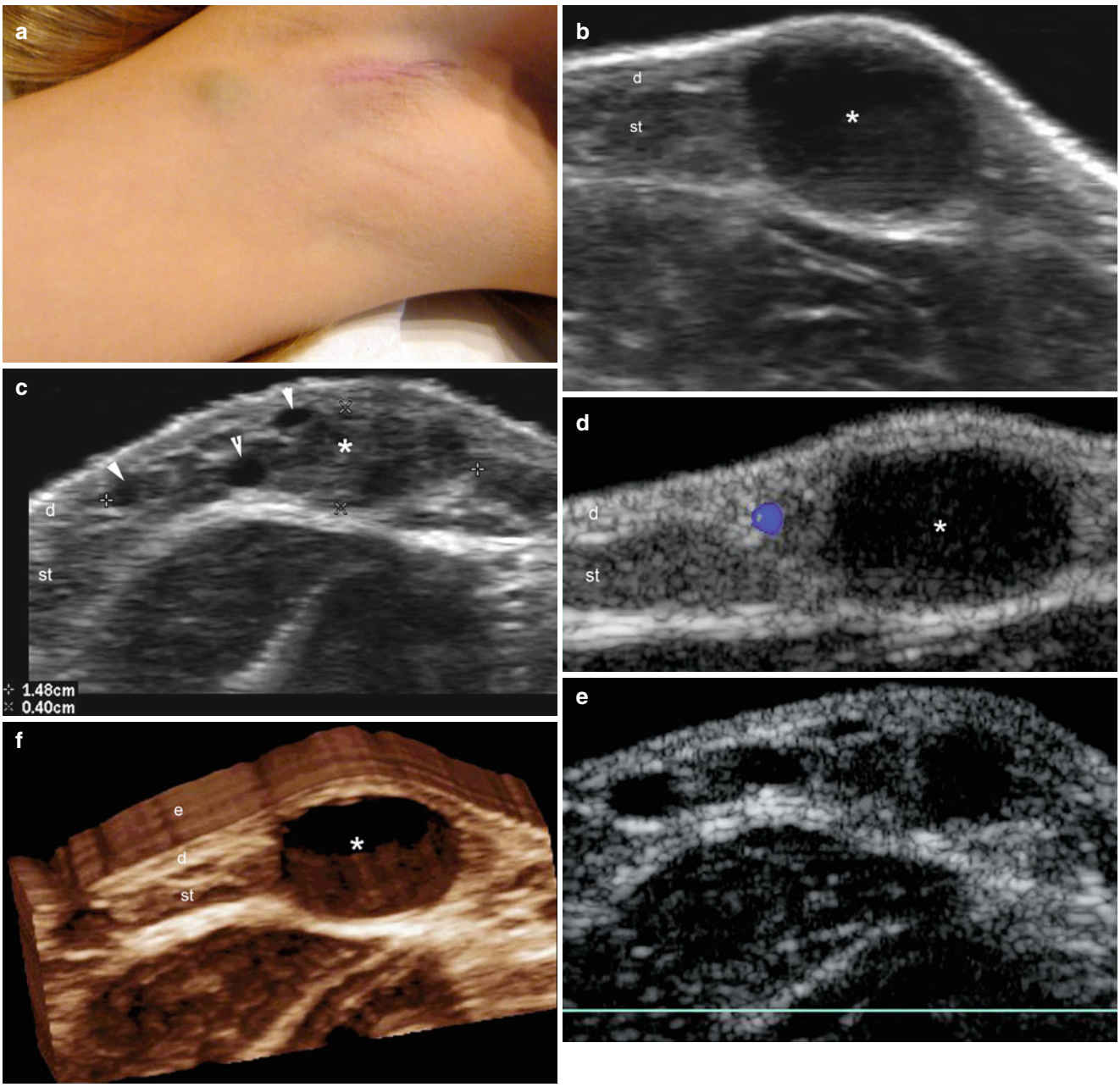

Fig. 7.43 (**a**–**f**) Low-flow lymphatic vascular malformation. (**a**) Clinical image shows a lesion with swelling in the inner aspect of the right arm. Notice the erythematous scar in the axilla secondary to a previous partial removal of the lymphatic malformation. (**b**, **c**) Grey scale ultrasound images (transverse view) demonstrate multiple well-defined round-shaped anechoic pseudocystic structures in the dermis and subcutaneous tissue. B (large pseudocyst, *) and C (multiple small pseudocysts–*arrows*) in between the normal subcutaneous tissue (*). (**d**, **e**) Color Doppler ultrasound images (transverse views) show lack of vascularity within the pseudocystic structures. (**f**) 3D reconstruction (5–8 s sweep) of the lesional area. *Abbreviations*: *e* epidermis, *d* dermis, *st* subcutaneous tissue

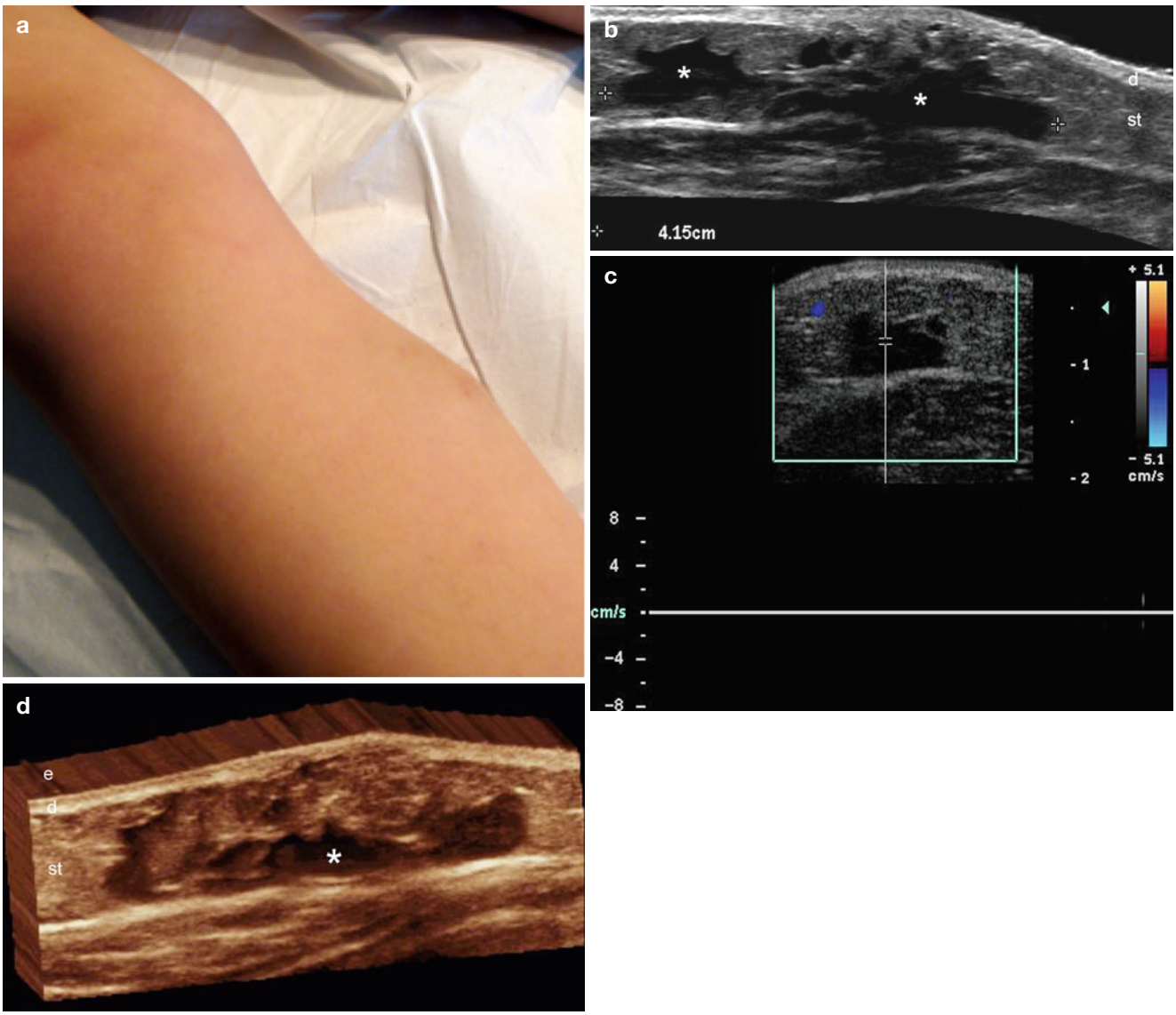

Fig. 7.44 (**a**–**d**) Low-flow lymphatic vascular malformation. (**a**) Clinical image shows swelling in the inner aspect of the right leg. (**b**) Grey scale ultrasound image (extended field of longitudinal view) demonstrates 4.15 cm long anechoic pseudocystic structures (*) mostly in the subcutaneous tissue. (**c**) Color Doppler ultrasound spectral curve analysis shows lack of vascularity within the pseudocystic spaces. (**d**) 3D ultrasound reconstruction of the lesion (*). *Abbreviations*: *e* epidermis, *d* dermis, *st* subcutaneous tissue

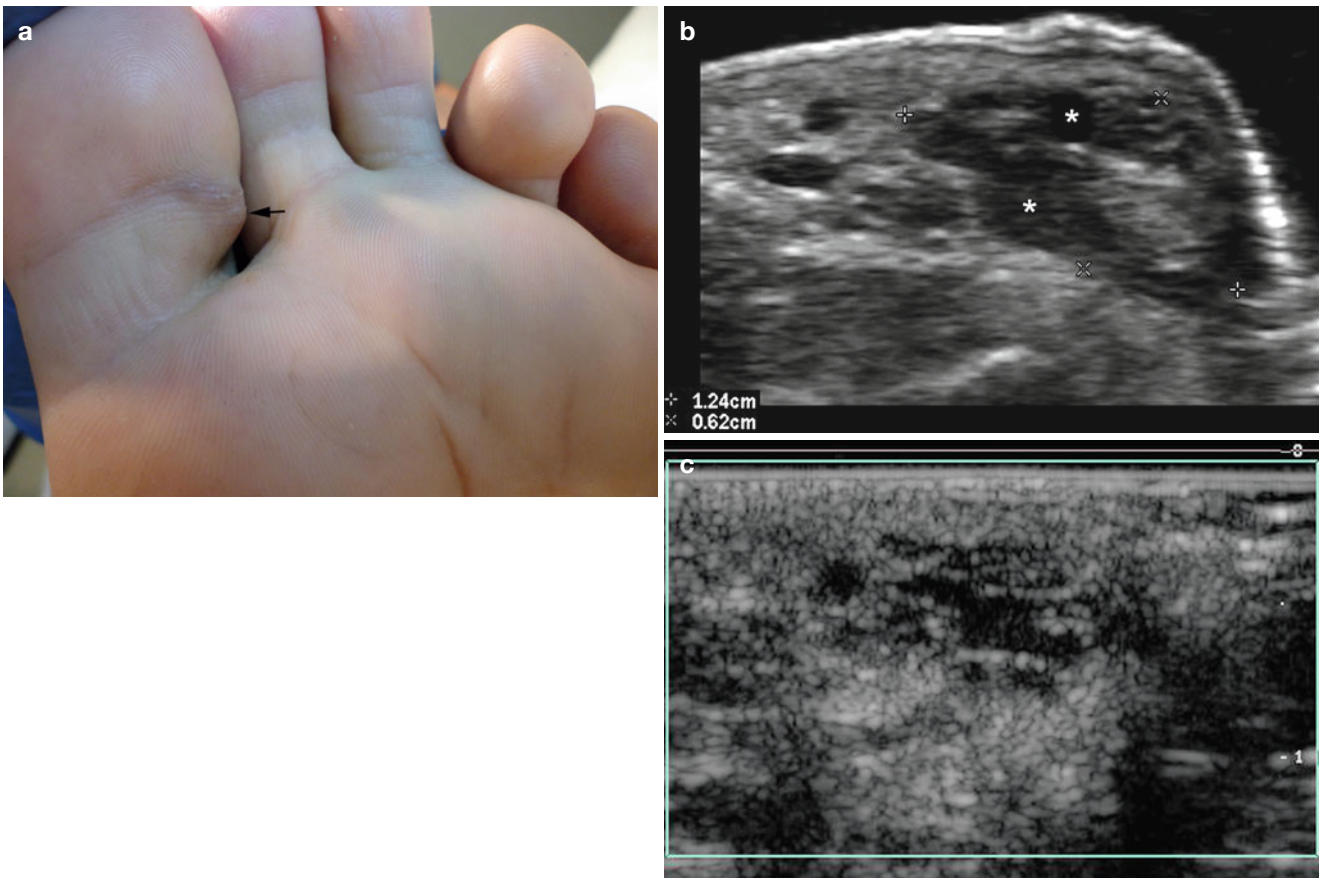

Fig. 7.45 (**a**–**c**) Low-flow lymphatic vascular malformation. (**a**) Clinical image demonstrates slightly erythematous swelling (*arrow*) in the lateral aspect of the left toe. (**b**) Grey scale ultrasound image (transverse view) shows 1.24 × 0.62 cm area with multiple anechoic tubules and pseudocystic structures (*) in the subcutaneous tissue. (**c**) Color Doppler ultrasound image (transverse view) demonstrates lack of vascularity within the tubules and pseudocystic spaces

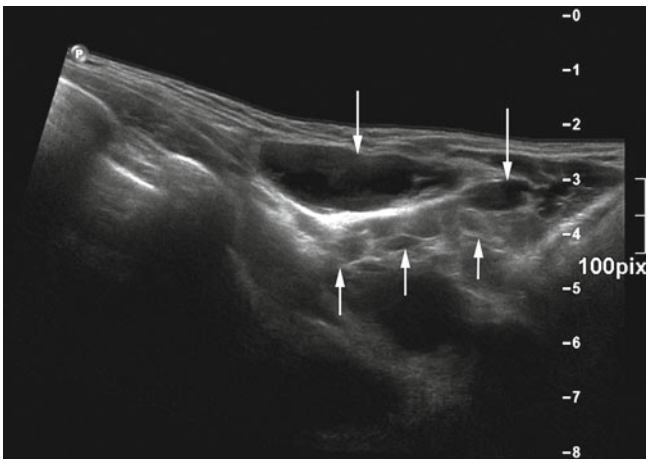

Fig. 7.46 Macrocystic lymphangioma consisting of variously sized fluid-filled cysts (*arrows*)

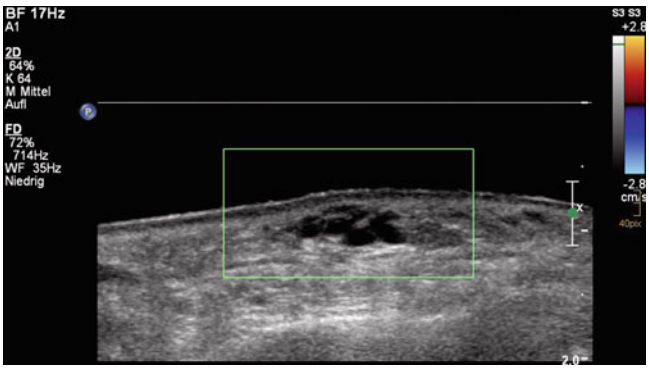

Fig. 7.47 Microcystic lymphangioma: subcutaneous lesion consisting of multiple equally sized tiny cysts without detectable flow (compression scan)

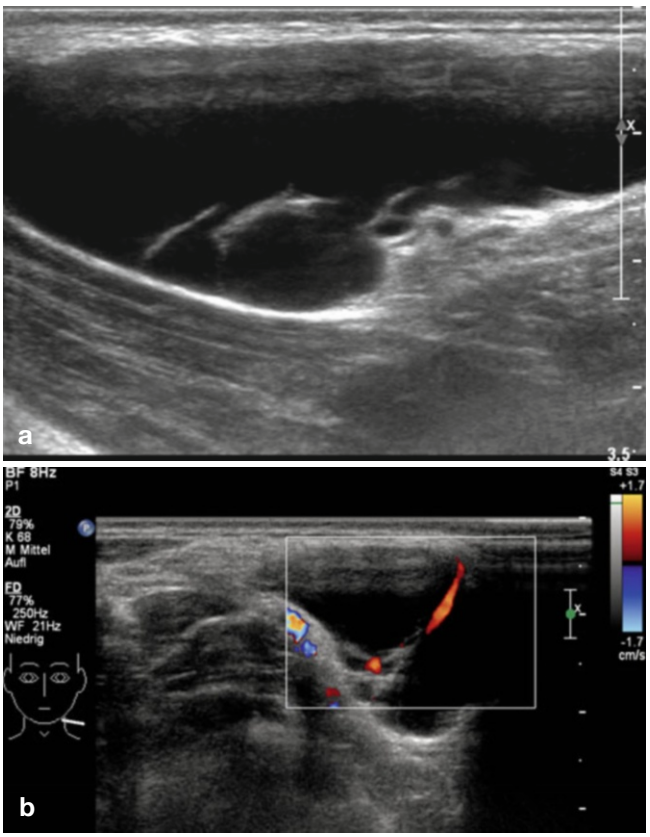

Fig. 7.48 Transverse grey scale (**a**) and Color Doppler ultrasound images (**b**) of a patient with lymphangioma. A small vessel is demonstrated inside a thick septum (**b**) in this otherwise avascular lesion

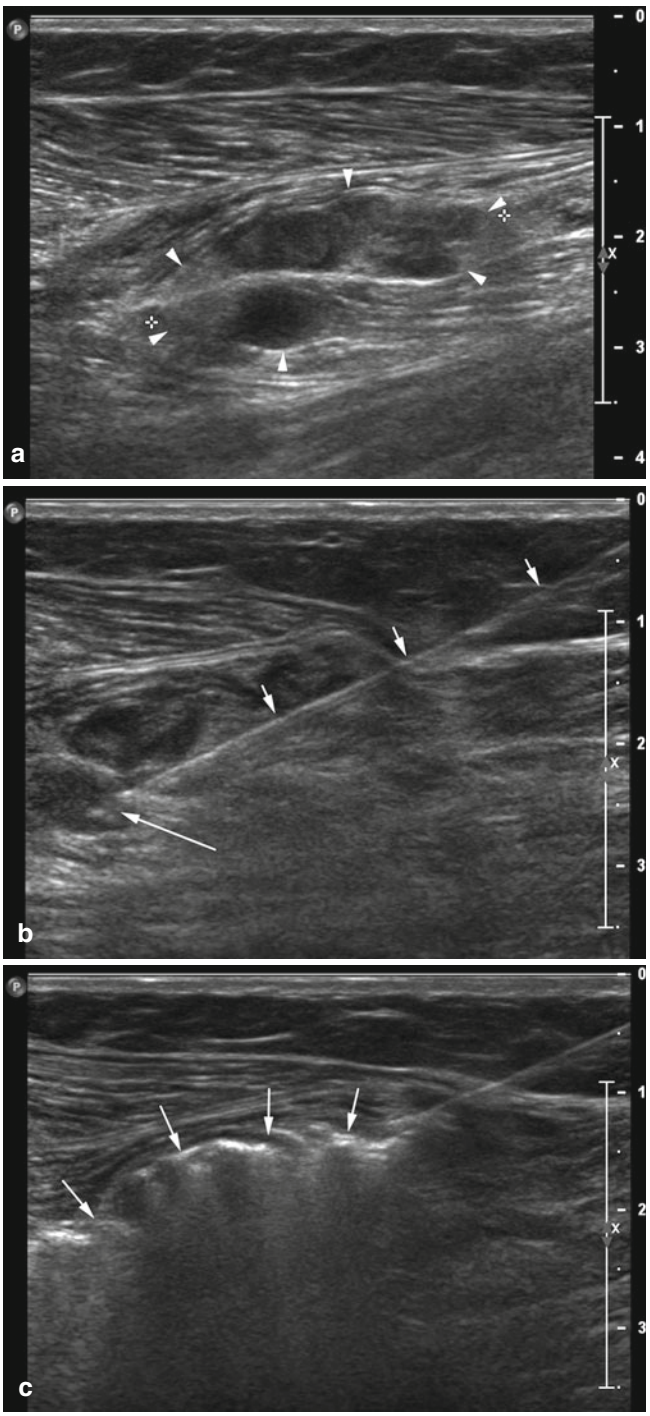

Fig. 7.49 (**a**) Transverse grey scale image of a small intramuscular venous malformation (*arrowheads*) (same patient as in Fig. 7.6). (**b**) Direct puncture under sonographic control with a 21-gauge needle (*arrowheads*). The needle tip (*arrow*) is positioned inside the deepest lying cavern. (**c**) Homogeneous distribution of polidocanol foam inside the lesions (*arrows*)

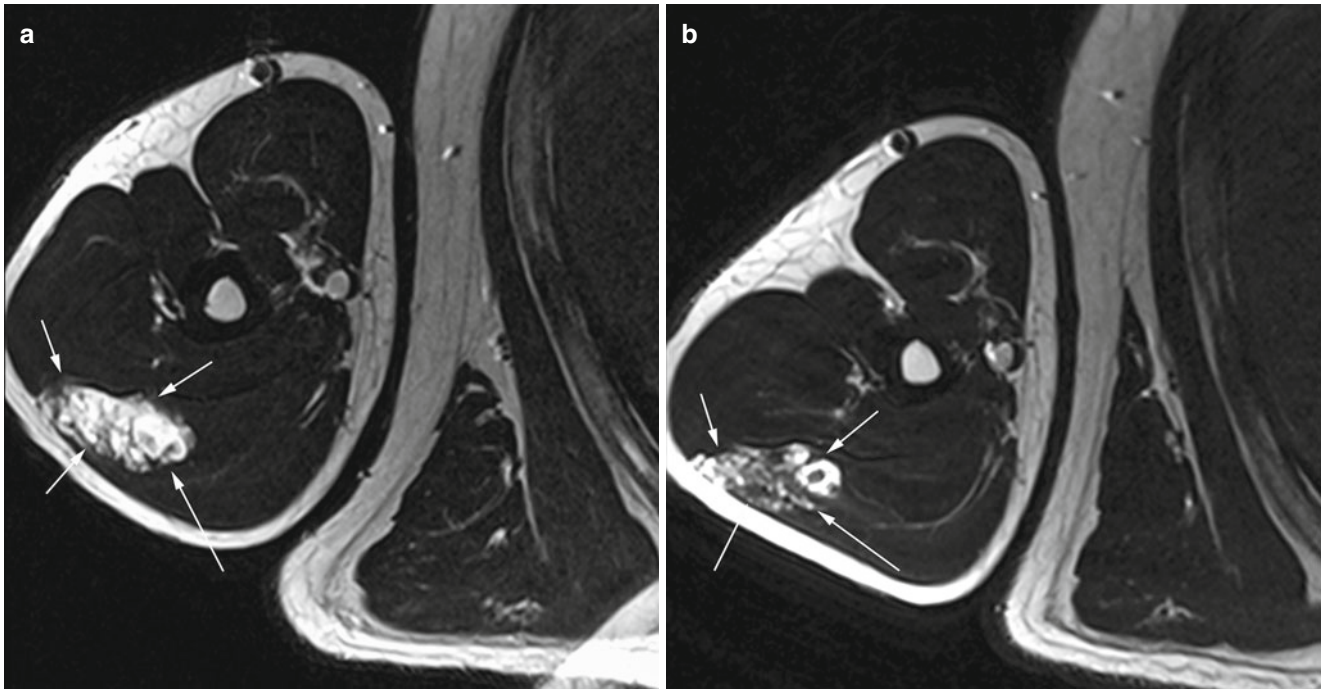

Fig. 7.50 (**a**, **b**) Transverse T2-weighted MR images of venous malformation (*arrows*) in the right triceps muscle, (**a**) before, (**b**) after sclerotherapy with polidocanol. Note marked reduction of hyperintense areas inside the malformation in (b), consistent with good response to sclerotherapy

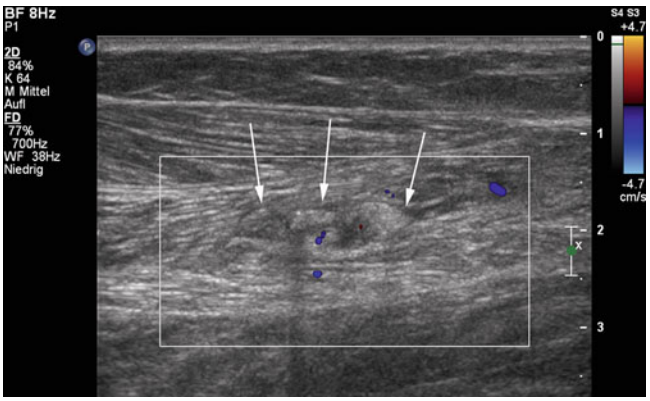

Fig. 7.51 Color Doppler ultrasound image after sclerotherapy of venous malformation: a marked reduction of lesion volume, fibrous remodeling (*arrows*) and no detectable flow is demonstrated confirming good response

7.7 Percutaneous Ultrasound-Guided Therapy

Traditionally the accepted treatment for a vascular malformation was surgery. Because of the complex architecture of vascular malformations, however, surgical resection often does not allow for complete excision of the lesion, or only at the risk of severe cosmetic impairment. This is especially true for complex AVMs with high flow. Generally speaking, malformations are lesions that respond to a variety of external stimuli: minor trauma (and thus also surgical incision) may result in accelerated growth of residual parts of a malformation with disastrous consequences. Therefore, current treatment concepts favor a multidisciplinary approach that on the one hand avoids overaggressive surgery, and overtly conservative approaches on the other. Treatment of vascular malformations has two major aims: complete destruction or resection of the lesion, if feasible, or at least amelioration of clinical symptoms by reduction of local blood flow and/or extent of the lesion. Ideally, the nidus of an AVM must be completely destroyed, complete thrombosis and later fibrous remodeling of a slow-flow malformation must be achieved, and cosmetic or functional impairment must be kept at a minimum. In this regard, sclerotherapy may be the sole treatment for a venous malformation, may be used in conjunction with arterial embolotherapy, or implemented as a preoperative or postoperative adjunct therapy.

While the nidus of an AVM is typically treated by transarterial catheter embolization, venous channels inside an AVM or slow-flow venous malformation (Fig. 7.49) may be attacked by a variety of sclerosing agents that include absolute ethanol, polidocanol (aethoxysklerol), and ethanolamine oleate. In experienced hands, percutaneous sclerotherapy is usually a safe procedure, however, certain complications exist and therefore the decision to treat must be based on a thorough clinical and imaging work-up. We generally recommend a complete color Doppler ultrasound examination with spectral wave analysis, including measurement of

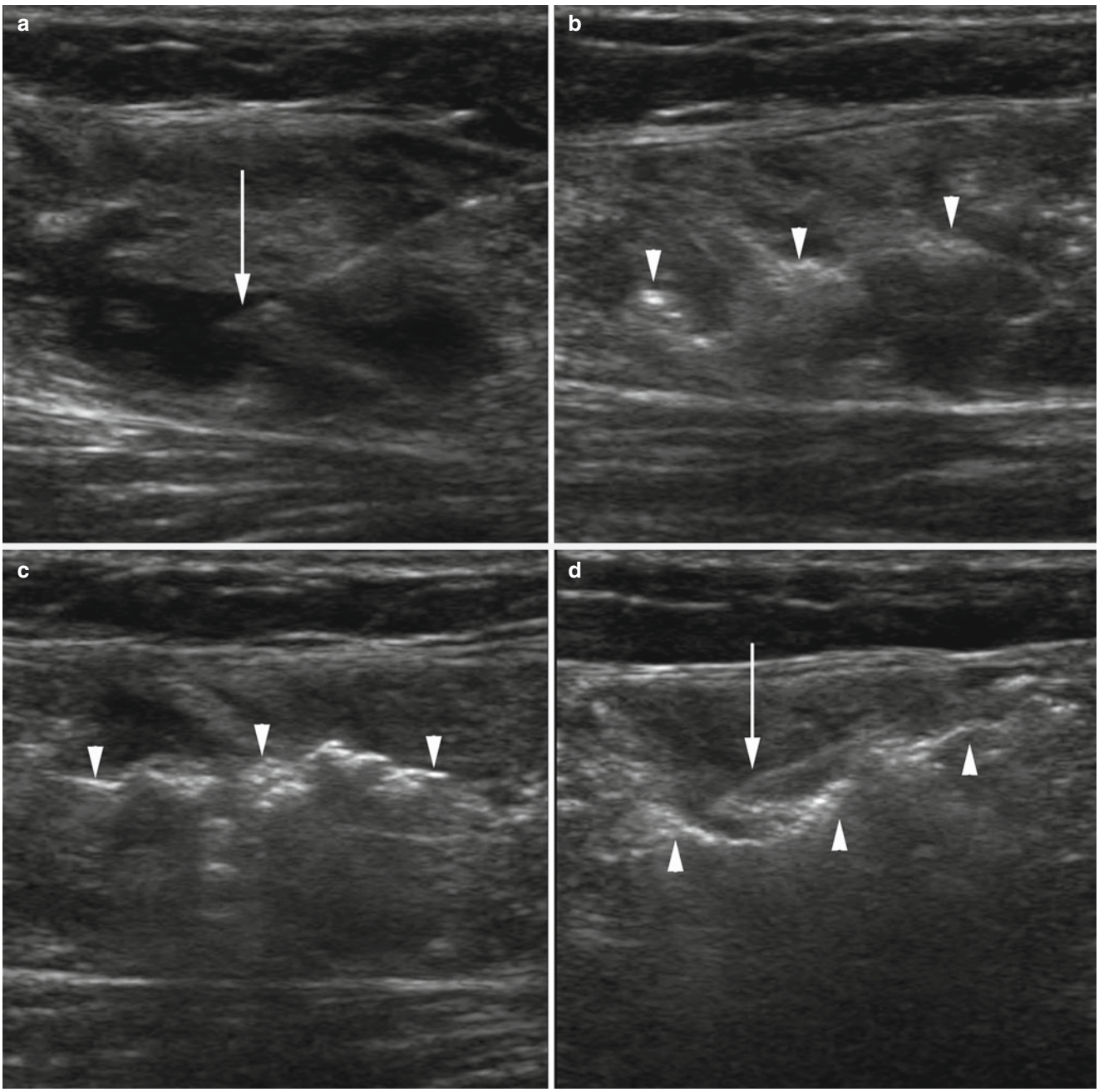

Fig. 7.52 (**a**–**d**) Sclerotherapy with polidocanol in a patient with a slow-flow venous malformation: initially the needle tip is positioned deep inside the lesion (*arrow* in **a**), with injection of polidocanol foam progressive filling of venous caverns is seen (*arrowheads* in **b** and **c**). The needle is repositioned to a more superficial location (*arrow* in **d**). Note the posterior acoustic shadowing in caverns already filled with echogenic foam (*arrowheads* in **d**) that prevents visualization of the deep lying area in the later phase of sclerotherapy

shunt flow in combined AVMs and MRI with inclusion of MRA. In the case of a combined AVM, conventional angiography is performed to define the configuration of the nidus and the existing feeders, and a first session of transcatheter arterial embolization is usually performed after diagnostic angiography. In selected cases, percutaneous sclerotherapy of the venous component is performed in the same session. For venous malformations, direct puncture percutaneous phlebography is performed and a first sclerotherapy session follows after definition of the venous drainage (see above). Patients with lymphangioma go directly toward sclerotherapy after diagnostic imaging with ultrasound and MRI.

The same imaging work-up detailed above is used to assess treatment success after sclerotherapy. Judging the effect of sclerotherapy is difficult because there is a high discrepancy

between the clinical and morphological response [21]; while some patients show good response in terms of regression of lesion volume as defined on imaging, clinical improvement can be unsatisfactory, and vice versa.

Teaching Point
Clinical improvement and results of imaging studies after sclerotherapy are highly discrepant.

To our knowledge, there are no reliable data on how to define a "good response" based on imaging criteria, but generally a reduction of lesion volume ≥50 % is considered acceptable (Fig. 7.50). This is true for low-flow venous malformations, but for high-flow lesions, an attempt to complete devascularization should be made. If only partial reduction is achieved, the risk of recurrence with increased perfusion of the persisting feeders and subsequent enlargement of the malformation is high. In general, better success rates are achieved in malformations with low flow and only small draining vessels. Another important aspect for better success rates is even distribution of the sclerosant throughout the malformation and a longer local dwell time in the target, which are achieved by multiple punctures and repositioning of the needle and effective reduction of venous drainage by compression of drainage veins, or the use of a sclerosant with better endothelial contact (i.e., foam). Given this reasoning, lesions with distinct margins on pre-interventional imaging, few drainage veins and no or slow drainage are good candidates for sclerotherapy.

Percutaneous sclerotherapy may be used to treat lymphangiomas [19]. Withdrawal of the cyst fluid before instillation of the sclerosant is mandatory, particularly in large lymphangiomas, to achieve better contact of the drug with the cyst wall and to reduce the volume of the sclerosant.

In general, multiple sclerotherapy sessions are needed for the treatment of larger malformations and especially large lymphangiomas.

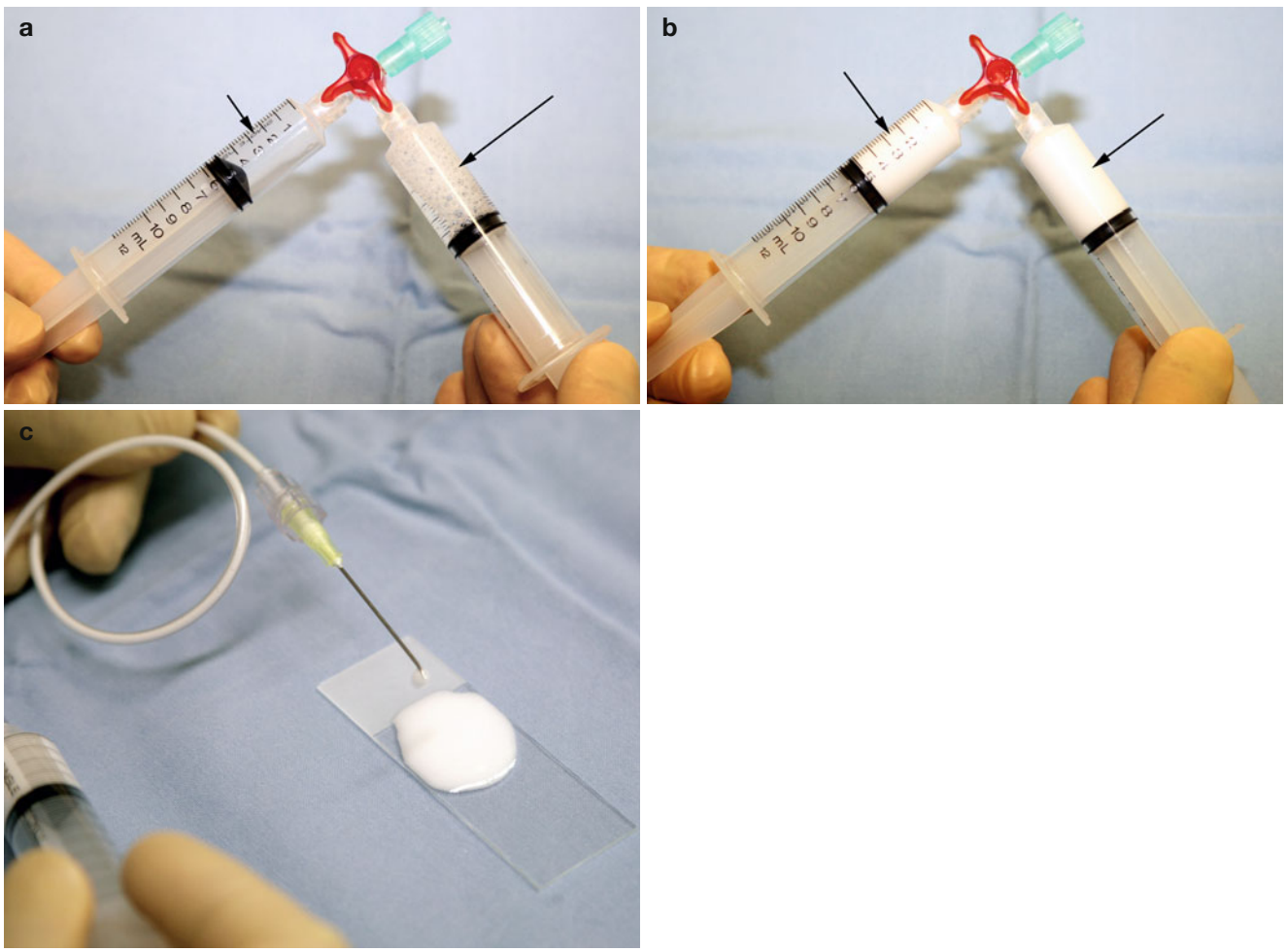

Fig. 7.53 (**a**) An equal amount of polidocanol (*long arrow*) and air (*short arrow*) is mixed by using a disposable three-way stopcock and two syringes. (**b**) Air and liquid polidocanol are pumped through the stopcock from one syringe into the other until dense foam is formed (*arrows*). (**c**) The stable foam is administered via a 21-gauge needle and tubing

7.7.1 Absolute Ethanol

Absolute ethanol has long been the main agent for treatment of lesions that are surgically inaccessible. Ethanol causes endothelial damage, thrombosis with later fibrosis, and occlusion of vascular channels. A response rate between 64 and 96 % is reported for venous malformations in terms of reduction of lesion size and volume and/or improvement of symptoms [12] (Fig. 7.51). The rate of complication is not to be underestimated with skin changes (blisters, necrosis), superficial cellulitis, deep vein thrombosis, pulmonary embolus, and cardiopulmonary collapse. It is possible for systemic alcohol contamination to also occur. Because of severe pain associated with the procedure, we generally only perform ethanol sclerotherapy under general anesthesia (a nerve block may be an alternative in selected cases). Blood-flow monitoring is mandatory because of the risk of cardiovascular reactions. Except for venous malformations with no detectable drainage or hemangioma, a tourniquet is used to reduce venous drainage and the sclerosant is injected slowly through an 18–22 gauge needle. In contrast to other researchers, we do not perform injection under fluoroscopic guidance, but with sonographic control only. For large cavernomatous malformations it is advised to gradually inject only small amounts of the sclerosant with frequent repositioning of the needle to achieve even distribution of the scelrosant inside the malformation. In our experience, this results in a better sclerosing effect throughout the lesion.

7.7.2 Polidocanol

Polidocanol (aethoxysclerol) is a substance that has been used with good success for the treatment of lower extremity and esophageal varices and thus an agent with good sclerosing potential for venous malformations [22]. It is a detergent consisting of 95 % hydroxypolyethoxydodecane, which induces overhydration of endothelial cells, resulting in a cascade of vascular injury, thrombosis, and fibrotic remodeling similar to ethanol. Because polidocanol has an anesthetic effect, it can be applied without any need for additional anesthesia, which makes it the agent of choice for sclerotherapy in an outpatient setting. Because severe cardiovascular complications are known, it should not be seen as a "Mickey-Mouse treatment," which is why the same precautions are to be taken as in ethanol sclerotherapy (blood-flow monitoring, use of tourniquets, etc.). We observe patients for at least half an hour after treatment, or longer depending on the extent of the lesion and the type of venous drainage. Generally, 1 ml of a 1 % solution of polidocanol is used for each centimeter of the lesion, with a maximum of 6–10 ml. The injection is done with real-time ultrasound guidance and repositioning of the needle or repeat punctures as specified above for ethanol treatment (Fig. 7.52). A special type of application using a polidocanol foam preparation has been presented in the literature for the treatment of varicose veins [23], which may also be used successfully for the treatment of venous malformations [24]. An equal amount of polidocanol and air is mixed by using a disposable three-way stopcock and two syringes. The air and liquid polidocanol are pumped through the stopcock from one syringe into the other until dense foam is formed [23] (Fig. 7.53). The stopcock may be gradually locked to reduce the opening of the hole and produce foam with tinier microbubbles and thicker texture. Afterward, the foam is injected as specified above under ultrasound guidance. In our experience, foam sclerotherapy has several advantages: foam provides better surface contact with the endothelium and therefore results in a better effect on the endothelial lining; it is highly echogenic and therefore the distribution of the sclerosant inside the malformations is better visualized with ultrasound compared with a liquid preparation.

Teaching Point

Polidocanol foam allows for better sonographic control of sclerotherapy and yields better results at a lower risk for complications.

Care must be taken to first fill the deep-lying caverns of a malformation (Fig. 7.52): if superficial parts fill with bubbles at the beginning of the injection, the deep-lying parts are no longer accessible because of overshadowing and a lack of needle visualization. Based on personal experience of foam sclerotherapy of varicose veins, because to our knowledge no data from larger controlled trials exist, we know that the risk of spilling the sclerosant into draining vessels and extravasation into the surrounding soft tissues is reduced with foam for the treatment of malformations.

Conclusion

Hemangiomas and vascular malformations are a complex subset of soft-tissue lesions. Their differentiation from other soft-tissue tumors and the correct classification of malformations and hemangiomas is important because it is the basis for adequate treatment. Ultrasound is the ideal first line modality for imaging and may be supplemented by MRI and MRA for further work-up. Invasive imaging such as arterial angiography or direct puncture phlebography is only needed for the planning and control of interventional treatment, but otherwise unnecessary. As hemangiomas and malformations are overtly complex in terms of clinical presentation, diagnosis, therapy, and prognosis, they must be covered by an interdisciplinary team of specialists dedicated to the management of these patients.

References

1. Mulliken JB, Glowacki J. Hemangiomas and vascular malformations in infants and children: a classification based on endothelial characteristics. Plast Reconstr Surg. 1982;69:412–22.
2. Burrows PE, Mulliken JB, Fellows KE, Strand RD. Childhood hemangiomas and vascular malformations: angiographic differentiation. Am J Roentgenol. 1983;141:483–8.
3. Enjolras O. Classification and management of the various superficial vascular anomalies: hemangiomas and vascular malformations. J Dermatol. 1997;24:701–10.
4. Kawanabe T, Wakita S, Harii K, Hayashi N, Inoue Y. Sclerotherapy of hemangiomas and vascular malformations in lips. Jpn J Plast Reconstr Surg. 1996;16:852–62.
5. Inoue Y, Wakita S, Yoshikawa K, et al. Evaluation of flow characteristics of soft-tissue vascular malformations using technetium-99 m labeled red blood cells. Eur J Nucl Med. 1999; 26:367–72.
6. Kramer U, Ernemann U, Fenchel M, et al. Pretreatment evaluation of peripheral vascular malformations using low-dose contrast-enhanced time-resolved 3D MR angiography: initial results in 22 patients. Am J Roentgenol. 2011;196:702–11.
7. Dubois J, Patriquin HB, Garel L, et al. Soft tissue hemangiomas in infants and children: diagnosis using Doppler sonography. Am J Roentgenol. 1998;171:247–52.
8. Paltiel HJ, Burrows PE, Kozakewich HPW, Zurakowski D, Mulliken JB. Soft tissue vascular anomalies: utility of US for diagnosis. Radiology. 2000;214:747–54.
9. Oe Y, Orr L, Laifer-Narin S, et al. Contrast-enhanced sonography as a novel tool for assessment of vascular malformations. J Angiogenesis Res. 2010;2:25.
10. Enjolras O, Riche MC, Merland JJ, Escnde JP. Management of alarming hemangiomas in infancy: a review of 25 cases. Pediatrics. 1990;85:491–8.
11. Taylor KJW, Ramos I, Carter D, Morse SS, Snower D, Fortune K. Correlation of Doppler US tumor signals with neovascular morphologic features. Radiology. 1988;166:57–62.
12. Hyodoh H, Masakazu H, Akiba H, et al. Peripheral vascular malformations: imaging, treatment approaches, and therapeutic issues. Radiographics. 2005;25:159–71.
13. Puig S, Casati B, Staudenherz A, Paya K. Vascular low-flow malformations in children: current concepts for classification, diagnosis and therapy. Eur J Radiol. 2005;53:35–45.
14. Puig S, Aref H, Chigot V, Bonin B, Brunelle F. Classification of venous malformations in children and implications for sclerotherapy. Pediatr Radiol. 2003;33:99–103.
15. Dubois J, Soulez G, Oliva VL, et al. Soft-tissue venous malformations in adult patients: imaging and therapeutic issues. Radiographics. 2001;21:1519–31.
16. Trop I, Dubois J, Guibaud L, et al. Soft tissue venous malformations in pediatric and young adult patients: diagnosis with Doppler US. Radiology. 1999;212:841–5.
17. Abernethy LJ. Classification and imaging of vascular malformations in children. Eur Radiol. 2003;13:2483–97.
18. Blei F. Congenital lymphatic malformations. Ann NY Acad Sci. 2008;1131:185–94.
19. Impellizzeri P, Romeo C, Borruto FA, et al. Sclerotherapy for cervical cystic lymphatic malformations in children. Our experience with computed tomography-guided 98 % sterile ethanol insertion and a review of the literature. J Pediatr Surg. 2010;45:2473–8.
20. Bloom DC, Perkins AJ, Manning SC. Management of lymphatic malformations. Curr Opin Otolaryngol Head Neck Surg. 2004;12:500–4.
21. Yun WS, Kim YW, Lee KB, et al. Predictors of response to percutaneous ethanol sclerotherapy (PES) in patients with venous malformations: analysis of patient self-assessment and imaging. J Vasc Surg. 2009;50:581–9.
22. Jain R, Bandhu S, Sawhney S, Mittal R. Sonographically guided percutaneous sclerosis using 1 % polidocanol in the treatment of vascular malformations. J Clin Ultrasound. 2002;30:416–23.
23. Tessari L, Cavezzi A, Frullini A. Preliminary experience with a new sclerosing foam in the treatment of varicose veins. Dematol Surg. 2001;27:58–60.
24. Bergan J, Cheng V. Foam sclerotherapy of venous malformations. Phlebology. 2007;22(6):299–302.